CHAPTER 1

INTRODUCTION

This chapter is an introductory chapter of the thesis that presents the motivation for the research undertaken herein, the specific research objectives and the research methodology adopted for the work.

1.1 Motivation

Orthogonal Frequency Division Multiplexing (OFDM) technology has become the technology of choice in most wireless communication networks of today. Wireless Local Area Network (LAN), Metropolitan Area Network (MAN), Personal Area Network (PAN), Regional Area Network (RAN), Digital Video Broadcast (DVB) and many such networks are built around OFDM system. The reason behind this is because OFDM system has advantages that no other system offers. Prominent among them are its efficiency in spectral usage because of the overlapping subcarriers, a far simpler channel equalization and lastly a very simple implementation by using Fast Fourier Transform (FFT) hardware.

However, the OFDM system is not without some problems of its own. Time and frequency synchronization and also the high peak-to-average power ratio (PAPR) are among the most common and serious problems in the Orthogonal Frequency Division Multiplexing (OFDM) system. Time and frequency synchronization produce offset errors leading to inter-carrier interference (ICI) and lower bit-error rates (BER). Many techniques have been developed to overcome these problems. For a burst transmission system like wireless LAN and wireless MAN, a certain preamble at the beginning of

the OFDM frame is exploited to estimate the offsets by exploiting the correlation properties of the preamble.

Our studies in the time synchronization show that Park's [1] method of time synchronization is a method that gives more accurate detection as compared to all other methods. Among the many bursty communication systems, the existing IEEE 802.16 standard for wireless MAN makes use of a preamble that is derived from a pseudo-noise (PN) sequence having good time as well as frequency domain correlation properties. However, when used in Park's method, it suffers from serious degradation if any frequency offset is present in the received frame. Frequency offsets, caused by mismatch between transmitter oscillator and receiver's oscillator is very common. Therefore, it is our motivation to design a new preamble that not only has better time and frequency synchronization properties but also is robust to the frequency offset. We also seek lower PAPR in the proposed preamble than the existing preamble.

Furthermore, it is also observed that, in the presence of frequency offset, no channel estimation can be carried out in time domain before FFT. Neither has any work been done to best of our knowledge that estimates and corrects the integer frequency offset in time domain. Therefore, it is also our endeavour to estimate and correct the integer frequency offset in the time domain leading to a new receiver design that allows the channel estimation in time domain.

1.2 Objectives of the Research

The objectives of this research, therefore, are:

1. To design a new Generalized Chirp Like (GCL) sequence - based preamble and evaluate its performance in both the time and frequency synchronization by comparing it with those of the existing Pseudo Noise (PN) sequence-based preamble of IEEE 802.16std based wireless MAN.

2. To design a new receiver that will correct the integer frequency offset in the time domain and evaluates its performance.

3. To carry out channel estimation in time domain using both the GCL based preamble and the existing PN sequence-based preamble of IEEE 802.16std and compare their performances.

1.3 Introduction to OFDM

Orthogonal Frequency Division Multiplexing (OFDM) is a multicarrier transmission technique that divides a channel into many sub-channels and transmits the data simultaneously over all of them. The history of OFDM dates back to 1960's when it was used in military HF radio link applications. Of late, this technology has become increasingly popular and is used in many systems such as: broadcast systems like Digital Audio/Video Broadcasting (DAB/DVB) [2], Asymmetric Digital Subscriber Line (ADSL) [3] and most wireless networks like Wireless Local Area Network (WLAN), Wireless Metropolitan Area Network (WMAN), Wireless Regional Area Network (WRAN), Wireless Personal Area Network (WPAN), and emerging Cognitive Radios etc.

OFDM is a little bit similar to Frequency Division Multiplexing (FDM). Both divide the channel into sub-channels and send the data bits or symbols over the subcarriers. In OFDM, the same data is sent over all the sub-channels while FDM usually sends different data streams over different sub-channels. But in an FDM system, to avoid interference among the sub-channels, one needs a guard-band between consecutive sub-channels causing inefficient spectrum utilization. On the other hand, OFDM divides its channel into many sub-channels and there are no guard-bands between adjacent sub-channels thus it is spectrally more efficient. In order to avoid the interference between the sub-channels, each OFDM subcarrier needs to stay orthogonal to all other sub-carriers and that is where the name of the technique originated from. Fig 1.1(a) and Fig 1.1(b) present the FDM and OFDM subcarriers

and associated bandwidth allocation. Further, Fig 1.2 presents the spectrum of an OFDM signal that shows the orthogonality of the OFDM subcarriers.

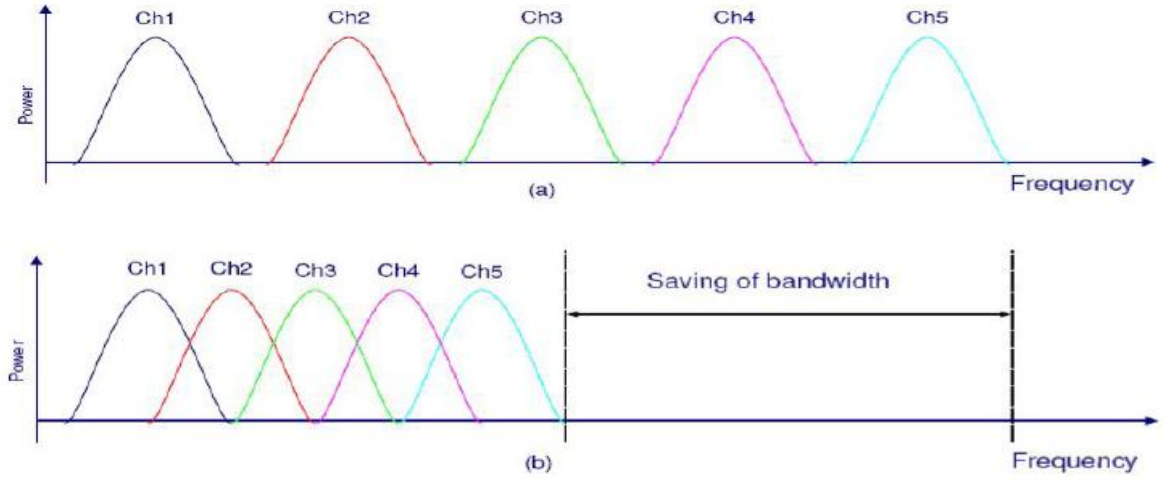

Fig.1.1 in (a) FDM and (b) OFDM Subcarriers

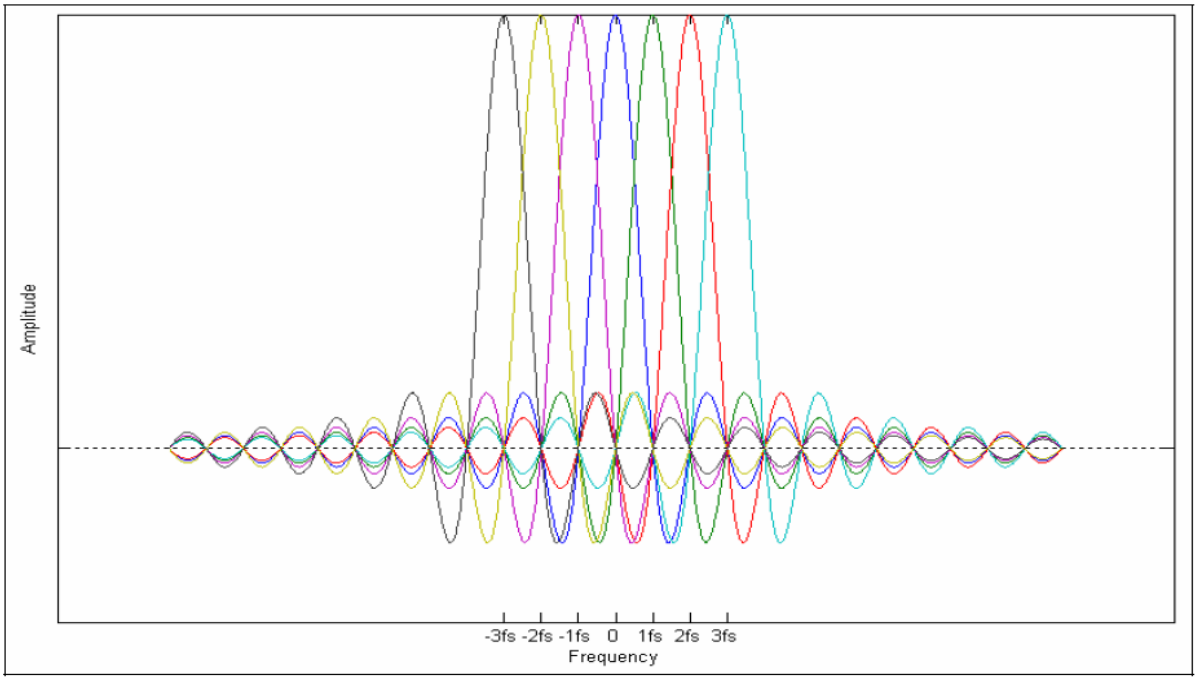

Fig. 1.2 Spectrum of an OFDM Signal

In a conventional radio communication system, radio waves are generated using oscillators. These oscillators generate the carrier waves and modulators inject the data signal on to these carrier waves. An OFDM system, on the other hand, generates both

the carrier and the data signal simultaneously using a microchip that implements a Fast Fourier transform/Inverse Fast Fourier transform (FFT/IFFT) [4].

FFT/IFFT are two operations that transform data between time domain and frequency domain. IFFT is used to transform frequency-domain data into time-domain data by correlating the frequency-domain data with its orthogonal complex exponential basis functions at frequencies that are 1/*T* apart where *T* is the OFDM signal duration. It is equivalent to mapping the data onto the sinusoidal basis functions. Fig 1.3 depicts the OFDM implementation using the FFT/IFFT blocks.

With FFT/IFFT, the transmitter and receiver do not require many separate oscillator circuits to derive the separate subcarriers. DFT avoids the interference between the adjacent subcarriers as long as the peaks of the individual waveform do not coincide ensuring orthogonality. Each of the subcarrier is detected by counting its peak. That way OFDM may place its subcarriers close to each other and thus achieve high spectral efficiency.

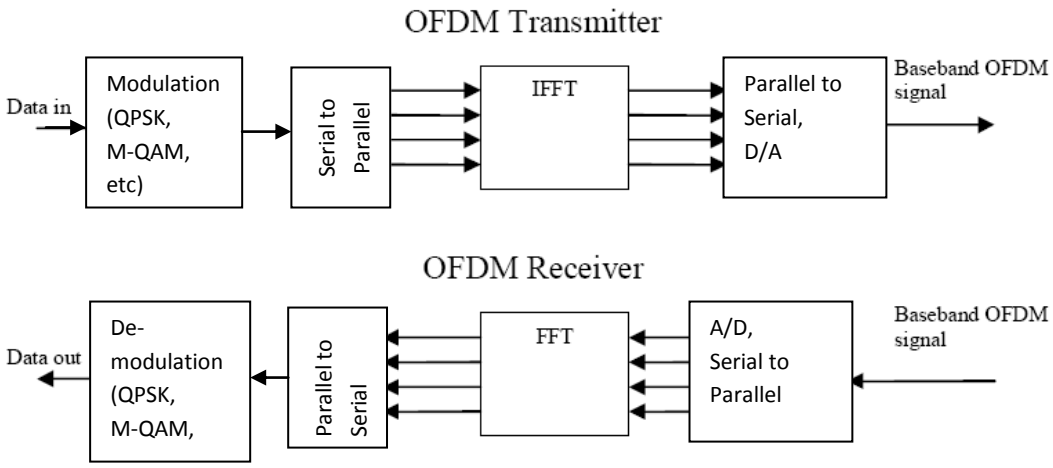

Fig.1.3 Basic OFDM Transmitter and Receiver

As a multicarrier transmission technique, OFDM has many advantages that make it attractive for communication system. Following are most notable advantages of the OFDM systems:

1. Efficiency in spectral use because of the overlapping subcarriers.

2. Equalization becomes simpler.
3. Simple implementation by using FFT.
4. With a specific channel coding and interleaving, the symbol lost due to frequency selective channel can be recovered.
5. With Cyclic Prefix, multipath channel effects such as inter symbol interference (ISI) and inter carrier interference (ICI) are mitigated.
6. If differential modulation is used, channel estimation is not required at the receiver.

Although OFDM system has all these beautiful properties, it still suffers from some shortcomings that degrade its performance if not attended to. Those shortcomings are as follows:

- It is very sensitive to time offsets and frequency offsets caused by lack of synchronization between transmitter and receivers. Time offset causes the symbol to experience ISI while frequency offset causes ICI among the subcarriers.

- It has a relatively large peak-to-average power ratio (PAPR) due to the many subcarriers that are used in the system. This high PAPR tends to reduce the power efficiency of the RF amplifier.

A lot of efforts have been made to overcome these problems. These efforts fall into the following receiver design issues: synchronization (time and frequency) problem, PAPR problem and channel estimation/equalization problem. Fig 1.4 shows the typical OFDM transmitter and receiver blocks in a bursty communication scenario.

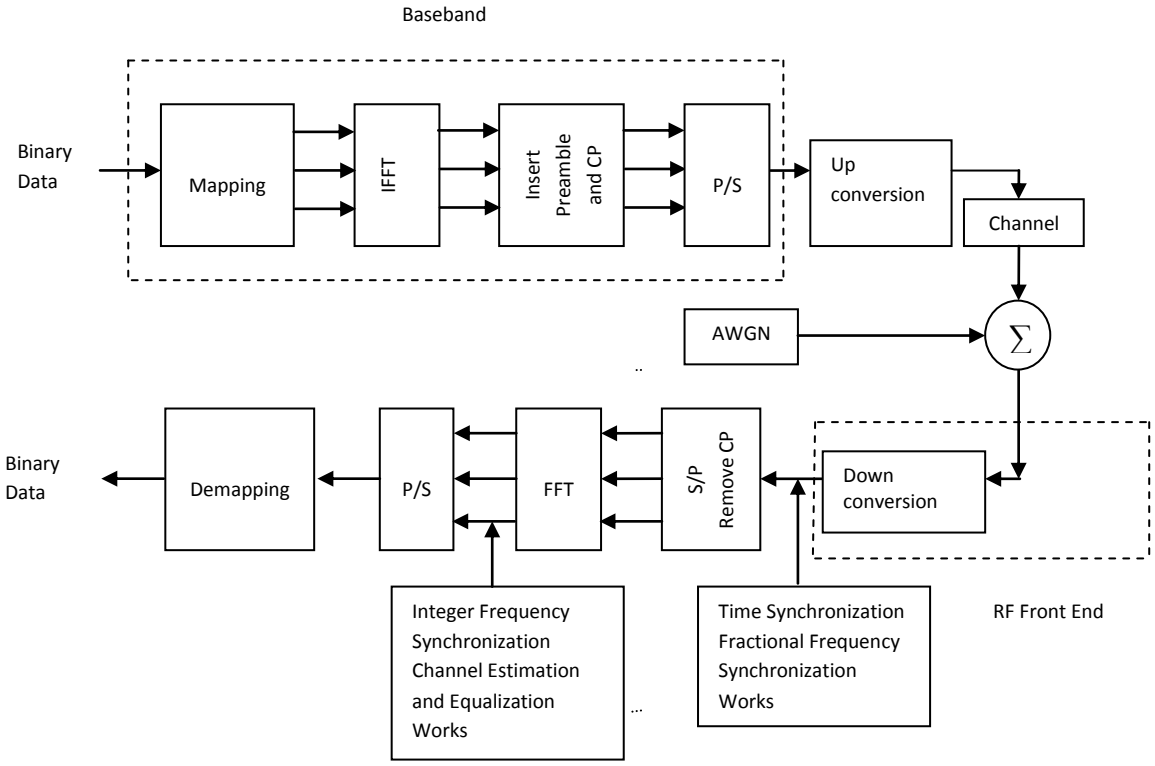

Fig.1.4 Typical OFDM Transmitter and Receiver System and Associated Works

The binary data bits, assumed to have been derived from a given application and received from link layer, serially enter the constellation mapper that converts them to complex symbols. These are then sent out as a block of symbols in parallel to IFFT block. The mapping is performed using either the Binary Phase Shift Keying (BPSK), Quadrature Phase Shift Keting (QPSK) or Quadrature Amplitude Modulation (QAM) modulation. The IFFT block helps modulate a set of subcarriers with these symbols and obtain the time domain OFDM signal that is transmitted. However, before its transmission, a cyclic prefix which is the copy of the last few samples of the OFDM symbol is added, so that the linear convolution of the signal with the wireless channel appears as a periodic convolution at the receiver. A suitable preamble is also appended to the OFDM symbols so that the frames can be synchronized and channel estimation obtained. Thanks to advancement in DSP technology today, all of this can be done using DSP chips in baseband. At this stage this baseband signal becomes ready for up-conversion to appropriate RF frequency and eventual transmission. Once up-converted, the OFDM signal is transmitted through the wireless channel which generally has multipath characteristics.

The received signal is this RF signal received together with white Gaussian noise. An RF front end consisting of narrow bandpass filter, down-converter and low-noise amplifier, not explicitly shown in the figure generates the signal that is then digitized and processed. When the signal is down-converted, frequency offsets set in as a result of the inconsistency in the oscillators at the transmitter and at the receiver. In order to perfectly demodulate the received signal, the receiver then starts to perform the synchronization in timing and frequency on the digitized signal. The time synchronization is needed to detect the start of the OFDM frame/symbol. In the typical OFDM receiver, this time synchronization can be obtained using the Schmdil & Cox's method [5]. By using this method, the frequency offset is also estimated though only the fractional part.

Once the time and fractional frequency offset is corrected, the cyclic prefix is removed. By removing the cyclic prefix, the block of received data becomes of same size as the transmitted block after IFFT. Doing FFT of the received block now gives the product of transmitted signal and channel frequency response. Once the remaining integer frequency offset is corrected, the suitable channel estimation and equalization can be carried out and the data can be successfully demapped or demodulated.

The synchronization is usually obtained from the useful properties of a pre-designed preamble [1,5, 6] or, sometimes from the cyclic prefix [7] itself. For channel estimation work, there are also some works that obtain these using scattered pilot subcarriers [8,9], as addition to the preamble based method [10,11,12]. Preamble, cyclic prefix and pilot are the properties of the OFDM frame and are designed purposely for synchronization and channel estimation.

1.3.1 A few observations:

- It is obvious that a good receiver scheme must be able to perform the time and frequency synchronization very well. In order to achieve better synchronization, the preamble based synchronization method critically depends on the preamble design.

In both the timing and integer frequency synchronization, correlation of the received preamble is a basic technique to estimate the offset of the time and frequency. The correlation is generally an autocorrelation of the received preamble using a suitable definition of a timing-metric. It can sometime be a cross-correlation between the received preamble and the stored preamble in the receiver.

In these methods, the correlation peak translates to the estimate of the offsets. The desired correlation peak, therefore, is an important issue in order to prevent a false detection of the estimation of the offset. The clutter-like sidelobes present in the correlation, depending on the characteristic of the used sequence in the preamble, might contribute to a false detection of the estimation of the offset.

- From Fig 1.4, we can see that the frequency offset is partly estimated and corrected in the time domain and the remaining offset in the frequency domain. We also see that the channel estimation is carried out in the frequency domain. However, it is possible to correct even the remaining integer frequency offset in the time domain. In turn, even the channel estimation can be carried out in the time domain which is otherwise very difficult to carry out in time domain particularly in the presence of frequency offsets in time domain. It is to be noted that pre-FFT channel estimation is helpful in estimating SNR that could be used in optimizing system performance by using them for adaptive power control, adaptive bit-loading or adaptive modulation. Therefore, a new receiver scheme is needed that can estimate and correct the frequency offset in the time domain and also estimate the channel in time domain.

1.4 Research Methodology

In this thesis, we divide the works into two major parts. First is to evaluate the performance of the proposed GCL-based preamble in the time and frequency

synchronization. Second is to evaluate the performance of the new receiver scheme for frequency offset correction and also the time domain channel estimation.

The performance of the preambles in the time synchronization is analyzed from the plateau-like shape of the timing metric for the Schmidl & Cos's method. However, for the Park's method, the performance is evaluated from not only the impulse-like peak shape of the timing metric but also from the probability of misdetection of the said peak.

In the time synchronization work, we will apply both preambles in Schmidl and Cox's technique. By obtaining the timing metric shape, we then analyze it to compare the performance of the two preambles. The same goes for the Park's method and an addition is made to obtain and analyze the probability of misdetection for various SNRs. To obtain the probability of misdetection in Park's method, we run the simulation for 10.000 iterations to obtain more accurate and convincing results.

The simulation is carried out on a test system that is built using the specifications of the IEEE 802.16 standard meant for WMAN. The simulation parameters we use in this thesis are according to the used system: the length of the preamble, the number of active subcarriers, the length of the cyclic prefix, the frequency offset and lastly the specific channel, SUI-channel.

The performance measure for the integer frequency synchronization is the probability of misdetection of the integer offset. The probability of misdetection is obtained for both preambles, the proposed GCL-based preamble as well as the standard stipulated PN sequence based preamble for various SNRs.

For the integer frequency synchronization work, we will apply both preambles in the frequency domain cross-correlation, obtain the correlation peak, and then analyze how many times the correlation peak gives wrong estimation of the integer offset as a function of SNR. The probability of wrong estimates is obtained from 1000 times iteration and the number of iteration gives the satisfying results.

In the new receiver scheme, the frequency offset correction performance is the probability of the misdetection of the symmetrical correlation. This probability is also obtained for various SNRs.

In the frequency offset correction, we will design the receiver to estimate and correct the frequency by providing the bank of multipliers and correlators. One of the correlations produces the symmetrical correlation and we will detect the symmetrical correlation. No more than 7 branches are needed since the maximum integer frequency offset is ±3.The probability of offset misdetection of the symmetrical correlation is done over 10.000 iterations and gives satisfying results.

Still in the new receiver scheme, the performance of the time domain channel estimation is the probability of misdetection of the impulse response from the preambles for various SNRs.

In the time domain channel estimation, we will again apply the preambles to the time domain correlation, obtain the impulse response peaks, and analyze how many times the correlation gives wrong estimate of the impulse response as a function of SNR. The probability is obtained for 10.000 times of iterations.

The simulation experiment for the new receiver is also built around IEEE 802.16 standard as explained before with identical simulation parameters.

1.5 Contribution of the Research

This study has resulted in three main contributions.

- First, a new and more robust preamble has been designed that is based on GCL sequence. The preamble has lower PAPR and better correlation property both in time and frequency domains and hence performs better in both time and frequency synchronization in a typical OFDM receiver. The time-domain preamble also works better in the presence of frequency offsets in time synchronization.
- Second, a new receiver scheme has been proposed which estimates and corrects integer frequency offsets in the time domain.

- Thirdly, having corrected the frequency offset in time domain, the stage is set for carrying out time-domain channel estimation reliably before FFT. Accordingly, a pre-FFT channel estimation is performed and tested with both kinds of preambles – the GCL based preamble and also the PN sequence based preamble. The channel estimates are helpful in various applications, such as SNR estimation, adaptive power control, adaptive bit-loading and adaptive modulation [13].

1.6 Thesis Outline

This report is divided into five chapters. The thesis starts with the introduction chapter outlining the motivation of the research and the research objectives, followed by the introduction of OFDM system. Chapter 2 dwells on the receiver issues in an OFDM system. It also presents the related literature on timing and frequency synchronization and also channel estimation. GCL sequence is introduced in this chapter and lastly mentions the GCL related work carried out in OFDM systems. Chapter 3 presents first, the comparison between the PN-sequence and GCL-sequence in their autocorrelation followed by the design of the GCL based preamble. The cause and the design of the time domain frequency offset correction then are described in this chapter. The performance evaluation for the time and integer frequency synchronization for the typical OFDM receiver together with the performance evaluation of the time domain frequency offset correction and time domain channel estimation for the new design of OFDM receiver are explained. The methodology for each mentioned works are the last explanation of Chapter 3. Chapter 4 presents the results and analysis of time synchronization, integer frequency synchronization, time domain frequency offset correction and lastly, time-domain channel estimation using PN as well as GCL sequence based preambles. Chapter 5 summarizes the thesis and offers recommendations for future research.

CHAPTER 2

OFDM RECEIVER AND RELATED LITERATURE

This chapter presents the basics of an OFDM receiver and gives the literature review of OFDM receiver issues such as: timing and frequency errors, the synchronization methods for both issues, the need of channel estimation, the methods of estimating and also the introduction of a sequence namely generalized chirp-like (GCL) sequence and its applications, particularly in OFDM system.

2.1 OFDM Receiver

In chapter 1, we presented the block diagram of an OFDM system which shows all the blocks of its transmitter and receiver parts including what particular step is undertaken in each block. In this chapter, we present the generation of the OFDM signal in the transmitter and the received OFDM signal mathematically.

An OFDM signal consists of a superposition of many subcarriers that are modulated by M-ary phase shift keying (MPSK) or M-ary quadrature amplitude modulation (MQAM). Mathematically, the complex baseband OFDM signal for the *k-th* symbol can be expressed as follows [14]:

$$s_k(t-kT) = \sum_{i=-N/2}^{N/2-1} x_{i,k} e^{j2\pi\left[\frac{i}{T_{FFT}}\right](t-kT)} \tag{2.1}$$

where T is the time between two consecutive OFDM symbols, T_{FFT} is the FFT-time, N is the number of FFT points, i is the index of the sub-carrier and the complex number,

$x_{i,k}$, represents the signal constellation point. Equation (2.1) is actually the IFFT of the QAM/PSK constellation points.

The effect of a time varying multipath channel can be modelled by a convolution with the time-varying channel impulse response of $h(t, \tau)$ [14].

$$r(t) = h(\tau,t) * s(t) + n(t) = \int_0^{\tau_{\max}} h(\tau,t)s(t-\tau)d\tau + n(t) \tag{2.2}$$

where $n(t)$ is additive white Gaussian noise, AWGN. Since a guard interval is added to each OFDM symbol such that its length is greater than the maximum excess delay of the channel, no ISI occurs. The frame consisting of many such OFDM symbols are so designed that the channel stays stationary over the length of the frame. With this, the channel impulse response is simplified to $h(\tau)$. Consequently, the demodulated OFDM symbol can be shown as [14]:

$$\begin{aligned} y_{i,k} &= \frac{1}{T_{FFT}} \int_{i=kT}^{kT+T_{FFT}} r(t)e^{-j2\pi i(t-kT)/TFFT}dt \\ y_{i,k} &= \frac{1}{T_{FFT}} \int_{t=kT}^{kT+T_{FFT}} \left[\int_{\tau=0}^{\tau_{\max}} h_k(\tau)s(t-\tau)d\tau + n(t) \right] e^{-j2\pi i(t-kT)/T_{FFT}}dt \end{aligned} \tag{2.3}$$

Because of the interval of the integration and $\tau_{\max} < \tau_{guard}$ then $s(t)$ could be replaced by $s_k(t)$ as in eqn. (2.1) [14]:

$$\begin{aligned} y_{i,k} = \frac{1}{T_{FFT}} \int_{t=kT}^{kT+T_{FFT}} \left[\int_{\tau=0}^{\tau_{\max}} h_k(\tau) \sum_{i'=-N/2}^{N/2-1} x_{i',k} e^{j2\pi\left(\frac{i'}{T_{FFT}}\right)(t-kT-\tau)} d\tau \right] e^{-j2\pi i(t-kT)/T_{FFT}}dt \\ + \frac{1}{T_{FFT}} \int_{t=kT}^{kT+T_{FFT}} n(t)e^{-j2\pi i(t-kT)/T_{FFT}}dt \end{aligned} \tag{2.4}$$

To simplify the integration, let $u = t - kT$ and change the order of integration, so the summation yields [14]:

$$y_{i,k} = \sum_{i'=-N/2}^{N/2-1} x_{i',k} \frac{1}{T_{FFT}} \int_{u=0}^{T_{FFT}} \left[\int_{\tau=0}^{\tau_{\max}} h_k(\tau)e^{-j2\pi i'\tau/T_{FFT}} d\tau \right] e^{-j2\pi(i-i')u/T_{FFT}} du + n_{i,k} \tag{2.5}$$

The output of the integration above will yield [14]:

$$y_{i,k} = \sum_{i'=-N/2}^{N/2-1} x_{i,k} h_{i,k} \frac{1}{T_{FFT}} \int_{u=0}^{T_{FFT}} e^{-j2\pi(i-i')u/T_{FFT}} du + n_{i,k} \tag{2.6}$$

The integration of the $h_k(\tau)$ term is actually the Fourier transform of the impulse response, which yields $h_{i,k}$. Thus, the integration part in Eq.(2.6) yields 1 if and only if $i = i'$, else it yields 0 (both i and i' are integer number). Thus the condition $i = i'$ as in the normal situation yields [14]:

$$y_{i,k} = x_{i,k} h_{i,k} + n_{i,k} \tag{2.7}$$

Eq. (2.7) implies that the receiver, post FFT, produces the encoded constellation symbols multiplied with channel frequency response plus, of course, the noise. Thus, if the channel frequency response is known or has been estimated, then the zero-forcing equalizer implemented by simply dividing $y_{i,k}$ term by term, with the channel frequency response would help demodulate $x_{i,k}$.

2.1.1 Time synchronization error

When there is an error in estimating the start of the OFDM symbol, the FFT time will also be incorrect. The FFT time synchronization error can be modelled as a shift in the interval of integration of the matched filter [14]. For a timing offset of δt, the ideal interval
$t \in [kT, kT + T_{FFT}]$ becomes $t \in [kT + \delta t, kT + T_{FFT} + \delta t]$ and Eq. (2.3) could be written as [14]

$$y_{i,k} = \frac{1}{T_{FFT}} \int_{i=kT+\delta t}^{kT+T_{FFT}+\delta t} r(t) e^{-j2\pi i(t-kT-\delta t)/T_{FFT}} dt \tag{2.8}$$

If $T_{guard} > \delta t$, then the ISI will not arise during (timing) error. This will only happen when the error is small enough for the channel impulse response to remain within the guard interval.

By repeating the derivation of Eq.(2.3) until Eq.(2.5) and replacing $u = t - kT - \delta t$ yields [14]:

$$y_{i,k} = \sum_{i'=N/2}^{N/2-1} x_{i,k} \frac{1}{T_{FFT}} \int_{u=0}^{T_{FFT}} \left[\int_{u=0}^{\tau_{max}} h(\tau) e^{-j2\pi i'\tau / T_{FFT}} d\tau \right] e^{-j2\pi[(i-i')u+i'\delta t]/T_{FFT}} du + n_{i,k} \tag{2.9}$$

Putting the $e^{-j2\pi i'\tau\delta t/T_{FFT}}$ out if the integral yields a timing error in demodulation of the received signal reflected as linear phase increase or progressive phase rotation across the subcarriers [14]:

$$y_{i,k} = x_{i,k} h_{i,k} e^{-j2\pi i\delta t/T_{FFT}} + n_{i,k} = x_{i,k} h_{i,k} e^{-j2\pi i\delta t'/N} + n_{i,k} \tag{2.10}$$

where $\delta t'$ is the timing error in samples.

2.1.2 Frequency synchronization error

Another error that typically happens in the receiver is a small mismatch in the frequency of the transmitter oscillator and that of the receiver oscillator. The error in frequency in the received signal can be represented by the expression where the frequency offset is denoted as δf and phase offset is θ, [14]:

$$r'(t) = r(t) e^{j(2\pi\delta ft+\theta)} \tag{2.11}$$

Applying Eq.(2.11) into Eq. (2.3) we obtain, [14]:

$$y_{i,k} = \frac{1}{T_{FFT}} \sum_{t=kT}^{kT+T_{FFT}} r(t) e^{j(2\pi\delta ft+\theta)} e^{-j2\pi i(t-kT)/T_{FFT}} dt =$$
$$e^{j2\pi\theta} \frac{1}{T_{FFT}} \sum_{t=kT}^{kT+T_{FFT}} \left[\int_{\tau=0}^{\tau_{max}} h(\tau) s(t-\tau) d\tau + n(t) \right] e^{j2\pi\delta ft} e^{-j2\pi i(t-kT)/T_{FFT}} dt \tag{2.12}$$

By repeating the derivation of Eq.(2.5), the received constellation points from Eq.(2.12) becomes [14]:

$$y_{i,k} = e^{j(\theta+2\pi\delta fkT)} \sum_{i'=-N/2}^{N/2-1} x_{i',k} h_{i',k} \frac{1}{T_{FFT}} \int_{u=o}^{T_{FFT}} e^{-j2\pi\left(\frac{i-i'}{T_{FFT}}\delta f\right)u} du + n_{i,k} \tag{2.13}$$

From Eq.(2.9), it can be seen that, due to the presence of the frequency error, the integral is not equal to zero when $i \neq i'$ neither it is 1 when $i=i'$ as in the idealized case in (2.7). Therefore, the orthogonality is destroyed. Eq.(2.14) mathematically expresses

the occurrence of the phase rotation in the first term, subcarrier attenuation and ICI seen in the second term in the received signal.

$$y_{i,k} = e^{j(\theta+2\pi\delta fkT)} x_{i,k} h_{i,k} \frac{1}{T_{FFT}} \int_{u=0}^{T_{FFT}} e^{j2\pi\delta fu} du + e^{j(\theta+2\pi\delta fkT)} \sum_{i'=-N/2}^{N/2-1} x_{i',k} h_{i',k} \frac{1}{T_{FFT}} \int_{u=0}^{T_{FFT}} e^{-j2\pi(\frac{i-i'}{TFFT}\delta f)u} du + n_{i,k} \quad (2.14)$$

The integral for the expression (2.14) is not equal to zero for $i \neq i$' neither it is one for $i = i$'; the situation is caused by the presence of the frequency offset. The evaluation yields in two terms, the first term (for $i = i$') accounts for equal phase rotation and attenuation of all subcarriers and the second term (for $i \neq i$') describes the ICI. When the frequency error is larger than half of the subcarrier spacing, the transmitted data symbol $x_{i,k}$, will get shifted to one or more positions in the frequency. Thus, the frequency error is often normalized to the subcarrier spacing, such that it is a decimal number. The ICI happens when the fractional part of the frequency error is not corrected and the integer part shifts the position of the subcarriers in the frequency direction.

2.1.3 Channel estimation issue

Repeating Eq (2.7) as shown in section 2.1 with simpler indexing, the perfectly received signal is shown in the equation [14]:

$$y_k = x_k h_k + n_k \quad (2.15)$$

with $\{x_k\}$and $\{y_k\}$are the transmitted and the received signal constellation points, while $\{h_k\}$ is the complex-valued frequency domain attenuation factor introduced by the time-frequency selective radio channel and $\{n_k\}$ is the AWGN noise.

From the equation (2.15), it can be seen that, although the signal is received with perfect synchronization, the received signal $\{y_k\}$needs to rid itself of the attenuation factor, $\{h_k\}$ such that what is transmitted can be approximately received in the receiver, regardless of the presence of the noise, as shown in the equation:

$$\hat{x}_k \approx y_k / h_k \tag{2.16}$$

The attenuation factor is, therefore, an important quantity that needs to be known at the receiver so the transmitted constellation symbols can be estimated. Hence, all OFDM systems employ special techniques to estimate the channel (attenuation) and use that to equalize and estimate the transmitted symbols.

The time error, frequency error and time-varying channel impulse response present in the received signal are the main impairments of the OFDM system. The system suffers badly if the three impairments are not corrected. Therefore, the pertinent algorithms to correct the impairments are explained starting with the time synchronization, frequency synchronization and lastly channel estimation.

2.2 Typical OFDM Receiver – Schmidl & Cox Receiver [5]

An OFDM receiver basically performs the reverse tasks of that at the OFDM transmitter. But, as the signal goes through the channel, the signal experience some impairments and the receiver needs to carry out certain tasks before it starts to demodulate and get back the transmitted data bit. In a bursty communication system, where the transmitter transmits packets of data, the receiver does not have the knowledge of the start of the signal to properly perform the demodulation. This is among the most common problems of a receiver popularly known as time synchronization problem.

A typical receiver, therefore, performs the time synchronization task first before anything. For bursty communication system, one of the widely known receiver scheme is the Schmidl and Cox receiver scheme, which carries out both the time and frequency synchronization. For clarity, Fig. 2.1 depicts the Schmidl and Cox receiver scheme.

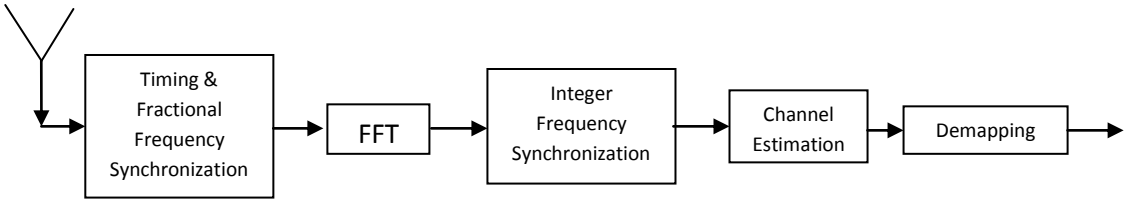

Fig. 2.1 Schmidl and Cox Receiver Scheme

The first synchronization is in timing synchronization (pre-FFT), which is to know the start of the symbol. Simultaneously, it also varies out fractional frequency synchronization. Now the received signal can be stripped of the cyclic prefix and be subjected to FFT. The second part is in frequency domain (post FFT) where the remaining integer frequency offset is corrected or synchronization and channel estimation is performed.

The time and fractional synchronization is achieved by performing autocorrelation of a suitably designed preamble while integer frequency synchronization is achieved by cross-correlation of the same preamble. Channel estimation is sometime done using another preamble or sometime using the same preamble. More details of all the synchronization and channel estimation will be given in the next section.

2.3 Time Synchronization

In the following sections, three preamble-based synchronization algorithms will be introduced. In all cases, packet detections are assumed to be performed successfully before all the synchronization algorithms take part.

2.3.1 Schmidl and Cox's time offset estimation

Schmidl and Cox algorithm [5] is a well-known preamble-based synchronization algorithm in OFDM system. This algorithm works for both timing offset estimation and also frequency offset estimation. In this algorithm, two preambles are used to carry out the estimation of time and frequency offsets. The first preamble is designed to have two identical halves for the purpose of time estimation. The second preamble

is designed for the purpose of remaining frequency offset estimation and channel estimation.

The two identical halves of the preamble are designed by assigning a BPSK modulated PN sequence on the even subcarrier, and zeros on the odd subcarrier in the symbol. Taking the IFFT of this arrangement will results in two parts that are identical to each other. Fig. 2.2 shows the identical halves symbol of Schmidl and Cox. It also shows a cyclic prefix added to the two identical halves.

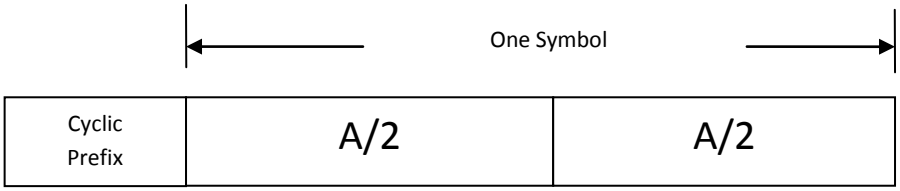

Fig. 2.2 Schmidl and Cox's Preamble

If L is the number of complex samples in one half of the symbol and d is the unknown arrival time, then the Schmidl and Cox timing metric, $M(d)$, algorithm can be defined as following:

$$M(d) = \frac{|P(d)|^2}{(R(d))^2} \tag{2.17}$$

where the identical halves correlation, $P(d)$, and the received energy of the second-half symbol to normalize the timing metric, $R(d)$, are defined as:

$$P(d) = \sum_{m=0}^{L-1} r^*(d+m) r(d+m+L) \tag{2.18}$$

$$R(d) = \sum_{m=0}^{L-1} |r(d+m+L)|^2 \tag{2.19}$$

When $M(d)$ reaches a peak it means that the autocorrelation of the preamble reach the whole part of the preamble. Fig. 2.3 presents the plot of Schmidl and Cox timing metric.

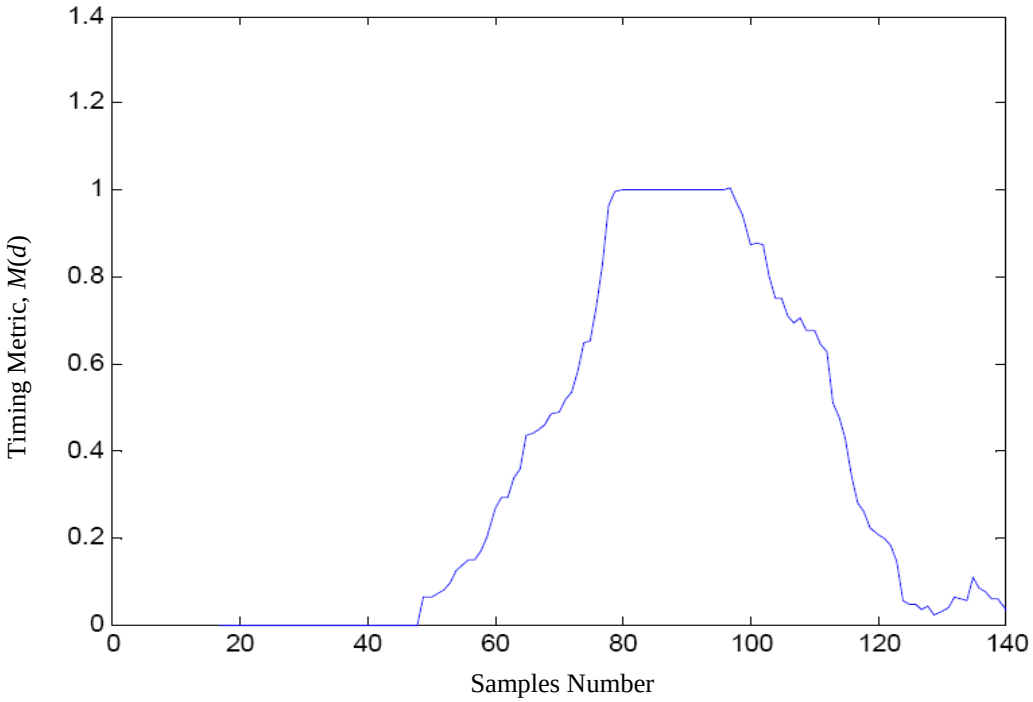

Fig. 2.3 Schmidl and Cox Timing Metric [15]

In time domain, if the conjugate of the sample from the first half is multiplied with the corresponding sample from the second half, at the start of the frame the product of these pair of samples will have approximately the same phase. Then the sum of the magnitude will be large.

The plateau of the Schmidl and Cox's timing metric peak is due to the presence of the cyclic prefix (CP) in the preamble. Since the CP is copy of the length of the last samples of the preamble, the plateau lasts according to the length of cyclic prefix. The timing metric starts to degrade when the samples do not correlate to each other anymore.

The peak of the auto-correlation is the sign of where the frame starts. But with the presence of noise , the start of the frame/symbol cannot be ascertained. In order to find the symbol timing, we can either:

- Find the maximum of the peak, or
- Locate a point to the left and another point to the right of the maximum peak, with each point having 90% of the maximum peak's magnitude. Then compute the average of the two points in the start of the frame.

This uncertainty is a drawback of the Schmidl and Cox algorithm.

2.3.2 Improvement by Minn and Barghava's time estimation method

To reduce the uncertainty of Schmidl and Cox algorithm, Minn and Barghava [6], designed a new preamble that has 4 identical quarters as can be seen in Fig. 2.4. The identical quarter are designed simply by taking the IFFT of the *N*/4 length of BPSK modulated PN sequence where *N* is the length of the symbol, copying and taking the negative value of it for the two other parts.

Fig. 2.4 Minn and Barghava Preamble

A new definition of the correlation which is applied to the preamble is written (*L* is length of *A*/4):

$$P_2(d) = \sum_{k=0}^{1} \sum_{m=0}^{L-1} r^*(d + 2Lk + m) r(d + 2LK + m + L) \tag{2.20}$$

Now the received energy is the correlation of the second positive-values with the negative-values of the preamble:

$$R_2(d) = \sum_{k=0}^{1} \sum_{m=0}^{L-1} r \mid d + 2LK + m + L \mid^2 \tag{2.21}$$

A plot in Fig. 2.5 presents Minn and Barghava's timing metric, $M_2(d)$, which is $|P_2(d)|^2$ normalized by $(R_2(d))^2$. It can be seen clearly that the plateau in Schmidl and Cox algorithm is much reduced.

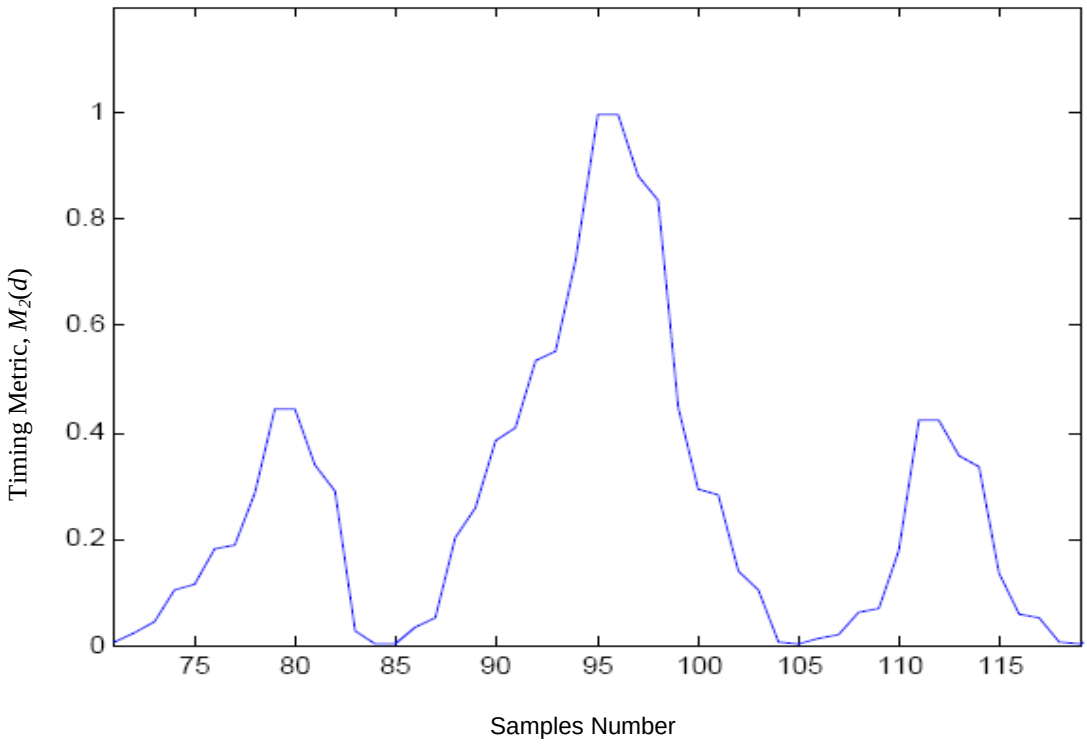

Fig.2.5 Minn and Barghava Timing Metric [15]

2.3.3 Improvement by Park et al.

The Park et al. algorithm [1] is another technique that also draws its inspiration from Schmidl and Cox's technique. Park et al. introduced another preamble that has conjugate symmetric parts. This new preamble came with a purpose to enlarge the difference between peak values of the timing metric with the other. To obtain a large difference between peak values, it is required to maximize the different pairs of product between them. The design of their preamble is presented in Fig. 2.6.

A/4	A/4*	A/4	A/4*

Fig. 2.6 Park et al. Preamble

The Park et al. preamble is also identical quarter but has a conjugate symmetric. The *A*/4 represents the IFFT of the BPSK modulated PN sequence with the length of *N*/4 and *A*/4* is the time-reversed conjugate symmetric of *A*/4. The new correlation and the received energy of the timing metric according to the designed preamble is:

$$P_3(d) = \sum_{k=0}^{N/2} r(d+k)r(d-k) \tag{2.22}$$

$$R_3(d) = \sum_{k=0}^{N/2} |\, r(d+k)\,|^2 \tag{2.23}$$

Fig. 2.7 presents Park et al.'s timing metric plot, $M_3(d)$, which is $|\, P_3(d)\,|^2$ normalized by $(R_2(d))^2$. There is a big difference between Schmidl-Cox's, Minn-Barghava's and Park et al.'s timing metric plots. The Park et al.'s conjugate symmetrical parts and the modified correlation produce an impulse-shaped timing metric thus allowing it to give more accurate symbol timing estimation.

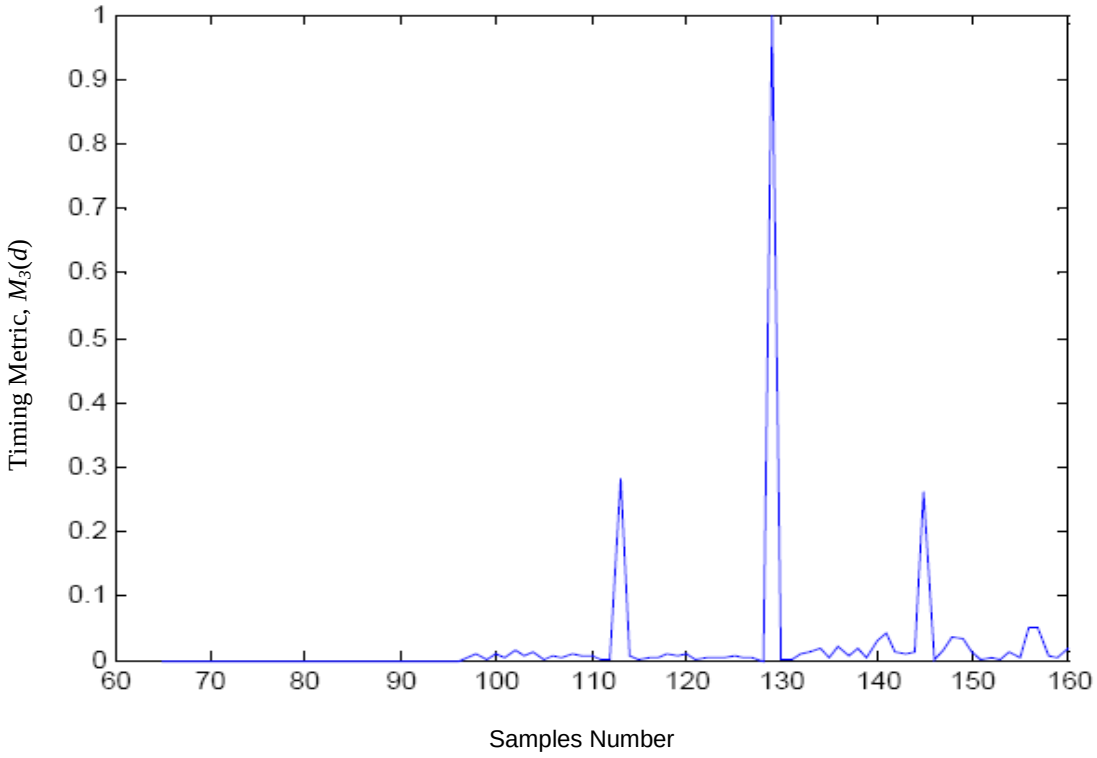

Fig. 2.7 Park et al. Timing Metric [15]

2.3.4 Other related works on time synchronization

Besides preamble based methods, a cyclic prefix based method is also very common in continuous OFDM system. Instead of padding preambles in front of the frame, a cyclic prefix is padded in front of every symbol [7]. This estimator has several

advantages: it has a high spectral efficiency by not using pilots; it is based on a relatively simple expression and hence it results in a reasonable implementation complexity; it can perform simultaneous time and frequency offset estimation. The main disadvantage of the estimator is that in presence of severe multipath its performance is reduced. Indeed, when multipath is present the range on which the signal is cyclic becomes smaller (going to zero when the channel is as long as the cyclic prefix) [16]. Another technique is to transform the preamble into cyclic prefix by assigning certain values to certain carriers [17]. The estimation uses a multidimensional generalization of Maximum Likelihood in [7].

2.4 Frequency Synchronization

2.4.1 Frequency error and effect

A frequency error is defined as the frequency difference between the oscillator at the transmitter and that at the receiver. Doppler shifts also contribute to the frequency difference especially in outdoor environment. This frequency mismatch is a big problem for a multicarrier system.

Multicarrier system such as OFDM divides its spectrum into many small subcarriers to obtain high efficiency spectrum. The subcarriers are overlapping to each other and staying orthogonal is the main idea for OFDM system. This orthogonality is a must in this system or otherwise a small offset in the subcarrier will cause one carrier to interfere with another carrier in the same OFDM symbol, called inter-carrier interference (ICI).

The frequency mismatch is usually different in different OFDM systems. In WiMAX system, the allowed frequency offset is up to 250 kHz at a channel bandwidth of 28MHz [18].

Frequency offsets are expressed often normalized to the subcarrier spacing. For example, the frequency offset mentioned above can be written as 2.28 offset normalized to the subcarrier spacing (with 256 subcarriers, the subcarrier spacing is 28 MHz/256 = 109.375 kHz. The normalized frequency offset, 2.28 calculated in Hertz (2.28 x 109.375 kHz) is equal to 250.23 kHz).This offset is then translated to

two parts namely the integer and fractional parts. In this case, the integer part which is an integer multiple of the subcarrier is 2 and the fractional part is 0.28.

Both the integer and fractional parts affect the OFDM system but in a different way. The integer offset causes common rotation of different subcarriers that will be still mutually orthogonal. The fractional, part on the other, hand causes ICI and attenuation in the transmitted signal.

Fig. 2.8 shows the ICI caused by the fractional frequency offset where one bin in one subcarrier interferes other bins in other subcarriers.

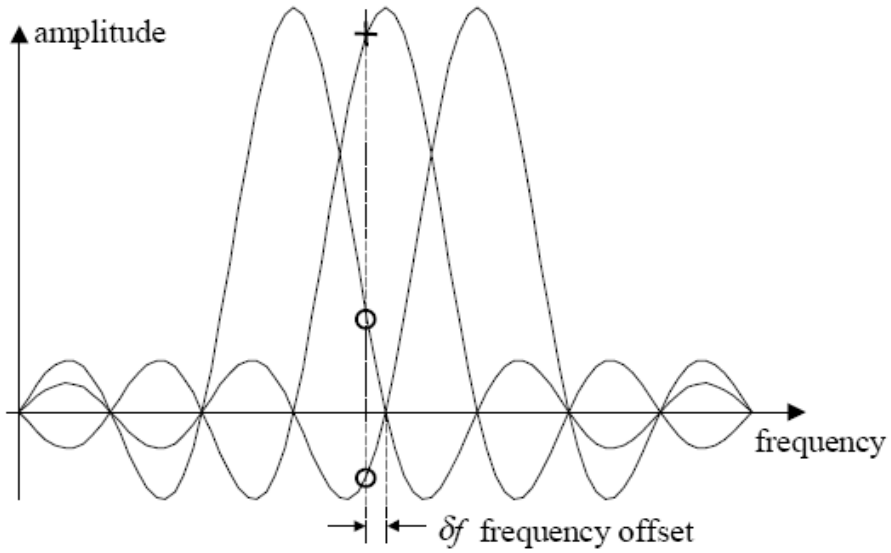

Fig. 2.8 Frequency Offset Effect [15]

2.4.2 Moose's frequency estimation

The first preamble-based frequency estimation algorithm was introduced by Moose [19] using the auto-correlation of the received signal in the frequency domain. In this algorithm, two repeated symbols are correlated to each other after FFT. Let R_1 be the FFT of the first symbol then the FFT of the second symbol is written as:

$$\boldsymbol{R}_{2,k} = \boldsymbol{R}_{1,k} e^{j2\pi\delta f(t/T)} \tag{2.24}$$

The subcarriers in the repeated symbols experience the same phase shift which is proportional to the amount of frequency offset. By exploiting the phase shift of the correlation, we can estimate the frequency offset directly [19]:

$$m = \sum_{k=-K}^{K} R_{1,k} R^{*}_{2,k} \tag{2.25}$$

$$\delta f' = \frac{-1}{2\pi} \angle m \tag{2.26}$$

Eq (2.26) can estimate only for the fractional part of the frequency offset.

2.4.3 Schmidl and Cox's frequency estimation

To estimate the frequency offset (fractional part), Schmidl and Cox in [5] utilize one symbol that has identical halves. This is the same symbol used in the timing synchronization. The samples of the identical halves in the symbol are correlated to each other and their main difference is the phase difference ϕ. The phase difference can be estimated ($\hat{\phi}$) from the phase angle of the identical halves correlation $(P(d))$. Equation (2.27) shows the estimation of fractional frequency offset.

$$\phi = \pi T \Delta f \tag{2.27}$$

$$\hat{\phi} = \angle P(d) \tag{2.28}$$

$$\hat{\Delta f} = \hat{\phi}/(\pi T) \tag{2.29}$$

The first estimation of Schmidl & Cox can estimate frequency offset up to half subcarrier spacing. Thus Schmidl & Cox's technique is quite similar with Moose's technique except that the Schmidl & Cox's estimation is in the time domain.

When the frequency offset is more than half subcarrier spacing then it needs to estimate the integer part too. Before estimating the integer part, the OFDM received signal needs to be corrected by the fractional part estimation $\hat{\Delta f}$, by simply multiplying the received signal samples with $e^{-j2\pi \hat{\Delta f}(i/N)}$, where Δf is the fractional part.

To estimate the integer offset, $\hat{z}$, a second symbol is designed such that the first and the second symbol are differentially modulated (on the even subcarriers, *k*), which means, $v_k = r_{2,k} / r_{1,k} = \{\pm 1, \pm j\}$. Both $r_{2,k}, r_{1,k}$ are the symbol 1 and symbol 2 in

frequency domain. The cross-correlation then is performed over frequency domain received symbols, $x_{1,k}, x_{2,k}$ and v_k :

$$\hat{z} = \max_{z} \frac{|\sum_{k} x^{*}_{1,k+2z} v^{*}_{k} x_{2,k+2z}|^2}{2\left(\sum_{k} |x_{2,k}|^2\right)^2} \tag{2.30}$$

2.4.4 Other related works on frequency synchronization

The frequency offset can also be estimated using the cyclic prefix once the time offset is estimated [7]. The frequency offset is estimated from the phase angle of the correlation between cyclic prefix with its corresponding part in the symbol.It is simpler but less robust compared to the auto-correlation preamble- based technique and can only estimate less than half subcarrier spacing of frequency offset.

The preamble turned into cyclic prefix based is also used to estimate the frequency offset just as the cyclic prefix based [17]. In this method, the length of preamble is made shorter into the length of cyclic prefix and is padded to the data symbol. The length of the data symbol is also made shorter so that the length of the symbol plus the preamble is equal to FFT length. The estimation technique in cyclic prefix is also applied in this method. The performance of this method depends on the number of preambles used in the correlation. To achieve the same performance of cyclic prefix based, this method requires at least 2 preambles in the correlation.

2.5 Channel Estimation

Channel estimation is the task to estimate the attenuation factor caused by the wireless channel. Channel estimation literatures show that the task commonly being performed in the frequency domain. This is due to the requirement of the synchronization accomplishment first before channel estimation.

In the section 2.5.1, some of the techniques to estimate the channel are presented. The techniques are divided into two major approaches, the frequency domain approach and the time domain approach.

The Eq. (2.15) shows that, in order to obtain the transmitted signal constellation points, the received signal must rid itself of the complex-valued attenuation factor from the channel regardless of noise presence. In order to do that, the attenuation factor from the channel needs to be estimated. Once estimated, equalization is performed to remove the attenuation factor from the received signal. After equalization, the signal is ready for demodulation.

2.5.1 Frequency domain channel estimation

In a burst transmission system, such as WLAN, the packet length is short enough to assume that the channel is constant during the length of the packet. Besides that, scattered pilots in the symbol causes delay of several symbols before the first channel estimates can be calculated [8]. In this case, the known data is transmitted in even subcarriers or odd subcarriers only, such that an interpolation technique needs to be performed to estimate the channel frequency response among the zeros subcarriers [8]. Hence, the simple way to estimate channel in packet transmission is to use a predesigned preamble. The preamble can consist of several symbols. The symbols in the preamble have known data values to the receiver. The existing techniques to estimate the channel in OFDM system usually done in the frequency domain like in [8] and [9] while in [10] it is converted back to time domain back and forth.

Other channel estimation in frequency domain is by Wiener Filtering or the Minimum Mean Square Estimator (MMSE) [11,12]. This method require a great computational complexity since, it needs to estimate an autocorrelation matrix and cross-correlation vector at the receiver [14].

2.5.2 Time domain channel estimation

Guoping etal. [20] presented a time domain channel estimation where the estimation is performed before FFT and then the estimation of the channel send to the FFT to obtain the frequency response. Fig. 2.9 shows the receiver scheme based on the time

domain channel estimation. After obtaining the frequency response, equalization and demodulation are performed to remove.

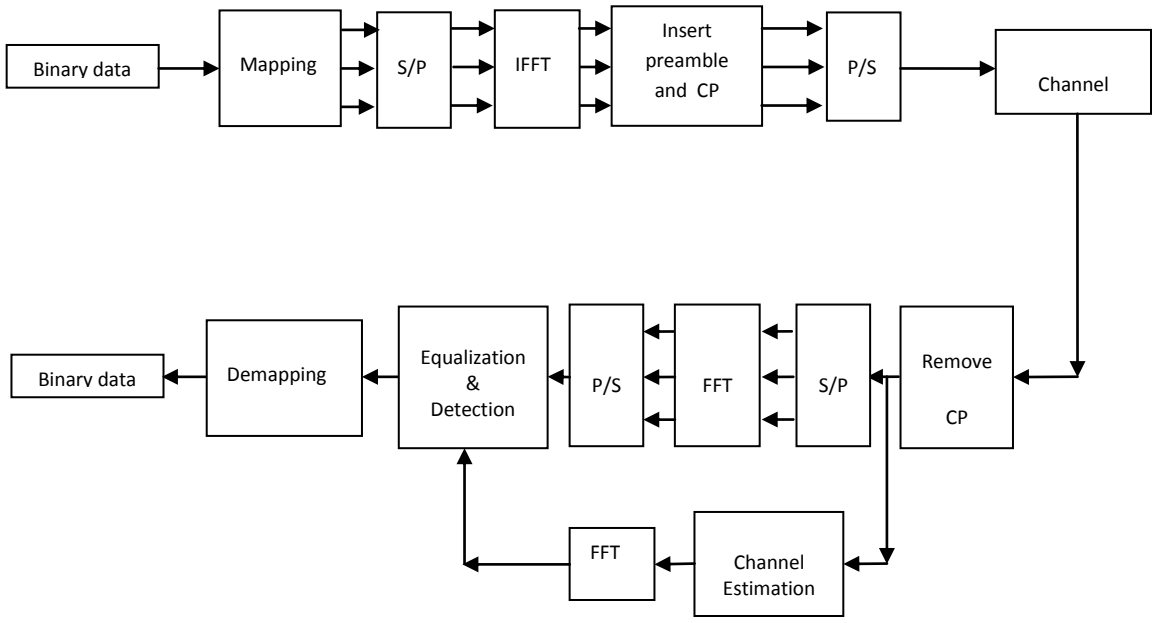

Fig. 2.9 OFDM system based on time-domain channel estimation [20]

The main idea of this work is to obtain the channel impulse response. Since the transmitted signal reaches the receiver through multiple paths, the result is that the received signal contains the multiple transmitted signals with different delays and amplitudes. When the received signal is correlated with its copy stored in the receiver, the multiple signals with its own delay and amplitude will appear as impulses. Each impulse has different samples away from the main impulse correlation according to its delay. Each impulse also has different amplitude appearing in the correlation according to its attenuation from the channel. These impulses are the channel impulse responses. Hence by capturing these impulses the channel is estimated.

Examining Guoping's receiver scheme in Fig. 2.9, it is seen that the receiver assumes perfect synchronization. In fact, to estimate the channel impulse response by performing cross-correlation, perfect synchronization is required. Otherwise, correlation gives clutter-like sidelobes instead of the desired impulse responses. It is also noticed that in Guoping's work the preamble is derived from m-sequence. The multiple m-sequence is received and is correlated with its copy stored in the receiver.

2.6 Generalized Chirp Like Sequence

Some polyphase sequences with interesting properties are also used in many communication applications. A polyphase sequence is a complex sequence whose elements can be represented as a complex root of unity i.e. $a_n = \exp(j\frac{2\pi x_n}{q})$ [21]. Frank and Zadoff [22] introduced a periodic sequence that has zero autocorrelation except for the period-multiple-shift terms. Zadoff-Chu [23] introduced another complex sequence that has an ideal periodic autocorrelation function. Both Frank-Zadoff [22] and Zadoff-Chu [23] sequences are known as CAZAC sequence with following properties:

1. Constant Amplitude (CA) where the magnitude of each element of the sequence is equal and constant.
2. Zero autocorrelation (ZAC) where the correlation is zero for all values except at $t = 0$.

Zadoff-Chu's sequence belongs to the class of so-called modulatable orthogonal sequences. Modulatable sequence is a complex sequence with ideal autocorrelation function [24]. They can be modulated by a string of complex numbers of unit magnitude retaining the ideal periodic autocorrelation function (all zero autocorrelation side lobe) and the optimal cross-correlation function (maximum cross-correlation magnitude is equal to $\sqrt{(N)}$ with N being the length sequence) .

Generalized Chirp Like (GCL) sequence is derived from Zadoff-Chu sequence [25]:

$$a_k = \exp\left(-j2\pi u\frac{k(k+1)+qk}{2N_G}\right) \tag{2.31}$$

k = 012...N_G-1 q is any integer

u = 1….. N_G-1 is the class index

Let $\{a_k\}, k = 0,1,2,...N-1$ be a Zadoff-Chu sequence of length $N_G = sm^2$ where s and m are also any integer. Additionally, let $\{b_k\}$ be any unique complex numbers with absolute value of 1 (i.e. all b_ks are on the complex unit circle).

Then GCL sequence $\{s_k\}$ can be written as:

$$S_k = a_k b_{(k) \bmod(m)} \tag{2.32}$$

where the index *k* is a reduced modulo *m.*

GCL sequence has the following properties [26]:

1. GCL sequence has constant amplitude and its N_G-point FFT has also a constant amplitude.
2. GCL sequence of any length has 'ideal' autocorrelation.
3. The absolute value of the cyclic cross-correlation between any two GCL sequences is constant and equal to $1/\sqrt{N_G}$.

GCL sequence, being one type of the CAZAC sequence, is optimal in terms of cross-correlation. In other words, GCL sequence is the best sequence among all CAZAC [27].

2.6.1 GCL sequence and its many applications

GCL sequence has been used in many communication applications because of its good correlation property. A comparison between three different families of spreading sequences for an all-digital direct sequence spread spectrum code division multiple access (DSSS CDMA) modem is presented in [28]. The families considered are binary Gold and Kasami and polyphase generalised chirp-like (GCL) sequences. GCL sequence is used to design Random Access Channel (RACH) for the Evolved Universal Radio Access (E-UTRA) with the major goal to minimize the latency procedure of RACH [29]. The cross-correlation property of this sequence is also used by Naoki Suehiro for co-channel interference Spread Spectrum Multiple Access (SSMA) systems [24]. SSMA systems that use this sequence are more stable than the conventional SSMA systems that utilized another kind of sequence.

2.6.2 GCL sequence application in OFDM system

Besides CDMA and SSMA system, we also found that GCL sequence is applied in the OFDM system as shown in the following literatures:

GCL sequence is used to improve the ranging performance of the OFDM PHY layer in [25] and in the OFDMA PHY layer using modified GCL sequence [30]. It has also been used to improve the performance of the Fast Cell Search in [27]. MIMO channel estimation is evaluated by using GCL sequence-based preamble [10]. Li [9] introduced Semi-Blind channel estimation using superimposed training sequence by adding GCL sequence to the data in frequency domain.

2.7 Observation

The synchronization and channel estimation literature studies have been presented in the sections 2.3.1 to 2.5.3. The synchronization and channel estimation works are basically preamble based which exploit the correlation of the preamble both in time and frequency domains. From the synchronization literatures, it is observed that GCL sequence has never been used as a preamble.

Observation from channel estimation literatures tells that the existing work [20], which is time domain channel estimation, assumes perfect frequency synchronization. However, no practical receiver structure carries out complete frequency offset correction in time domain. Hence, there is a need to perform even the integer-frequency offset correction in time domain so the method of [20] or other better methods can be used to estimate the channel in time domain.

2.8 Summary

In this chapter, the design issues of an OFDM receiver are introduced and literature reviews of the preamble based methods to synchronize the time and frequency offsets are explained. From the literature it is known that Schmidl and Cox's technique [5] is a well-known technique for preamble-based synchronization. While Schmidl and Cox method has an uncertainty in the timing synchronization, Park et al. [1] method, which is an improvement from the Schmidl and Cox method, gives more accurate result. Schmidl and Cox's method also estimates the frequency offset and is best known for its ability to estimate the integer part as compared to other technique.

Channel estimation can be performed either in the frequency domain or in time domain. Guoping's time domain channel estimation method [20] estimates the channel impulse response with the assumption that the system is perfectly synchronized (time and frequency).

Since the synchronization and channel estimation literatures are mainly preamble based methods, this chapter also introduced a polyphase sequence that can also be used as a preamble. GCL sequence is introduced together with its application in some of the communication systems.

Next chapter will present the design of the preamble, the application of the preamble in the synchronization tasks, the methodology of evaluating the performance of the proposed preamble, the results and the analysis thereof.

CHAPTER 3

DESIGN OF GCL BASED PREAMBLE, NEW RECEIVER SCHEME AND THE METHODOLOGY

As mentioned before, there are two problems that have been addressed in this thesis. The first problem is the design of a new synchronization preamble to be used with conventional packet-based OFDM system, and the second problem is the problem of a new receiver design that seeks to estimate and correct the frequency offset before FFT.

In this chapter, first we make a comprehensive presentation on the design of GCL based preamble for synchronization purposes and demonstrate its benefit in conventional OFDM systems, and then we present our work on the design of a new OFDM receiver as comprehensively as possible.

This chapter begins by stating the technical objective, the motivation behind it and as to how the advantages arising from using it will be measured. In the end, it presents the methodology for the time synchronization, integer frequency synchronization, time domain frequency offset correction and lastly the methodology for the time domain channel estimation.

3.1 The Technical Objective

The objective of contained in this chapter is

- to design GCL sequence based preamble and

- to evaluate the performance the proposed preamble in the time and integer frequency synchronization in conventional OFDM system.
- To design and develop a new method to estimate and correct integer-frequency offset in time domain and evaluate its performance.
- To carry out time-domain channel estimation after integer frequency offset correction
- To evaluate the performance of the time domain channel estimation using a PN sequence based preamble as well as a GCL sequence based preamble.

As mentioned in Chapter 2, the GCL sequence has some interesting properties. Its auto-correlation like a delta function, so does the auto-correlation of its Fourier transform (or, for that matter, its inverse Fourier transform). The preamble based synchronization, used in packet based OFDM system, uses the sharpness of these auto-correlation peaks to accurately locate the start of the symbol and also, in frequency domain, estimate the integer frequency offsets. Hitherto PN sequences served this purpose very well. However, GCL sequences too have very good auto-correlation shapes and can easily serve that purpose. Furthermore, the GCL sequence based preambles have lower PAPR than PN sequence based preamble leading to better SNR at receiver or alternatively, longer range for the same transmitted power. The motivation to design the GCL based preamble and use it in the conventional OFDM systems comes from their afore-mentioned useful properties. In the subsequent subsection, these properties of GCL sequence will be investigated in more detail.

3.2 Comparison of PN Sequence and GCL Sequence

Sequences have been used in communication systems for many purposes [21]. A very common sequence that has been used quite often is a binary sequence called Pseudo Noise (PN) sequence. This sequence is a simple sequence and it is easy to implement in the hardware. Communication systems such as OFDM system and even CDMA system use this sequence for synchronization.

PN sequence is a sequence of binary numbers (0,1) where the occurrence of "1" or "0" in the sequence has equal probability.

PN sequence is generate by shift-register and is given by the polynomial:

$$p(z) = p_n z^{n-1} + p_{n-2} z^{n-2} + \ldots\ldots\ldots\ldots + p_0 \tag{3.1}$$

where n is the length of the sequence , p's are the feedback coefficient of the shift-register and z's are the shift-registers.

For example, if we generate a common PN sequence of length 200 and obtain its autocorrelation, the result could typically be as in Fig. 3.1. From the figure, it can be seen that the autocorrelation of a PN sequence, produces an impulse like peak at the zero lag and low sidelobes at all other lags.

$$Rpp(l) = \sum_{z=1}^{200} p^*(z)\, p(z+l) \tag{3.2}$$

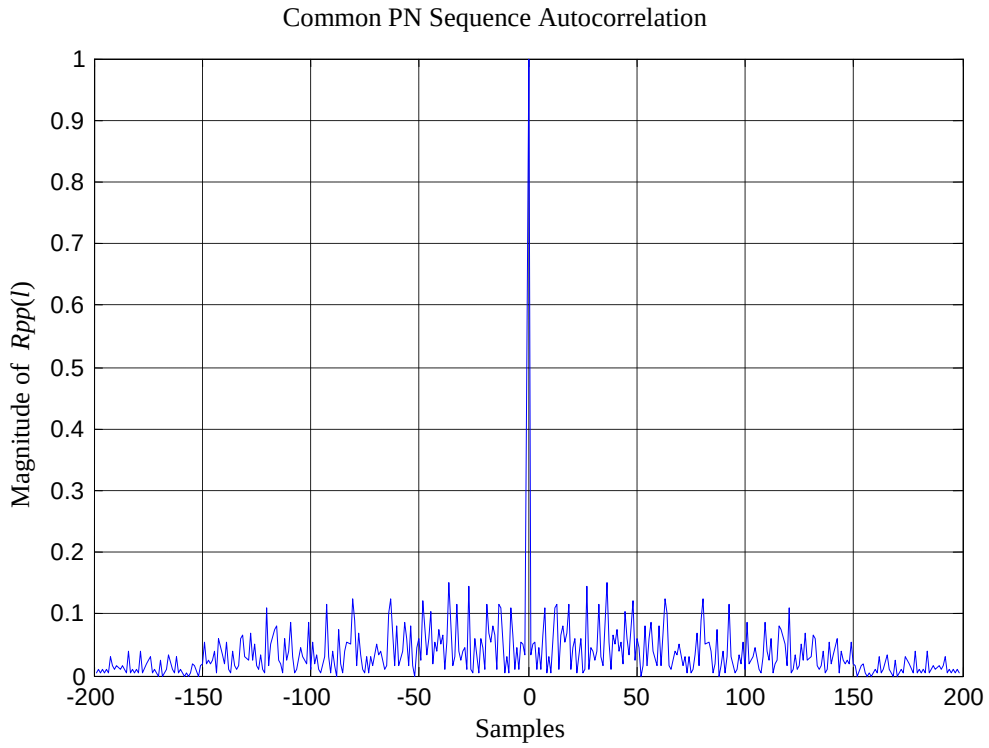

Fig. 3.1 Common PN Sequence Autocorrelation

Besides this binary PN sequence, there also exists a complex valued sequence called GCL sequence that has been used for various applications in communication systems.

As has been explained in the previous chapter, a GCL sequence can be generated by using the expression as shown below:

$$g_k = \exp\left(-j2\pi u \frac{k(k+1)+qk}{2N_G}\right) \tag{3.3}$$

$k = 0,1,2,...N_G\text{-}1$, q is any integer

$u = 1,..... N_G\text{-}1$, is the class index

N_G is the length of the sequence

For comparison with the common PN sequence, we also generate GCL sequence with the same length and produce its autocorrelation. Fig. 3.2 shows the autocorrelation of GCL sequence, $Rgg(l)$.

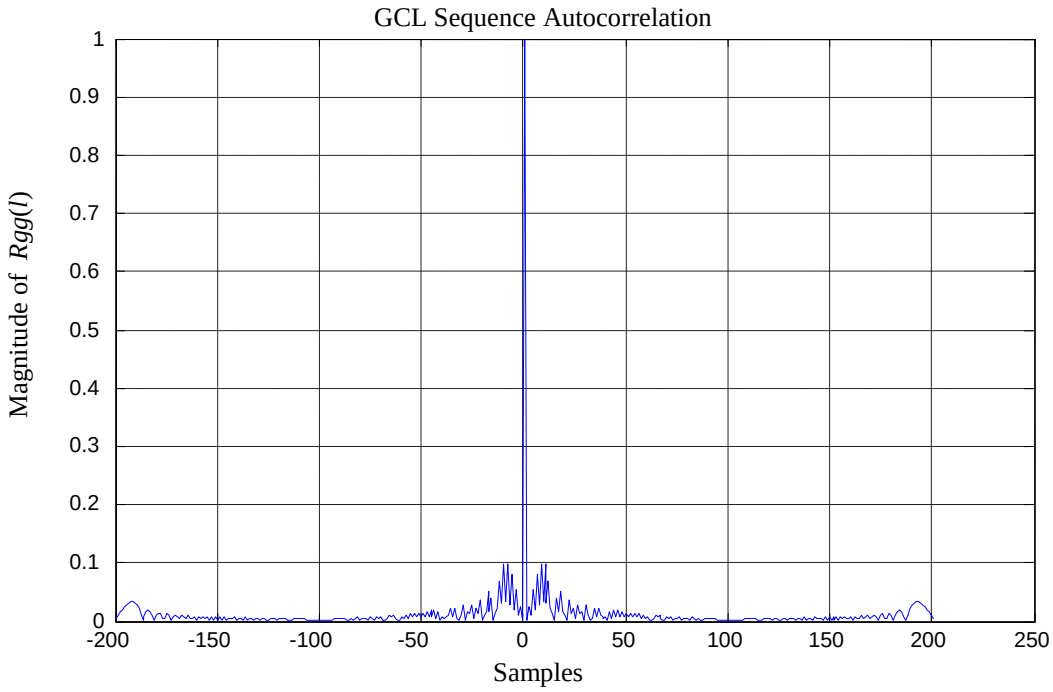

Fig. 3.2 GCL Sequence Autocorrelation

From the figure, it can be seen that GCL sequence also produces an impulse like peak at zero lag and substantially lower sidelobes at the remaining lags.

From both Fig. 3.1 and Fig. 3.2, it can be seen that GCL sequence has a better correlation property compared to that of the common PN sequence. The autocorrelation of sequence is suitably used in synchronization in the communication systems, particularly in OFDM systems, where the peak of the correlation is used to estimate the start of the symbol.

Since the autocorrelation property of GCL sequence is good to be used as preamble, we further investigate the GCL sequence based preamble in a typical OFDM based IEEE 802.16a system. We use the OFDM system based on the standard IEEE 802.16a, because the standard, that covers wireless metropolitan area network (W-MAN) and protected by the industry consortium called WiMAX, is one of the popular OFDM system example and readily available.

IEEE 802.16a standard is also useful to evaluate the performance of the proposed GCL based preamble as it provides a specific PN sequence based QPSK modulated preamble to be used for the purpose of synchronization that can be used for comparing the performance.

3.3. Design of the Preambles

PN sequence based preamble used in this thesis is obtained from the IEEE 802.16 Standard which is in a QPSK modulated form [18]. Basically, the PN sequence-based preamble is chosen from the IEEE 802.16 because the standard is one of the OFDM system standards, the most favorite wireless communication technology in these recent years as many countries try to apply it to provide excellent connectivity. Table 3.1 presents the QPSK modulated PN sequence taken from the IEEE 802.16 Standard [18].

Table 3.1 IEEE 802.16 Standard Preamble

Subcarrier	Complex Symbol									
-100:-91	1-j	1-j	-1-j	1+j	1-j	1-j	-1+j	1-j	1-j	1-j
-90:-81	1+j	-1-j	1+j	1+j	-1-j	1+j	-1-j	-1-j	1-j	-1+j
-80:-71	1-j	1-j	-1-j	1+j	1-j	1-j	-1+j	1-j	1-j	1-j
-70:-61	1+j	-1-j	1+j	1+j	-1-j	1+j	-1-j	-1-j	1-j	-1+j
-60:-51	1-j	1-j	-1-j	1+j	1-j	1-j	-1+j	1-j	1-j	1-j
-50:-41	1+j	-1-j	1+j	1+j	-1-j	1+j	-1-j	-1-j	1-j	-1+j
-40:-31	1+j	1+j	1-j	-1+j	1+j	1+j	-1-j	1+j	1+j	1+j
-30:-21	-1+j	1-j	-1+j	-1+j	1-j	-1+j	1-j	1-j	1+j	-1-j
-20:-11	-1+j	1-j	-1+j	-1+j	1-j	-1+j	1-j	1-j	1+j	-1-j
-10:-1	1-j	-1+j	1-j	1-j	-1+j	1-j	-1+j	-1+j	-1-j	1+j
0	0									
1:10	-1-j	1+j	-1+j	-1+j	-1-j	1+j	1+j	1+j	-1-j	1+j
11:20	1-j	1-j	1-j	-1+j	-1+j	-1+j	-1+j	1-j	-1-j	-1-j

21:30	-1+j	1-j	1+j	1+j	-1+j	1-j	1-j	1-j	-1+j	1-j
31:40	-1-j	-1-j	-1-j	1+j	1+j	1+j	1+j	-1-j	-1+j	-1+j
41:50	1+j	-1-j	1-j	1-j	1+j	-1-j	-1-j	-1-j	1+j	-1-j
51:60	1+j	-1-j	1-j	1-j	1+j	-1-j	-1-j	-1-j	1+j	-1-j
61:70	-1+j	-1+j	-1+j	1-j	1-j	1-j	1-j	-1+j	1+j	1+j
71:80	-1-j	1+j	-1+j	-1+j	-1-j	1+j	1+j	1+j	-1-j	1+j
81:90	1-j	1-j	1-j	-1+j	-1+j	-1+j	-1+j	1-j	-1-j	-1-j
91:100	1-j	-1+j	-1-j	-1-j	1-j	-1+j	-1+j	-1+j	1-j	-1+j

Since the preamble is used for the synchronization purposes, the preamble is designed to have identical halves property with the length of 256 samples as suggested by Scmidl & Cox [5]. The arrangements are as follows:

- First, the 200 samples sequence is alternated with zeros. The zeros are placed in the even subcarriers and the odd subcarriers are occupied with the sequence (in this case is the QPSK modulated PN sequence). Together with the DC offset, this arrangement will make up to 201 samples.
- Additional zeros are padded to both ends of the alternate sequence; 28 samples are positioned in the front end and 27 samples are put in the back end. These additional zeros act as the guard bands. DC offset is right at the middle of the preamble (as shown in the table).

The same approach is applied to the GCL sequence-based preamble. A length of alternate 200 GCL sequence and zeros, padded up with zeros at both ends form the GCL sequence-based preamble. To obtain the time domain preamble, the 256 samples preamble is passed through the IFFT.

Similarly for Park's method, the preamble is obtained the same way as in the Schmidl and Cox's preamble.

Section 3.31 and 3.3.2 resent the autocorrelation property of both sequences in frequency domain and in time domain.

3.3.1 Frequency domain autocorrelation

The transmitted and received signals are in time domain. Hence, in an OFDM system, the transmitted signal is obtained after an IFFT. The frequency domain correlation, as

a matter of fact, is needed to perform frequency synchronization task in OFDM receiver. Fig. 3.3 and Fig. 3.4 depict the autocorrelation of the standard PN sequence based preamble from Table 3.1, $R_{PNPNFD}(l)$ and GCL sequence, $R_{GG\,FD}(l)$ in the frequency domain without alternate zeros.

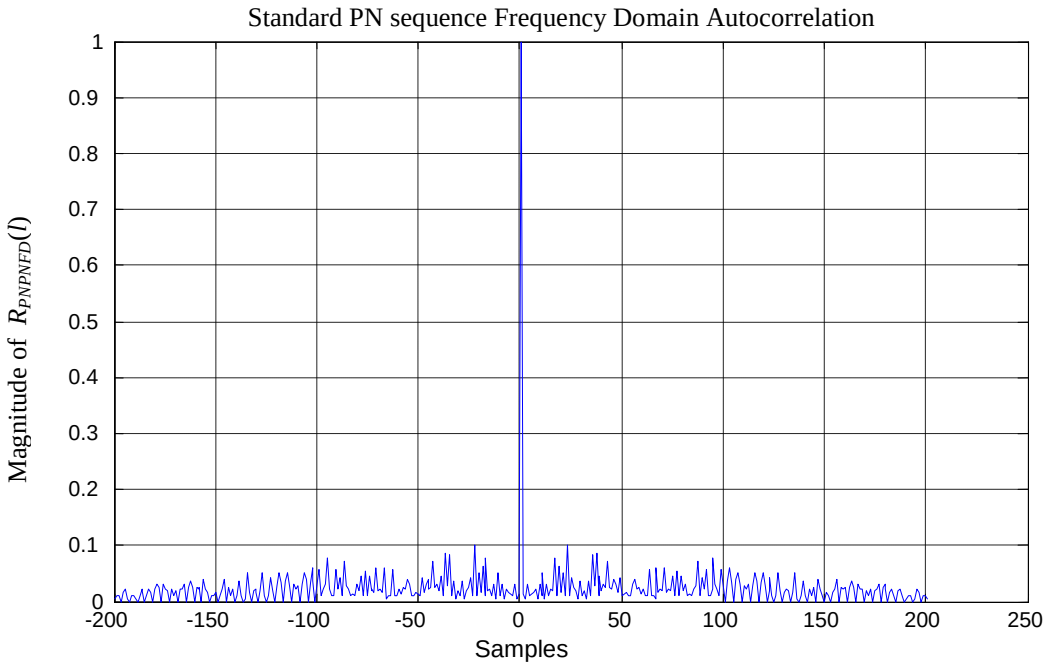

Fig. 3.3 PN sequence Autocorrelation in Frequency Domain

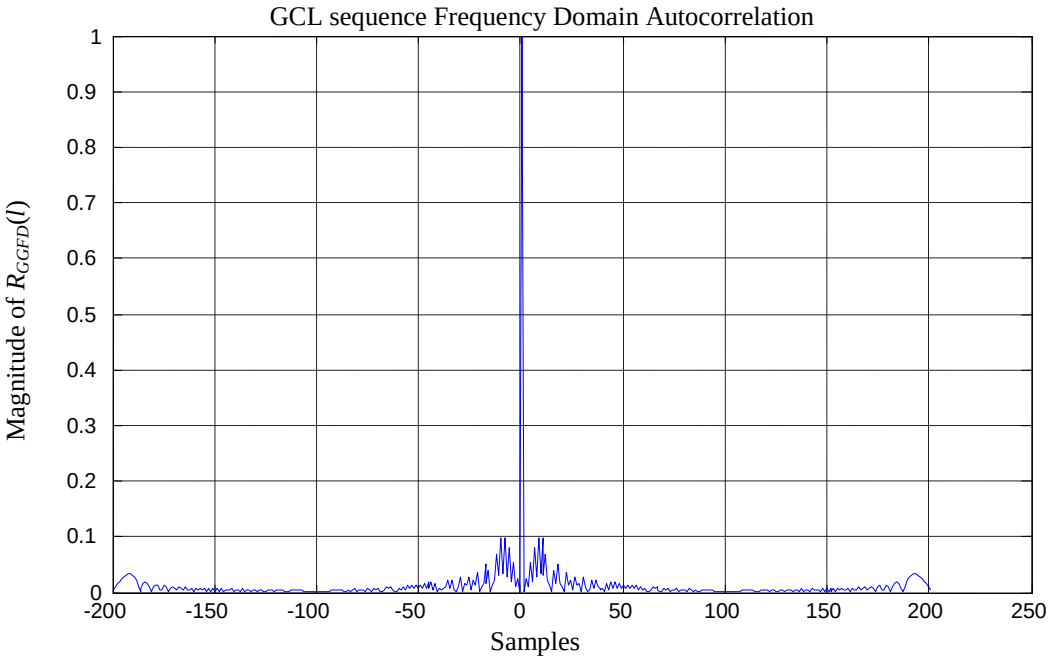

Fig. 3.4 GCL sequence Autocorrelation in Frequency Domain

As can be seen from the two figures, the autocorrelations of the PN and GCL sequences show the characteristics of the sequences in the frequency domain. In Fig. 3.3, the autocorrelation of the PN sequence with a length of 200 samples has more energy in its sidelobes as compared to that of the GCL sequence based preamble in Fig. 3.4. The autocorrelation of the GCL sequence only has some energy in its sidelobes near the main peak of the correlation while the rest are very low sidelobes. On the other hand, the PN sequence autocorrelation produces sizeable sidelobes for the rest of the correlation samples.

This frequency domain correlation is further used particularly for the integer frequency offset estimation. The integer offset estimation, carried out post FFT in the OFDM receiver, uses the correlation peak of the frequency domain correlation to determine how far the frequency has shifted from its original position.

3.3.2 Time domain autocorrelation

The time domain sequence is as important as the frequency domain sequence especially in OFDM receiver applications. The time domain sequence is generated by taking the inverse fast Fourier transform (IFFT) of the frequency domain sequence. In order to obtain time domain sequences, both 200 sample long frequency domain sequences are padded with zeros on both sides such that the overall length of the individual sequence becomes 256 to satisfy the FFT point requirements. The autocorrelation of this time sequence is used to determine the start of the OFDM symbol. Therefore, it is also necessary to see the autocorrelation of the sequence in time domain. Fig. 3.5 and Fig.3.6 present the autocorrelations of the PN, $R_{PNPNTD}(l)$, and GCL sequences, $R_{PNPNTD}(l)$, in the time domain. It can be seen from Fig. 3.6 that the normalized autocorrelation of GCL based preamble has much smaller sidelobes than those in Fig. 3.5 as they are on PN sequence based preamble.

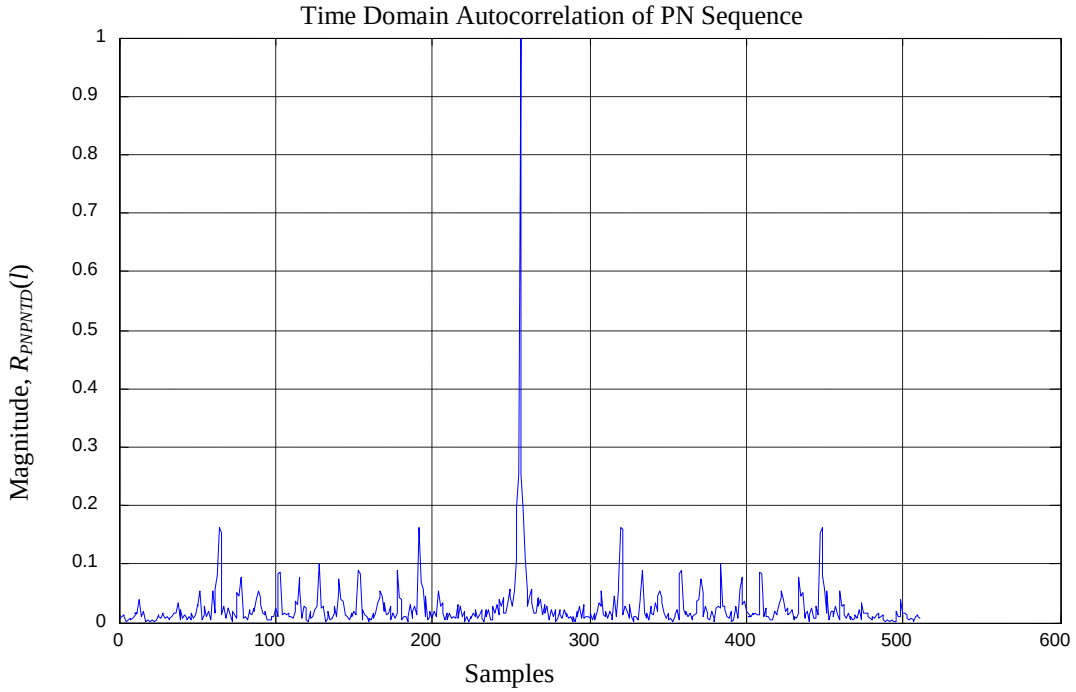

Fig. 3.5 Time Domain Autocorrelation of Standard PN sequence

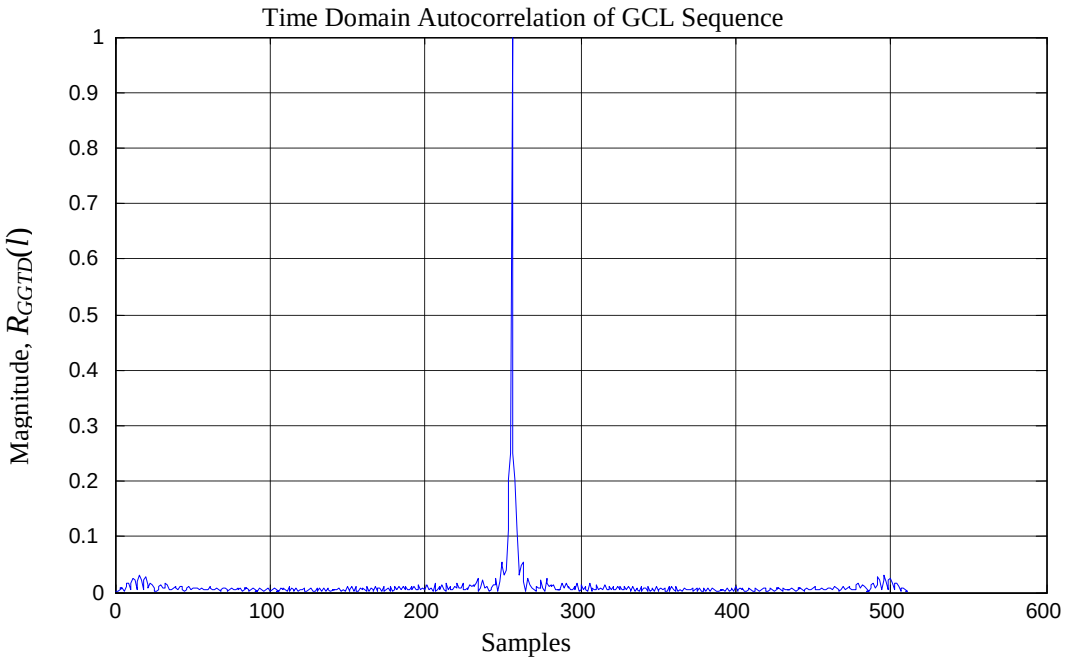

Fig. 3.6 Time Domain Autocorrelation of GCL sequence

Furthermore, by comparing Fig. 3.3 and Fig. 3.5, it can be seen that the time domain autocorrelation of the PN sequence has higher sidelobes compared to its frequency domain autocorrelation. On the other hand, Fig. 3.4 and Fig. 3.6 show that the GCL

sequence maintains the autocorrelation sidelobes in both domains even though it has slightly better sidelobes in the time domain. Noticing the autocorrelation behavior of both sequences in different domains, it can be said that IFFT changes the property of the autocorrelation of the PN sequence in time domain while the GCL sequence is able to maintain its correlation property through IFFT.

Although the correlation of GCL sequence in frequency domain and time domain seems similar, but we also calculate their peak to sidelobe ratio as the characteristic of their domain correlation. From our calculation, it is known that the frequency domain correlation of GCL sequence has ratio of 10 and the time domain correlation has ratio of 4. This means that the frequency domain has much lower sidelobe magnitude compared to that of the time domain correlation. Therefore, it is an advantage to utilize the frequency domain correlation in a certain task which based on frequency domain correlation.

This time domain correlation will be further used particularly for the timing offset estimation. The timing offset estimation uses the correlation peak of the time domain correlation to determine the start of the symbol.

3.3.3 Time domain waveform

The autocorrelation of the individual sequence (PN or GCL) in the time domain is basically the autocorrelation of its pertinent time domain waveform shown in the Fig. 3.7 and Fig. 3.8, respectively. As can be seen from the two figures, the PN sequence time domain waveform and the GCL sequence time domain waveform are different. The PN sequence time domain waveform appears to be random while the GCL sequence time domain waveform appears clearly with its two identical halves.

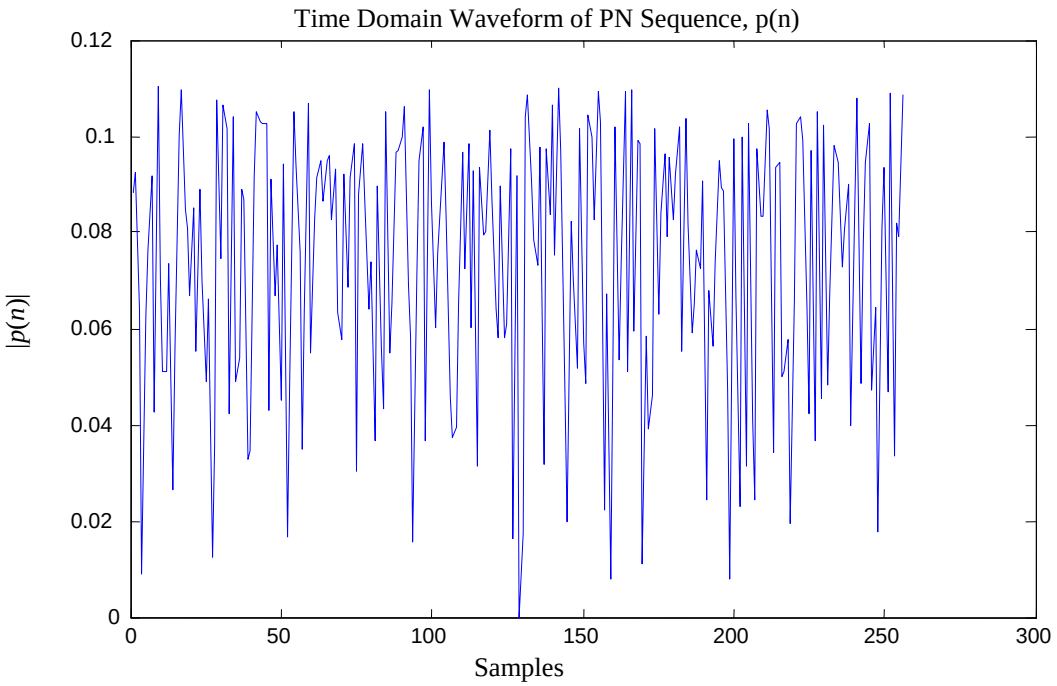

Fig.3.7 PN Preamble Time Domain Waveform

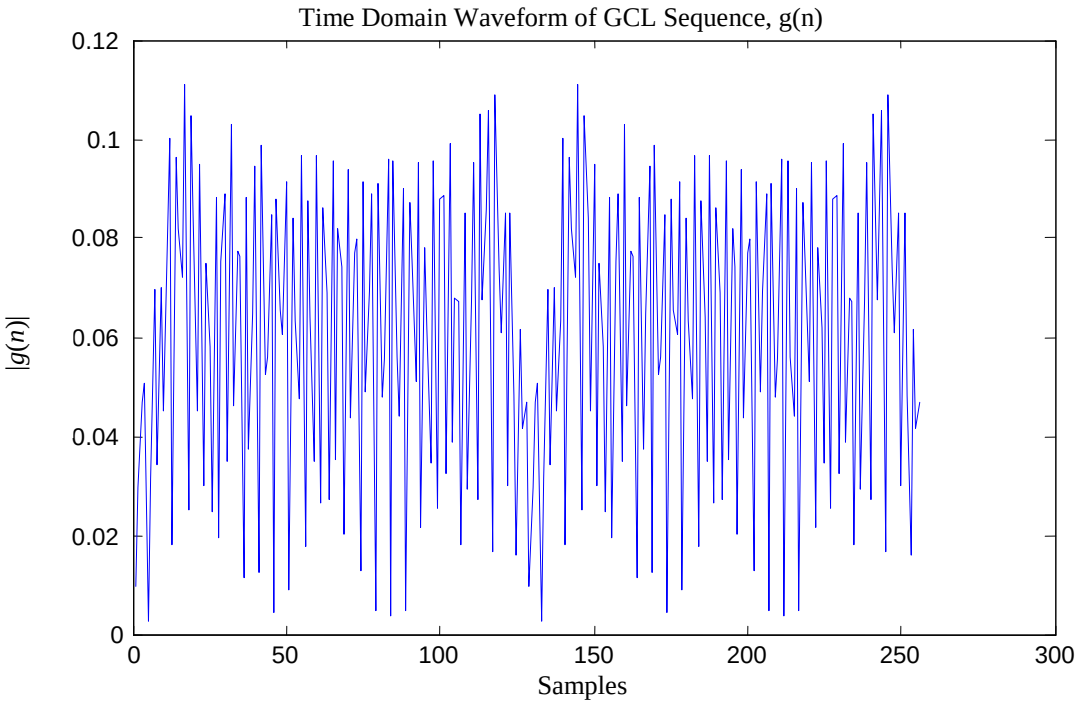

Fig.3.8 GCL Preamble Time Domain Waveform

By using the time domain waveform, some comments on PAPR can also easily be made. For the same peaks, the average of the waveform appears more in GCL based waveform. It is further verified by calculating the PAPR of the two waveforms. The

standard PN preamble has PAPR of 3 dB and the proposed GCL preamble has PAPR of 1.802 dB. The proposed GCL preamble has almost 1.2 dB PAPR advantage as compared to the standard PN preamble. This advantage translates to 1.2 dB SNR advantage or alternatively, this advantage extends the 10 km range to 11.5 km assuming free space propagation.

3.4 New Receiver Scheme

In Guoping et. al.'s work [20], a time-domain channel estimation is presented which estimates the channel in the time domain. This time domain channel estimation, however, assumes that the frequency offsets are not present. While the basic technique in estimating the channel in the time domain is to cross-correlate the received signal with the local copy of the preamble, the cross-correlation itself requires the received signal to be free from any frequency offset otherwise it cannot give the expected result. In conventional receivers, however, the integer frequency offsets are estimated post FFT. Our literature review shows that the integer frequency offsets have never been estimated in time domain before FFT without which the time-domain channel estimation is not feasible. Hence, the design of the new proposed receiver is motivated by this need to correct the frequency offset in the time domain so time domain channel estimation can be carried out accurately.

There are other advantages of doing time domain channel estimation. The knowledge of channel before FFT allows the signal power and hence the noise power to be evaluated up front. The channel and SNR thus estimated up front can be quickly shared with transmitters which can use them for adaptive power control on subcarriers or adaptive modulation etc [13]. At receiver itself, this can be used for receiver diversity techniques to further improve the received SNR.

In addition to accurately estimating and correcting integer frequency offsets, we also evaluate the performance of time domain channel estimation. To do so, we, once again, make use of both PN sequence and GCL sequence based preambles.

The new receiver design is motivated by the need to carry out integer frequency offset correction before implementing a time domain channel estimation based receiver. Unlike conventional receiver, it synchronizes the received frames, corrects their

frequency offsets, both fractional and integer, and estimates the channel all in time domain. The FFT is performed only for channel equalization and demodulation.

3.4.1 Presence of frequency offset and its impact

As mentioned earlier, in time domain channel estimation, the presence of frequency offsets destroys the cross-correlation between the received preamble and the local copy. The frequency offset affects the cross-correlation in such a way that not only the peak correlation gets shifted but also high unwanted clutter-like sidelobes result. As will be shown later, this causes inaccuracy in estimating the channel impulse response.

If $r(t) = x(t) \otimes h(t)$ is the received signal and, $x(t)$, the transmitted signal, then the cross-correlation between the received signal, $r(t)$,with the local copy of the transmitted signal, $x(t)$, will produce a symmetrical correlation plot as shown in Fig. 3.9 :

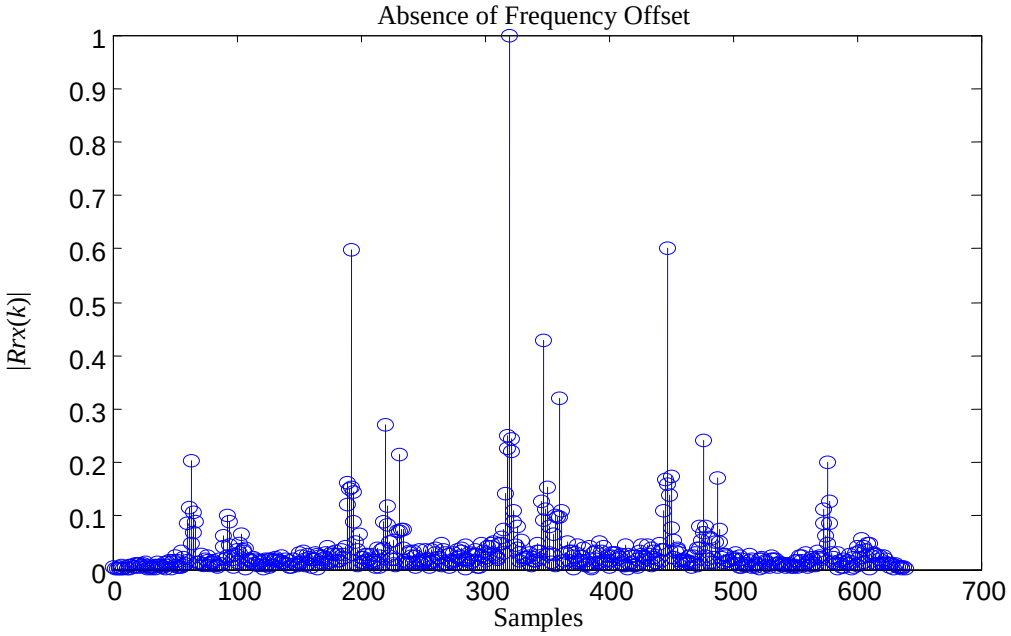

Fig. 3.9 Normal Cross-correlation

It can be seen in the figure above that the main impulse peak appears right at the middle of the correlation as it should. The other prominent impulse like peaks, albeit small in size, which appear next to the main peak are remaining part of the channel

impulse response. In this figure, there are two remaining taps of the channel impulse response next to the main peak and they appear clearly. The 3-tap channel impulse response is the result of choosing SUI channels which have 3 taps for most profiles.

From Fig. 3.9, it is also observed that, besides the main peak correlation, there are two other correlation peaks with magnitude of about half the main peak. This is because the correlation results not only from whole symbol being identical but also from identical halves in each symbol. Each of this peak is located 128 samples away from the main peak, since each identical half has a length of 128 samples. Thus, while the whole preamble (two identical halves) correlation produces the main peak, each half produces the half size correlation peak.

If, $r(t) = x(t)e^{j2\pi(I_f)i/N} \otimes h(t)$ is the received signal with integer frequency offset, I_f, and $x(t)$ is the transmitted signal, then the cross-correlation between the received signal, $r(t)$, with the local copy of the transmitted signal, $x(t)$, will not produce symmetrical plot but instead an asymmetrical plot as shown in Fig. 3.10:

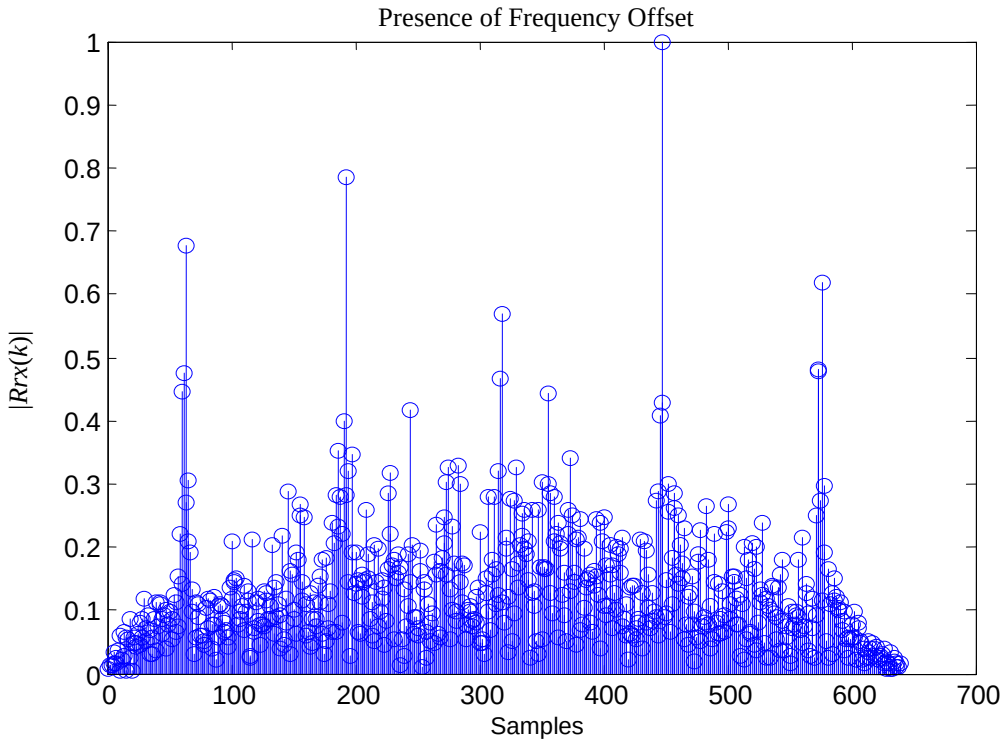

Fig. 3.10 Cross-correlation with the Presence of Frequency Offset

Fig. 3.10 shows the result of cross-correlation in the presence of the frequency offset. From the figure, we can see that the cross-correlation has an impulse peak which is located not at the zero lag (or in the middle of the correlation) but in some other location. It can also be seen that the correlation from identical halves are higher than what is expected. In addition, the clutter is so significant that no valid conclusions can be drawn from it. Given this situation, the channel impulse response is no longer as easily detectable as in Fig. 3.9, and it is overtly shadowed by the unwanted noisy clutter-like sideboles.

In conclusion, the frequency offset, which is represented by the multiplication with a complex exponential factor $e^{j2\pi(I_f)i/N}$, in the received signal, has modified the original signal ($x(t)$), such that the correlation result is not symmetrical anymore.

3.4.2 Frequency estimation and correction scheme

In order that the correlation results are symmetric, the frequency offset needs to be corrected by ridding the received signal completely from the frequency offset. The correction is mainly for the integer part since the fractional part is assumed to have been corrected beforehand as in conventional receiver schemes. Since the received signal contains an exponential complex as the frequency offset factor ($e^{j2\pi I_f(i/N)}$), then this particular factor can be eliminated by multiplying it with its opponent factor ($e^{-j2\pi I_f(i/N)}$).

Since the integer frequency offset is unknown to the receiver, the receiver needs to multiply the received signal with a multiple of suitable complex exponential signals in parallel branches as a bank of multipliers. By performing this multiplication, the received signal will be frequency corrected.

The only way to know whether a signal is corrected with the right complex exponential is when a bank of these multiplied signals are cross-correlated with a local copy of the preamble. The corrected signal will have a symmetric cross-correlation while the others will not be symmetrical. This is because the corrected signal, which is acquired by multiplying with the right complex exponential signal, is

the same signal as stored in the local copy. Fig. 3.11 shows the scheme of multiplication and cross-correlation.

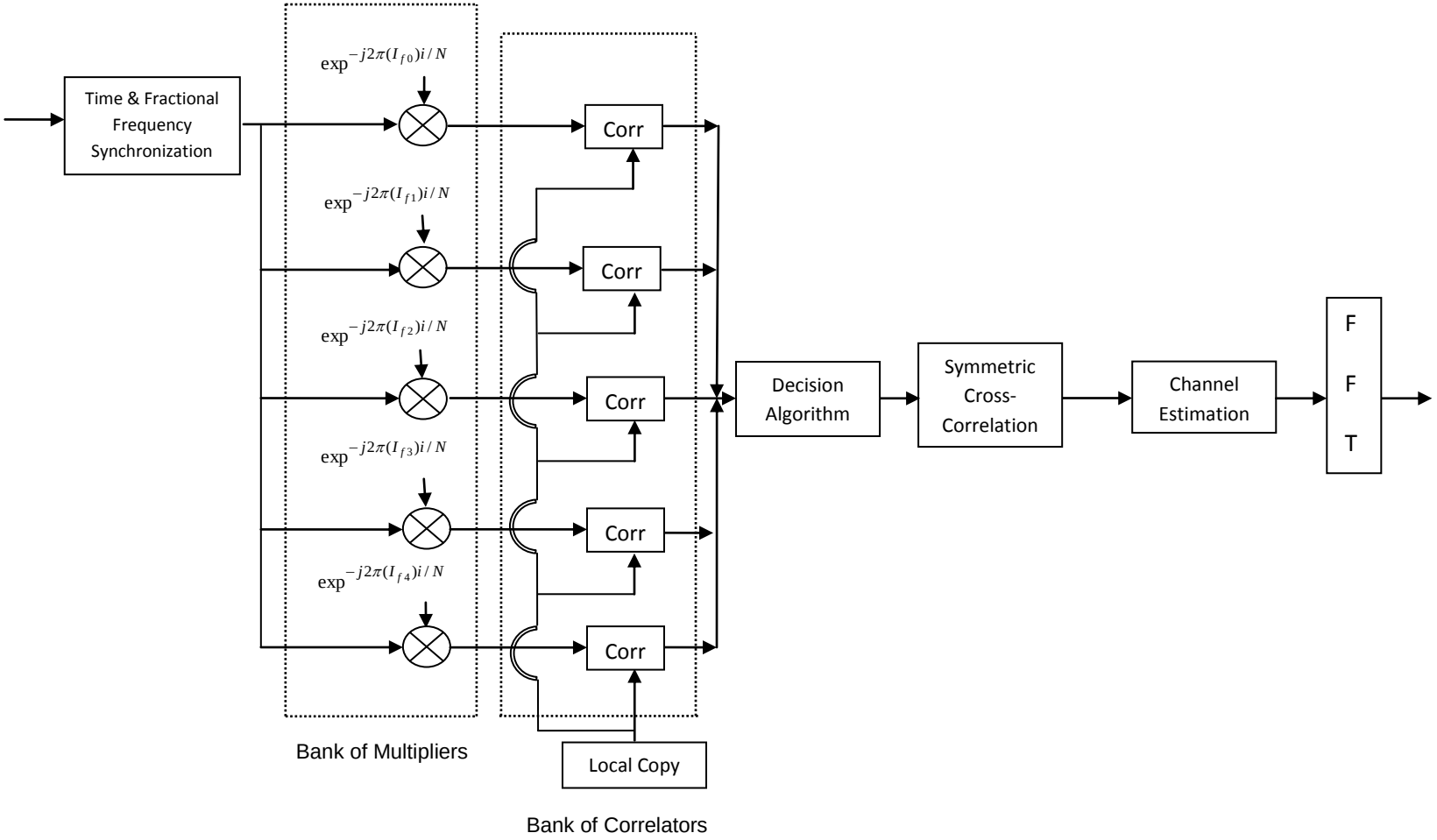

Fig. 3.11 Bank of Multipliers and Cross-correlators Scheme

The number of multipliers depends on the maximum number of integer frequency offset that is allowed in an OFDM system. Since, in this thesis, we use the IEEE 802.16a standard system, the maximum allowable of frequency offset is not more than integer 3 and, hence, no more than 7 branches ($2 \cdot |\pm 3| + 1 = 7$).

As mentioned earlier, the received signal is multiplied with these multipliers and then correlated with the local copy. All outputs of the correlators will produce unsymmetrical correlation but only one that will produce the symmetrical correlation, which means its signal has been fully corrected from the frequency offset.

The decision algorithm as pictured in Fig. 3.11 is used to decide which multipliers will result in a symmetrical cross-correlation. The decision algorithm first searches for the main (highest) peak location in each correlation plot. The highest peak should be a single peak and located in the middle of the correlation plot. When there is more than one main peak, then definitely the correlation is unsymmetrical. Once the correct located single main peak is found, the next thing is to find the two other high peaks resulting from identical halves at fixed locations relative to the main peak. Their location should be at 128 samples away to the right and the left of the main peak. Each second peak is located exactly 128 samples away; therefore if the second peak occurs higher in a different location, the correlation is unsymmetrical. Hence, if the required peaks are located at the correct location, the algorithm chooses the particular correlation to be used in the channel estimation. This decision also indicates that the received signal is frequency corrected. Fig. 3.12 depicts the flowchart of the detection algorithm.

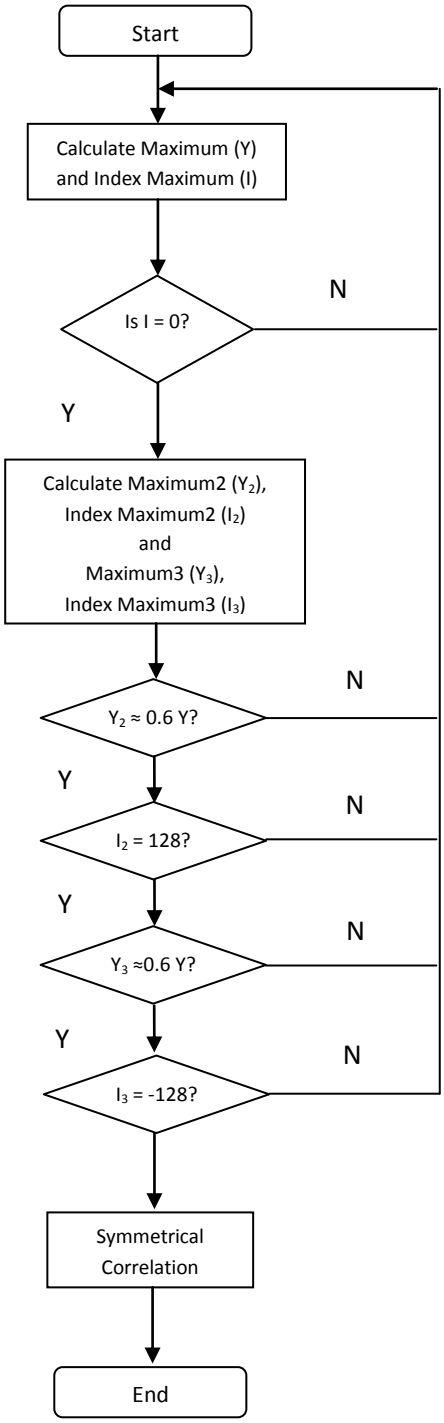

Fig. 3.12 Flowchart of Symmetrical Detection

Fig. 3.13 and Fig. 3.14 depict the unsymmetrical and symmetrical plots of the cross-correlation signals. The unsymmetrical plot shows that the frequency offset is not exactly corrected. The symmetric plot confirms that the frequency offset is exactly corrected.

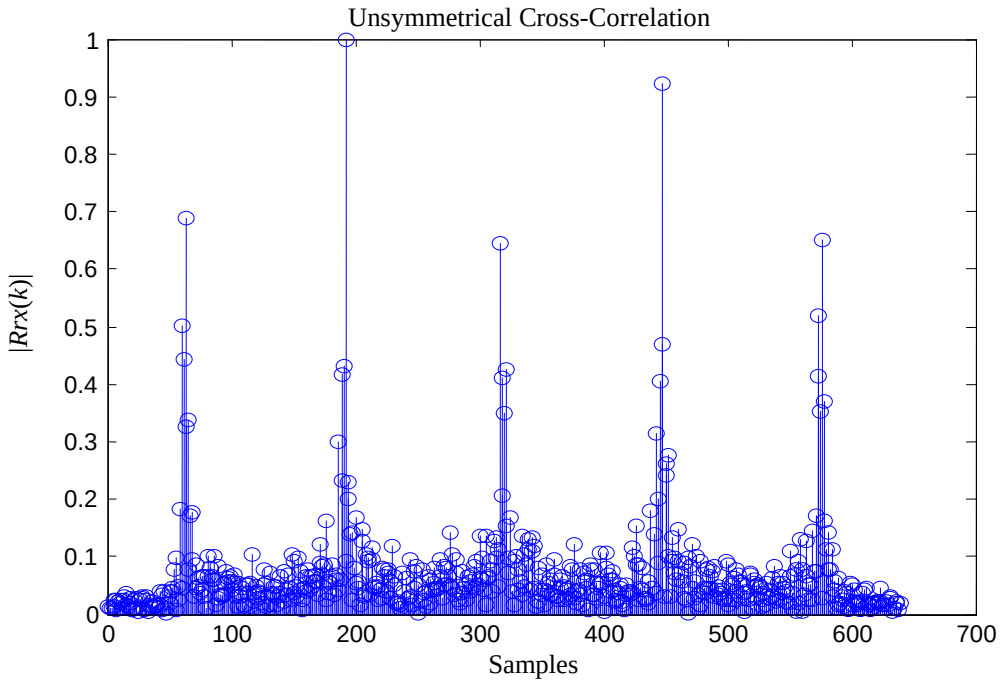

Fig. 3.13 Unsymmetrical Cross-correlation

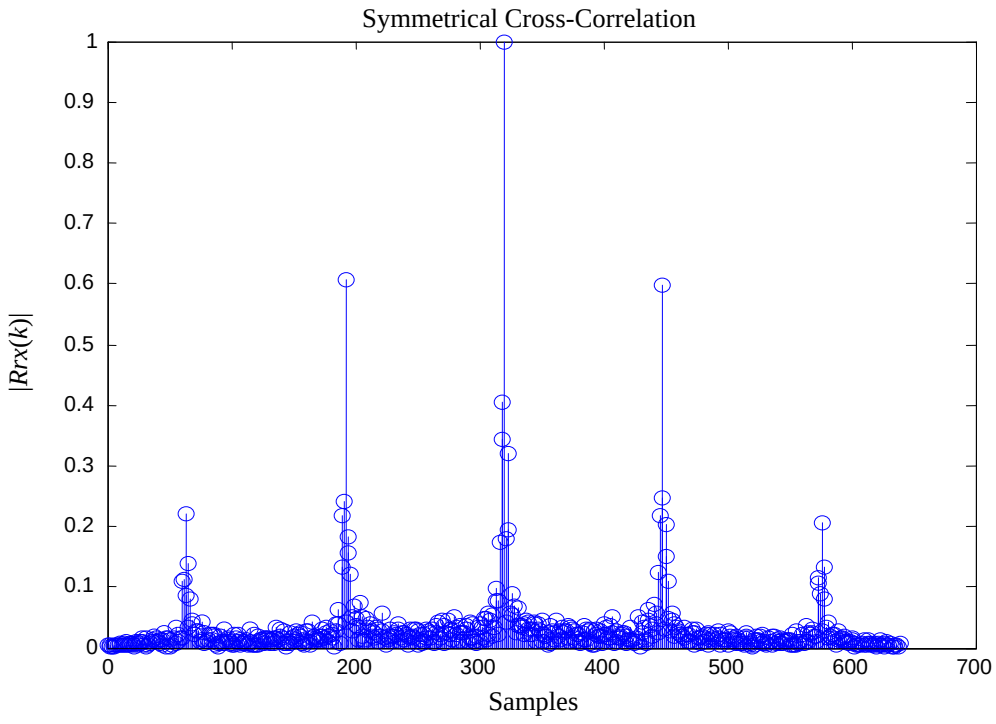

Fig. 3.14 Symmetrical Cross-correlation

The proposed receiver scheme offers a new design of receiver where time, frequency (fractional and integer frequency offset), SNR and also channel estimation are

performed in the time domain. The advantage of the proposed receiver scheme as compared to a typical receiver scheme is that the proposed receiver manages to estimate and correct timing offset, frequency offset, SNR and also estimates the channel impulse response in the time domain and in a simpler way. The integer frequency offset estimation and correction is heavy in the hardware implementation because of the presence of banks of multipliers and correlators. Fig. 3.15 depicts the time domain channel estimation based OFDM receiver.

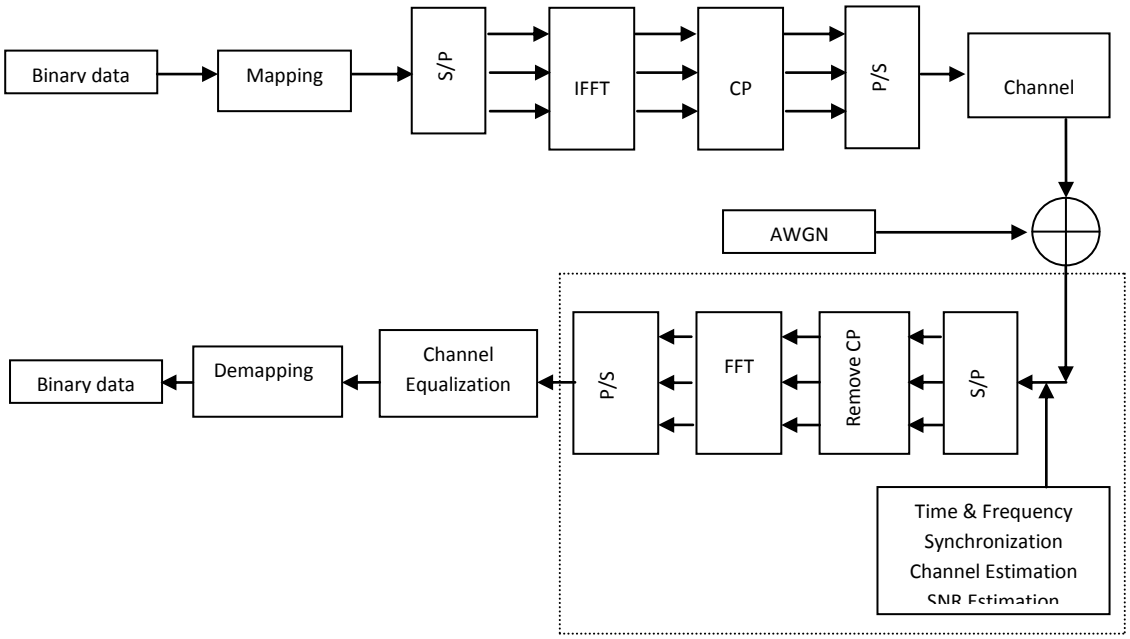

Fig. 3.15 OFDM Receiver Scheme based on Time Domain Channel Estimation

3.4.3 Time domain channel estimation

The received signal can be written as:

$$r(n) = s(n) + w(n) \tag{3.4}$$

where, $s(n) = x(n) \otimes h(n)$, $\otimes$ denotes convolution, $x(n)$ is the transmitted signal, $h(n)$ is the channel impulse response and $w(n)$ is the additive Gaussian white noise.

If we correlate the received signal with the local copy of the transmitted preamble, the resulting cross-correlation is as follows (* denotes complex conjugate of x):

$$
\begin{aligned}
R_{rx}(k) &= E[x^*(n)r(n+k)] \\
&= \frac{1}{N}\sum_{n=1}^{N} x^*(n)r(n+k) \\
&= R_{sx}(k) * h(k) + R_{wx}(k)
\end{aligned}
\tag{3.5}
$$

where

$$
R_{wx}(k) = \frac{1}{N}\sum_{n=1}^{N} x^*(n)w(n+k) \tag{3.6}
$$

is the cross-correlation value of $x(n)$ and $w(n)$.

$$
R_{sx}(k) = \frac{1}{N}\sum_{n=1}^{N} x^*(n)s(n+k) \tag{3.7}
$$

is the cross-correlation value of $x(n)$ and $s(n)$.

Since $x(n)$ and $w(n)$ are uncorrelated, then their cross-correlation value can be treated as zero. Then the cross-correlation of the received signal and the transmitted signal can be simply written as:

$$
\begin{aligned}
R_{sx}(k) &= \frac{1}{N}\sum_{n=1}^{N} x^*(n)s(n+k) \\
&= \frac{1}{N}\sum_{n=1}^{N} x^*(n)\sum_{m=-\infty}^{\infty} h(m)x(n+k-m) \\
&= \frac{1}{N}\sum_{m=-\infty}^{\infty} h(m)\sum_{n=1}^{N} x^*(n)x(n+k-m) \\
&= \sum_{m=-\infty}^{\infty} h(m)R_{xx}(k-m)
\end{aligned}
\tag{3.8}
$$

$$
\text{where } R_{xx}(k) = \begin{Bmatrix} P_0 & if\ k\ =\ 0 \bmod N \\ \dfrac{-P_0}{N} & if\ k\ \neq\ 0 \bmod N \end{Bmatrix} \tag{3.9}
$$

Under assumption that N is large, $R_{xx}(k)$ can be approximated as $R_{xx}(k) \cong P_0\delta(k)$. Therefore, (3.4) can be simply written as:

$$
\begin{aligned}
R_{rx}(k) &= \sum_{k=-\infty}^{\infty} h(m) R_{xx}(k-m) \\
&= \sum_{k=-\infty}^{\infty} h(m) P_0 \delta(k-m) \\
&= P_0 h(k)
\end{aligned}
\tag{3.10}
$$

The basis of the time domain channel estimation technique is that the correlation of the received signal with preamble's local copy produces an scaled impulse response as in Eqn. 3.9.

Since the cross-correlation between the received signal and transmitted signal gives impulse like peaks where the impulse response taps are, catching the peaks of cross-correlation is also catching the channel impulse response of the signal. The training symbol used for channel estimation is the same training symbol used for synchronization. As the training preamble signal has two identical halves, the cross-correlation of the received training symbol with the local copy results in repetition of impulse response at two other locations. As shown in Fig. 3.16, the correlation has two side peaks with magnitude half of the magnitude of the main peak and each peak appears 128 samples away from the main peak on either side of the main peak. This is due to the presence of two identical halves in the preamble. Each peak is followed by a few other peaks. These other peaks are the taps of the impulse response which appear according to its tap height and delay locations.

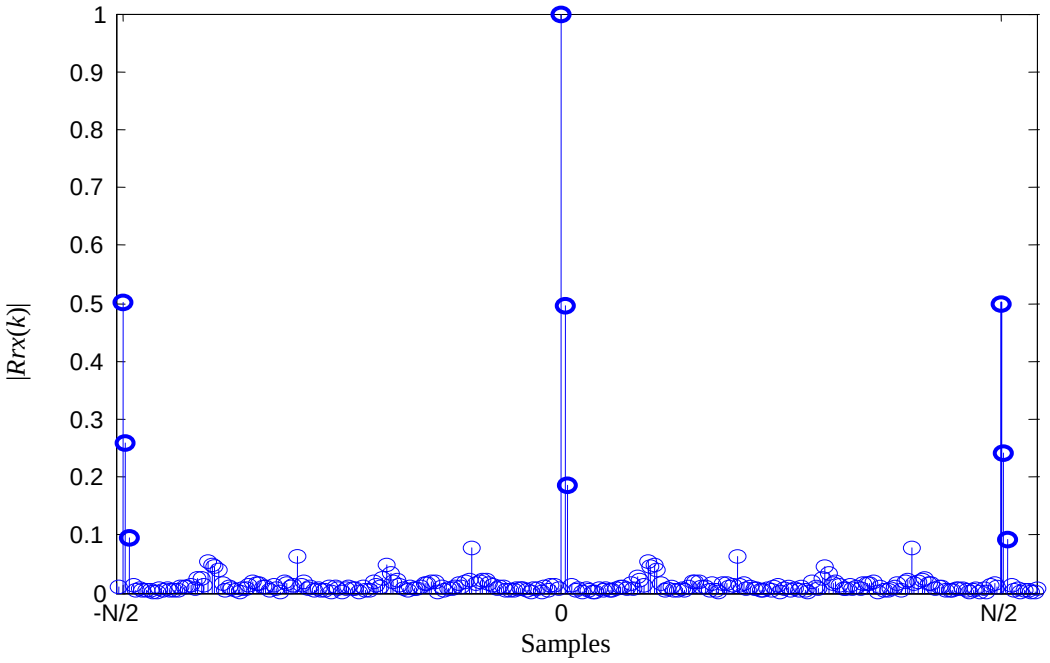

Fig. 3.16 Tap Catching Channel Estimation

Estimating the channel impulse response, therefore, is to catch these taps accurately. The taps are caught by selecting the three most significant taps in any or all of the three regions (-*N*/2 to -1, 0 to *N*/2 -1 or *N*/2 to *N*). In the proposed technique, each tap at a given location is added with the other respective taps from the other regions and averaged. By catching each tap in each region, missing one of the taps might be prevented because if one tap in one region does not appear then it might appear at the correct tap location in another region. The correct tap at the other region will then occupy a place in taps-catching.

After capturing three most significant taps as stipulated in SUI channels, the channel impulse response is padded with suitable number and locations of zeros to obtain 256 sample long channel impulse response. This is then transformed to the frequency domain to obtain 256 samples long channel frequency response which is then used in equalizing the distortion/ISI caused by the channel. If $\hat{h}(n)$ is the estimate of the channel impulse response, the channel frequency response can be written as:

$$\hat{H}(k) = DFT\{\hat{h}(n)\} \tag{3.11}$$

To show the realization of a typical channel frequency response estimated using the proposed technique, Fig. 3.17 depicts the realization of SUI-6 channel frequency response which is frequency selective.

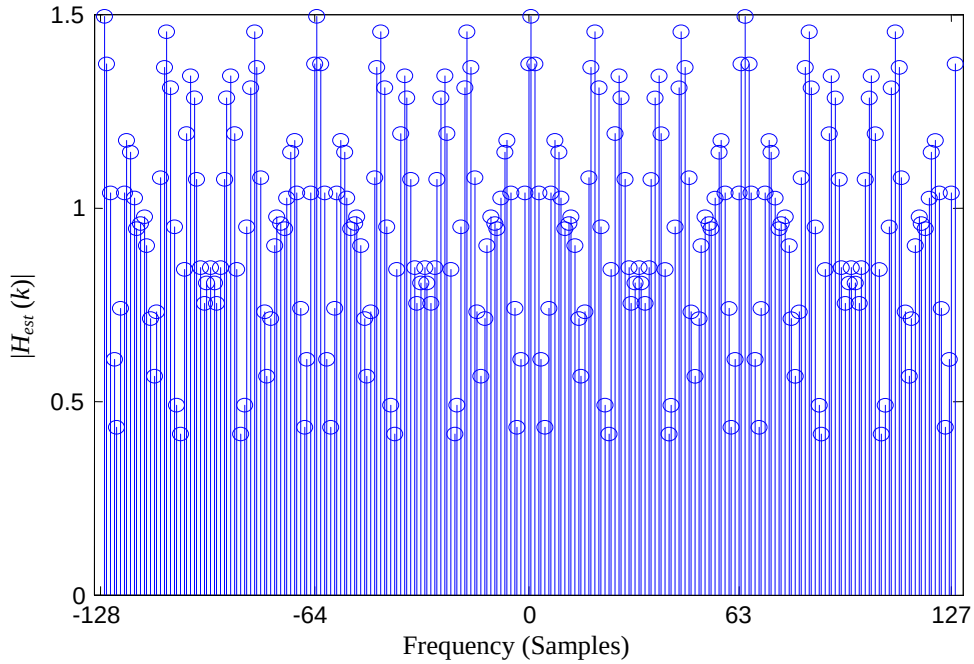

Fig. 3.17 The Frequency Response of SUI-6

3.5 The Performance Evaluation

3.5.1 Performance evaluation of time synchronization and integer frequency synchronization

In order to evaluate the performance of the proposed GCL preamble and the standard PN preamble, we will apply the proposed GCL preamble and the standard PN preamble into the time synchronization and also into the frequency synchronization blocks of IEEE 802.16a system.

The receiver of IEEE 802.16 a system is shown in Fig. 3.18:

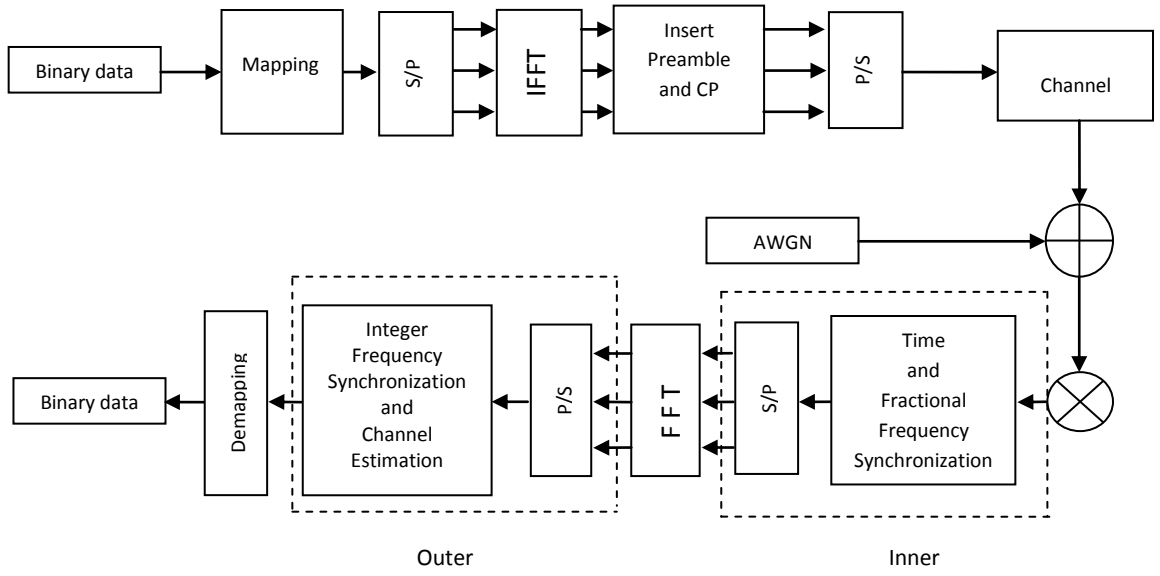

Fig. 3.18 Typical Receiver Scheme of OFDM System

An OFDM system has a receiver design which commonly consists of two parts, namely the inner receiver and the outer receiver.

- The inner receiver is a part where the estimation of the unknown parameters (e.g., time and fractional frequency synchronization) are performed in the time domain. After time synchronization and fractional frequency synchronization, the cyclic prefix is removed.
- In the outer receiver, the symbol is sent through FFT to obtain the frequency domain signal and thus performs other synchronization task such as integer frequency synchronization. It is here where channel estimation and equalization are also performed in the frequency domain.

The typical receiver scheme is basically based on Schmidl and Cox [5]. In Schmidl and Cox's method, there are three offset estimations that need to be carried out. The first is the time offset, followed by the fractional frequency offset estimation and finally the integer frequency offset.

The typical receiver scheme has two main tasks, time synchronization and integer frequency synchronization. The two synchronizations are chosen because they perform correlation based approach to estimate the offset. The correlation method for the time synchronization is autocorrelation in the time domain while the integer

frequency synchronization is performed by a cross-correlation approach in the frequency domain.

The time synchronization is evaluated by two methods, Schmidl and Cox's method [5] and Park et. al. method [1]. Park's method is evaluated since basically it has a similar training symbol as Schmidl and Cox's but its performance is much better. The preamble acts as the training symbol and the same training symbol is used for estimating time offset and integer frequency offset. In other words, the estimations need only one preamble.

In Schmidl and Cox's method, the time-domain preamble is so designed to have identical halves by assigning zeros on the even subcarrier and PN sequence on the odd subcarrier with consideration where the DC offset is in the even subcarrier. Taking the IFFT of this preamble will result in two identical parts in a symbol with the same length $N/2$ (N is the N-point FFT). The number of FFT point, N-point FFT, used is 256 points. The preamble is then sent through the multipath channel. Standford University Interim (SUI) channels [31] as provided for the standard IEEE 802.16 d are used. A processing delay of 200 samples is assumed. The receiver then starts to correlate the received signal. In Schmidl and Cox's method the correlation is performed between two corresponding samples which are $N/2$ samples apart as shown in Schmidl and Cox's timing metric in the previous chapter. The correlation, thus, gives a correlation peak with a plateau at the peak in cyclic prefix length. The expected result from this method thus is the correlation peak shape which has a plateau.

The Park's method has training symbol that has four parts which consist of conjugate and symmetrical parts as explained in chapter 2. The training symbol is designed by assigning the PN sequence on the odd subcarriers and the zeros on the even subcarriers just like in the Schmidl and Cox's preamble. Taking the IFFT of the designed preamble will result in the identical and symmetrical part which has $N/4$ samples length each, $N/4$ shorter compared to Schmidl and Cox's. By noticing the identical and symmetrical property in the preamble, the autocorrelation is performed in $N/4$ samples away according to Park's timing metric described in the previous

chapter. The expected result from this method is an impulse like correlation peak as described in Park's method.

Once the timing synchronization is done, the integer frequency error estimation is started where the time error is assumed to be corrected first. With perfect timing synchronization, the cyclic prefix is removed from the preamble and then the frequency domain of the preamble is obtained through FFT. The integer frequency error estimation is performed by using a modification to the Schmidl and Cox's method. Here we use the same one symbol long preamble instead of using another preamble on another symbol as in Schmidl and Cox's method and use it for integer frequency offset estimation. In this method, after obtaining the frequency domain preamble, the zeros subcarriers are removed from the preamble; then only the cross-correlation with the frequency domain local copy of the preamble is performed. The expected result from this cross-correlation is a sharp peak as shown in Fig. 3.3 and Fig. 3.4.

3.5.2 Performance evaluation of time domain frequency offset correction and channel estimation

In order to evaluate the performance of the time domain frequency offset correction, we will detect the symmetrical correlation plot as described in the decision block from Fig. 3.11. The correction of frequency offset in the new receiver scheme is determined by the presence of symmetrical correlation. The performance of this frequency correction is therefore measured by the probability of detecting the symmetrical correlation versus SNR.

The range of the SNR is taken from -7 to 3 dB. The reason of the SNR range is that to observe the probability of symmetrical correlation in the false alarm condition. The simulation is run 10.000 times under SUI-6. The integer frequency offset introduced in this work are 2 and 3.

The cross-correlation of the received preamble in the time domain with its local copy results in the impulse responses. The taps are expected to appear higher than other clutter like sidelobes of the cross-correlation in order for them to be caught. If the unexpected sidelobes appear higher than the desired taps, then the possibility to catch

the wrong taps is bigger. A good cross-correlation is then necessary in this algorithm such that the right taps are caught easily instead of other sidelobes.

Therefore, the key point of to evaluate the performance of the time domain channel estimation is to analyze the possibility of catching the right taps at the right positions between the standard PN preamble and the proposed GCL preamble. The evaluation performance is translated into the probability of miss-detection of the three channel impulse response (taps).

It is known that the time domain cross-correlation of GCL sequence is better than that of PN sequence since it has lower undesired sidelobes. Therefore it is expected that the probability of misdetection of the taps catching of GCL based preamble is lower than that of PN based preamble.

3.5.3 Simulation parameters

The simulation parameters are taken from the IEEE 802.16std [18]. The reason is because this particular IEEE standard is the most popular OFDM system example and now is readily available. The main parameters are the number of subcarriers, the number of active subcarriers, the *N*-point FFT and the frequency offset that is normalized to subcarrier spacing. Table 3.2 shows the chosen value for each parameter [18].

Table 3.2 OFDM System Parameters [18]

OFDM System Parameter	
Number of Subcarriers	256
Number of Active Subcarrier	200
N-Point FFT	256
Cyclic Prefix Length (samples)	64
Frequency Offset (for frequency estimation)	2

One OFDM symbol has 256 samples and 64 samples of cyclic prefix. In each symbol only 200 subcarriers are used while the remaining is nulled to provide guard bands and to deal with a carrier leakage and a DC carrier. To evaluate the performance of

the conventional preamble and the proposed preamble, we use three different channels such as SUI-2, SUI-3 and SUI-6 each of which represents a different type of terrain in the SUI channels.

3.5.4 Stanford University-Interim channel

The Standard University-Interim (SUI) channels are the specific channel model for IEEE 802.16 Standard. The SUI-channel represents the channel characteristics such as delay spread, doppler spread, line-of-sight (LOS) and non-line of-sight (NLOS) conditions that are typical in the US [31]. SUI-channels have 6 kinds of channels and are presented in the Appendix.

3.6 Methodology

3.6.1 Time synchronization methodology

In the time synchronization, we will apply both preambles in Schmidl and Cox's method. This implies obtaining the timing metric and analyzing it to compare the performance of the two preambles. The Schmidl and Cox's method basically produces an autocorrelation peak with a plateau of length with the same length of the cyclic prefix length. It is observed that the start of the symbol can be chosen anywhere over the length of the plateau. Hence, it is important to recognize the start and stop of the plateau, and perhaps its shape as well. The plateau shape critically depends on SNR. At very low SNR, it may not appear as a plateau at all. It is known that the Schmidl and Cox's method gives uncertainty of time synchronization because of the plateau shape. This method is not good enough to determine the start of the OFDM symbol. The Schmidl and Cox's method is among the first such method for synchronization and today it has been much improved that the timing metric produces a sharp peak as in Park's method [1].

Accordingly, we only analyze the shape of the plateau when we apply both PN based preamble and GCL based preamble to Schmidl and Cox's method to obtain its timing metric at various SNR, particularly low SNR.

We further estimate the performance of the proposed preamble by applying it to Park's method that produces much sharper impulse like peak. For the Park et al.'s method, the results will also be presented in terms of probability of miss-detection as a function of SNR.

As mentioned in the previous chapter, both Schmidl-Cox and Park et al. generate their preamble in the same way but use different definition of timing metric.

3.6.2 Integer frequency synchronization methodology

In the same manner as in time synchronization, for integer frequency synchronization, we will apply both preambles in the frequency domain cross-correlation, obtain the correlation peak, and then analyze how many times the correlation peak gives wrong estimation of the integer offset as a function of SNR. In other words, the performance of frequency offset estimation method based on the proposed preamble is evaluated in terms of probability of wrong estimate as a function of SNR.

3.6.3 Time domain frequency offset correction methodology

At the beginning of this time domain frequency offset correction, we will multiply the received signal in the time domain which still contains the integer frequency offset (after time and fractional frequency synchronization) with the complex exponential signals (in the bank of multipliers) and then correlate each output from the multipliers with the local copy of the preamble (in the bank of correlators). This implies obtaining the symmetrical correlation plot and analyzing how symmetric the result of the correlation is.

With the correct complex exponential signal, the cross-correlation that is being carried out afterward should produce the expected symmetrical plot. But, the symmetrical correlation critically depends on the SNR. In other words, when the SNR is low such that the signal power is lower than the noise power, large correlation peaks result even from the sidelobes. This condition, thus, will disturb the detection of the symmetrical correlation plot. The detection depends on the presence of the main peak and, relative to that, the two side peaks at correct location as explained in 3.4.2.

3.6.4 Time domain channel estimation methodology

In order to evaluate the time domain channel estimation, we will apply the proposed GCL preamble and the standard PN preamble into the time domain channel estimation. We also use the SUI-channels which have three taps, so the estimation problem is to try and catch all the three taps correctly (at the right position). The performance is a probability of misdetection of the channel taps and is presented as a comparison of probability of misdetection between the two preambles in order to analyze which preamble is better suited for the OFDM system.

3.7 Summary

Chapter 3 began by presenting the comparison between the PN sequence-based preamble and the GCL sequence-based preamble in terms of the correlation property both in the time domain and the frequency domain. The GCL preamble shows better property of correlation, both in frequency and time domain and thus is proposed to be used as the preamble for the purpose of synchronization.

In order to validate the better performance of GCL sequence in the OFDM receiver, a typical OFDM receiver is described which uses Schmidl and Cox's method for time synchronization and integer frequency offset estimation. However, as Schmidl and Cox's method has been much improved with Park's method for time synchronization, the chapter also explains the Park's method.

Accordingly, the performance of GCL based preamble in time synchronization is obtained for both the Schmidl and Cox's method and Park et al.'s method. Its performance for the integer frequency synchronization is, however, evaluated using Schmidl and Cox's method.

This chapter also presented a new technique for time domain frequency offset correction and time domain channel estimation. The former is the pre-requisites to be able to perform the latter. This resulted in a new receiver design that carries out all synchronization tasks, both time and frequency synchronization and even channel estimation, before FFT.

The chapter explains that the presence of the frequency offset in the received signal destroys the symmetry in the cross-correlation of the received signal with the local copy of the transmitted signal. To eliminate the frequency offset (the integer part) in the received signal, this work proposed a bank of complex exponential multipliers and a bank of correlators. Once the appropriate branch that corrects the frequency offset is selected, the resulting correlation, a symmetrical correlation that it is, is used to estimate the channel impulse response.

CHAPTER 4

RESULTS AND ANALYSIS

In this chapter, we present our results in the time synchronization, integer frequency synchronization, time domain frequency offset correction and time domain channel estimation. The time synchronization is evaluated by the Schmidl and Cox's timing metric shape and also Park's timing metric shape. In addition, we also produce the probability of miss-detection for Park's method. PN based preamble as well as GCL based preamble are used to evaluate the time synchronization and their performance will be analyzed in the timing metric and the probability of miss-detection. The integer frequency synchronization is evaluated by the probability of miss-detection of the integer offset in the Schmidl and Cox's method using PN based preamble and GCL based preamble.

The performance of the time domain frequency offset correction as the probability of misdetection of the symmetrical cross-correlation will be compared to the frequency domain integer frequency synchronization from the Schmidl and Cox based typical OFDM system. And lastly, the time domain channel estimation is evaluated by the probability of miss-detection of the channel taps using PN based preamble and GCL based preamble.

4.1 Time Synchronization Results and Analysis

In the time synchronization, the purpose is to obtain the timing metric plot as shown in Fig. 2.3 for Schmidl-Cox and Fig. 2.7 for Park et al. by applying different preamble to each of the timing metric. In order to obtain the expected timing metric plot, the main point of the preamble designed for this synchronization is its identical halves for

Schmidl and Cox's method and symmetrical and conjugate parts for Park's method. Fig. 4.1 depicts the phase of GCL preamble that shows the symmetrical and conjugate phase.

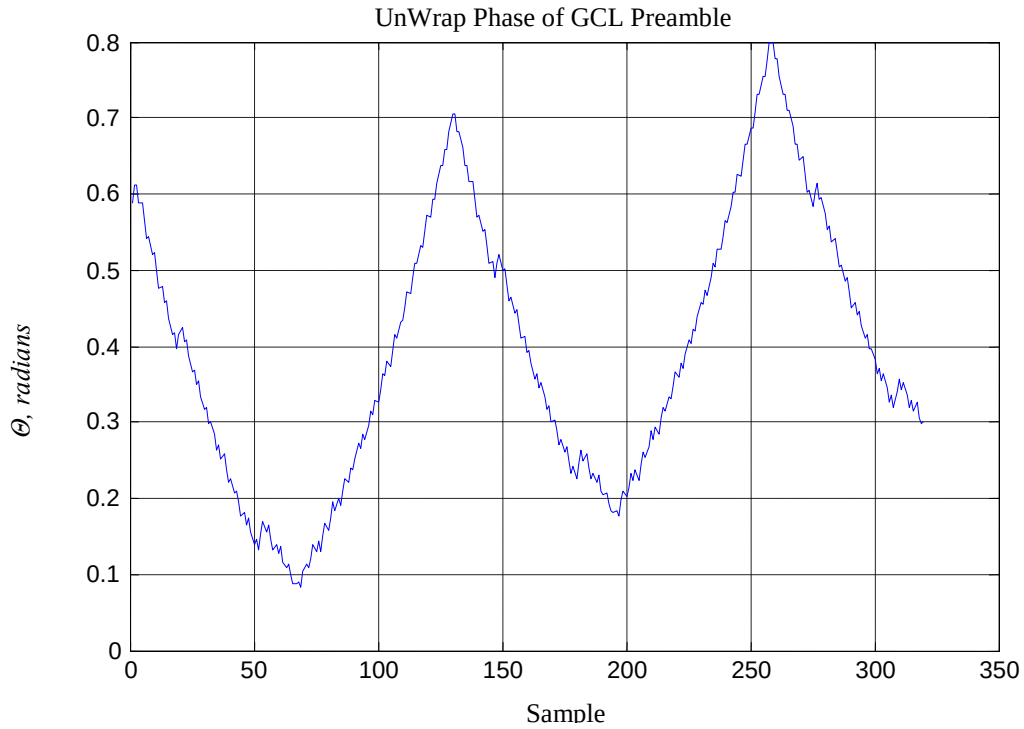

Fig. 4.1 Phase of GCL Preamble

As seen from the figure, the preamble in general has two identical halves showed by two curves with the same shape. But, if each curve is observed in detail, it shows the symmetric and conjugate part of the preamble.

The purpose of using different preambles for different timing metrics is to look for a better timing synchronization. Two well-known timing metrics by Schmidl-Cox and Park et al. are used to analyze the standard preamble and the proposed preamble. The needed preamble of both timing metrics is arranged to have alternate with the zeros on certain frequency; zeros on the even frequencies. The purpose of the arrangement is to have certain properties that will be used in the timing metric correlation.

4.1.1 Plateau results in Schmidl and Cox and their analysis

Fig. 4.2 to 4.4 present three plots of the timing metric of the PN sequence-based preamble in three different channels (i.e., SUI-2, SUI-3 and SUI-6) for the Schmidl

and Cox's method. Here, the correlation is summed over 128 samples. The CP length is 64 samples which gives a plateau a length of 64, that of the CP. Next, Fig. 4.5 to 4.7 present the timing metric for GCL preamble under the SUI-2, SUI-3 and SUI-6 for the same Schmidl and Cox's method.

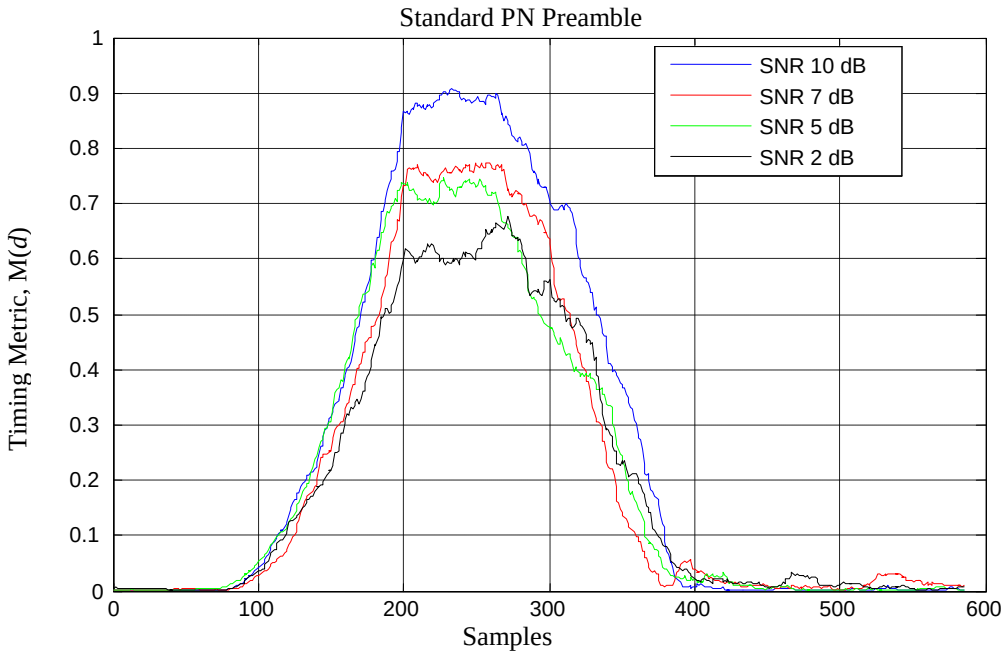

Fig. 4.2 Standard PN Preamble in Schmidl and Cox for SUI-2 Channel

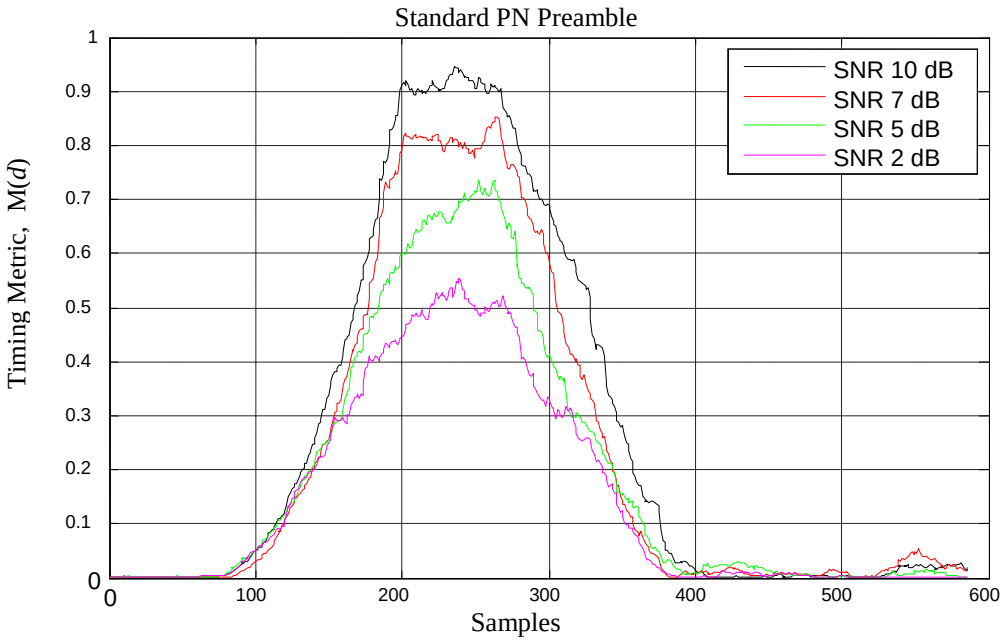

Fig. 4.3 Standard PN Preamble in Schmidl and Cox for SUI-3 Channel

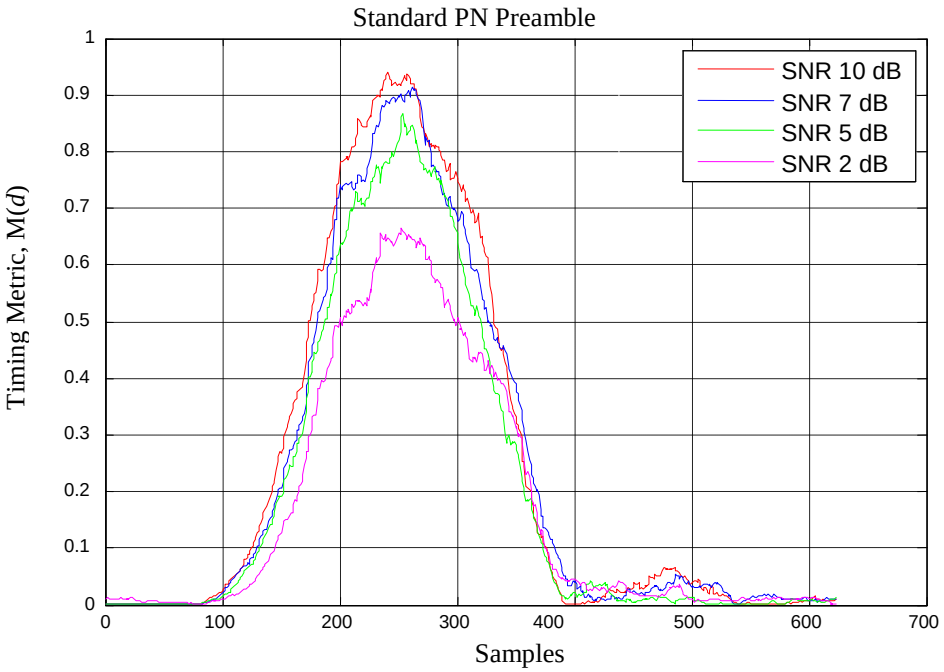

Fig. 4.4 Standard PN Preamble in Schmidl and Cox for SUI-6 Channel

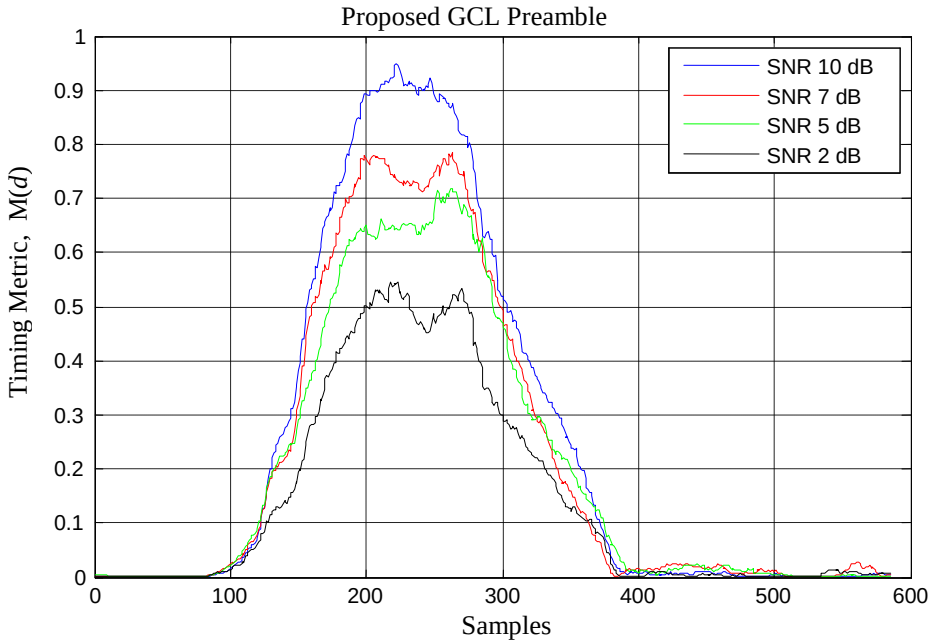

Fig. 4.5 Proposed GCL Preamble in Schmidl and Cox for SUI-2 Channel

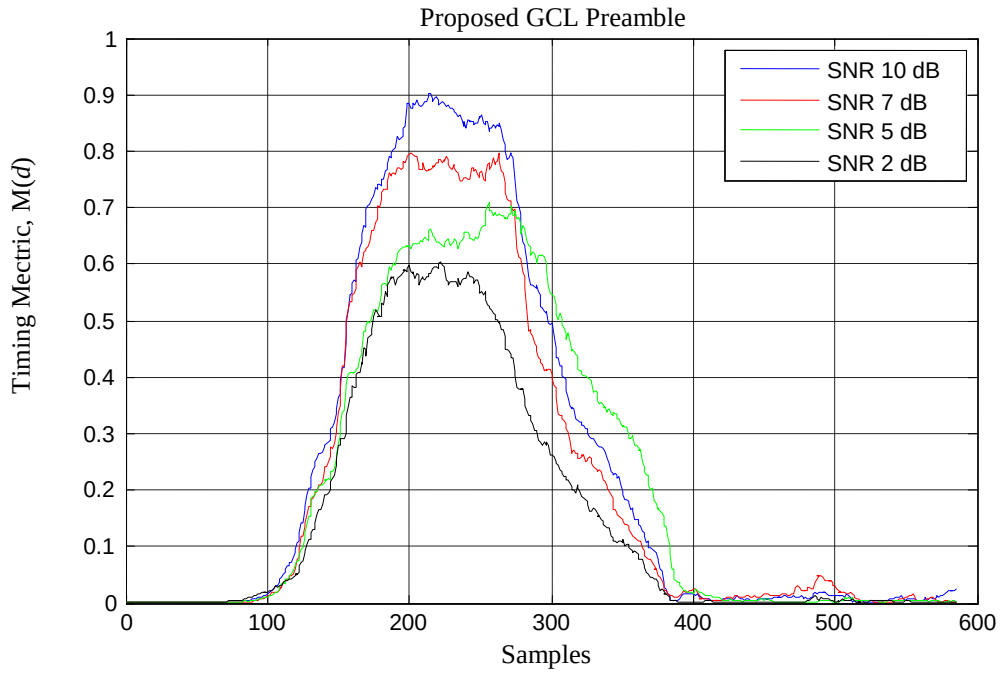

Fig. 4.6 Proposed GCL Preamble in Schmidl and Cox for SUI-3 Channel

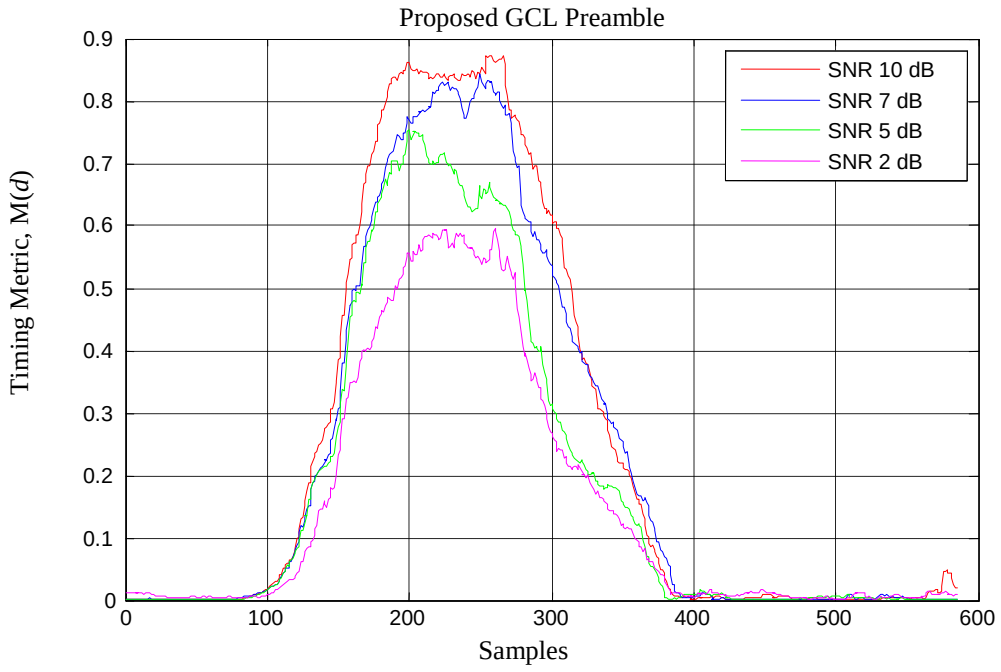

Fig. 4.7 Proposed GCL Preamble in Schmidl and Cox for SUI-6 Channel

In Schmidl and Cox's timing metric, the results of both preambles are found similar in terms of shape and magnitude. In every SUI-channel, the shapes of timing metric for both preambles appear like a Gaussian shape with no significant plateau. The

magnitude for each SNR in each preamble is more or less similar. However, for SNRs lower than 5 dB, it can be seen that the proposed GCL preamble maintains the plateau shape of the timing metric while the standard PN preamble does not. This would prove more suitable for use as a preamble in Schmidl & Cox based synchronization.

4.1.2 Park et al.'s result and analysis

Park's timing metric, as has been explained in the Chapter 2, relies on the property of the symmetric and conjugate symmetric parts in its time waveform. The correlation with the symmetric part will give an impulse like peak instead of a broad plateau which has been the motivating factor in his proposal. Fig. 4.8 and Fig. 4.9 show the results for both preambles in the AWGN channel without frequency offset. The processing delay, in this case, is 400 samples.

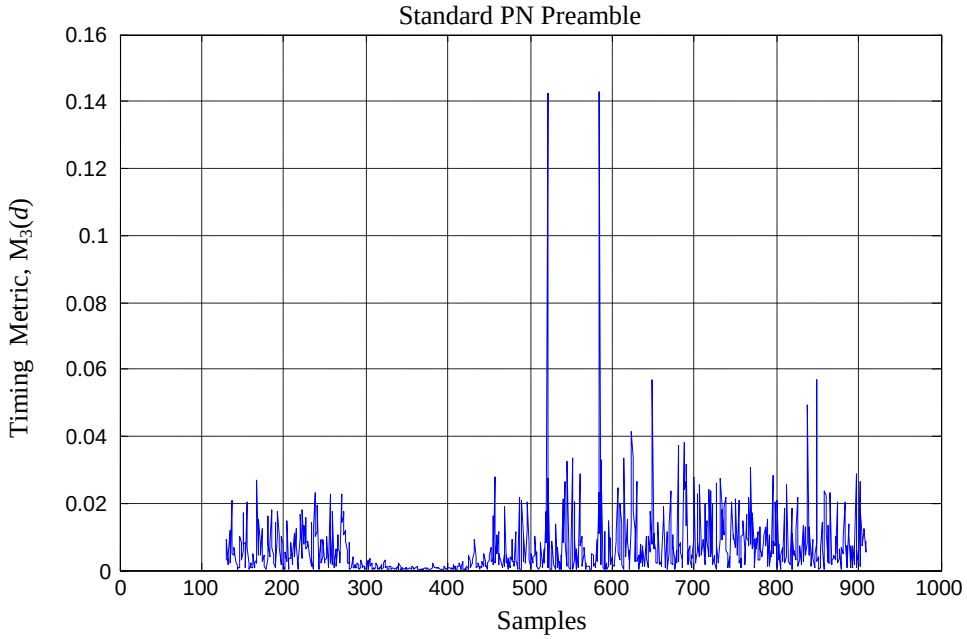

Fig. 4.8 Standard PN Preamble at SNR 10 dB no Frequency Offset

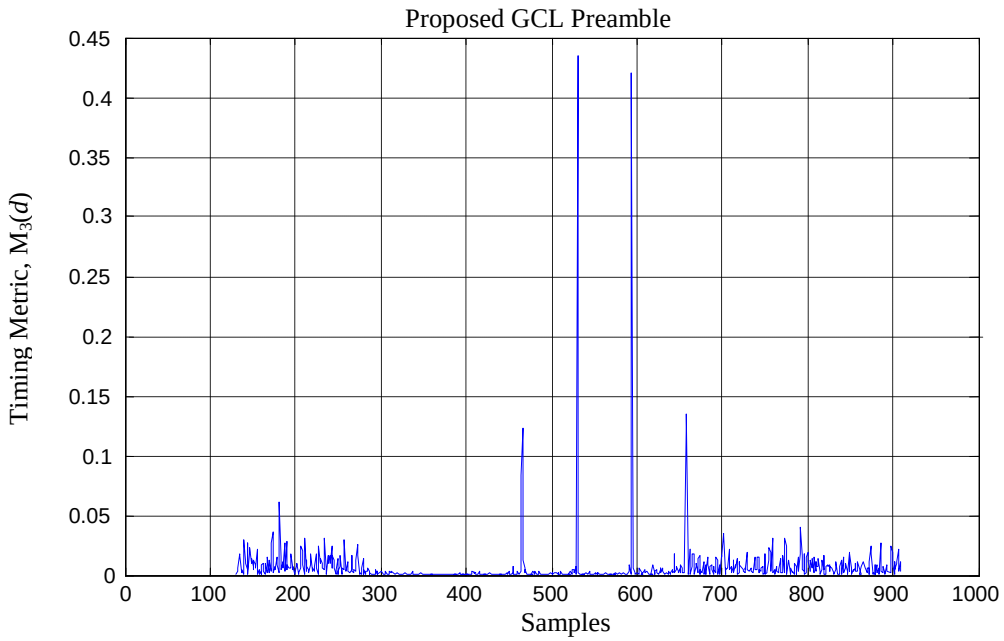

Fig. 4.9 Proposed GCL Preamble at SNR 10 dB no Frequency offset

As can be seen from the Fig. 4.8 and Fig. 4.9, Park's timing metric gives an impulse like peak which consists of two major peaks and two minor peaks. This is due to the length of the cyclic prefix that has been used in this simulation. Each symmetric and conjugate part has a length of ¼ of the symbol length, same as the cyclic prefix. Therefore, the timing metric correlation contains two parts that can be correlated to each other with the same length of the correlation summation. Fig. 4.10 depicts the correlation of Park's method in the preamble.

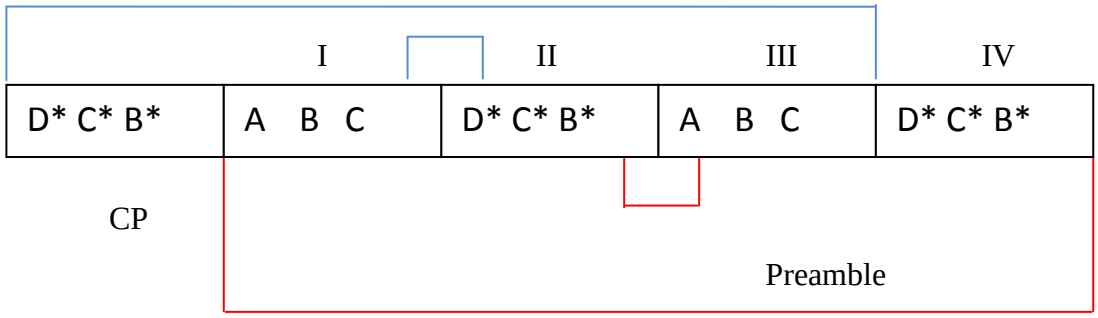

Fig. 4.10 Park's Timing Metric Correlation Scheme

Fig. 4.10 shows that there are five parts altogether consists of one part of CP and another four parts from the preamble itself (I,II, III and IV) with each part has the same length. It is seen from the figure that the correlation is intended to correlate the

corresponding symmetric samples over some length. There are two major correlations which are shown as in blue line and red line. The blue line correlation is the correlation starts with the CP part up to the third (III) part of the preamble. The summation over these four parts produces one major impulse peak. The second correlation is the red line where the correlation is taken over the first (I) part up to the fourth (IV) part of the preamble. The summation over these four parts also produces another one major impulse peak.

The major impulse peak appears only when there are four parts that are corresponding to each other and summed over. When there are only two parts which are corresponding to each other then the minor impulse peak is produced.

When there is no frequency offset, the method gives a good detection of the start of the symbol in spite of the noise being present as shown in those figures.

4.1.3 Presence of frequency offset and its impact on time synchronization

To see the performance of the preambles when frequency offset is introduced, Fig. 4.11 and Fig. 4.12 present the results of such condition for both preambles.

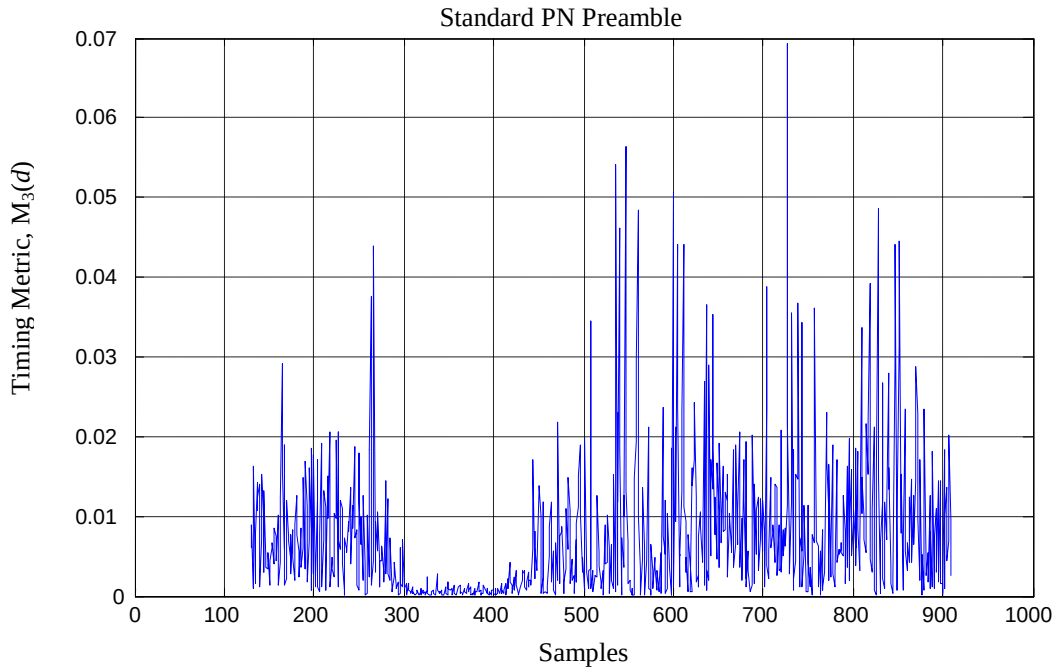

Fig. 4.11 Standard PN Preamble at SNR 10 dB with Frequency Offset 2.5

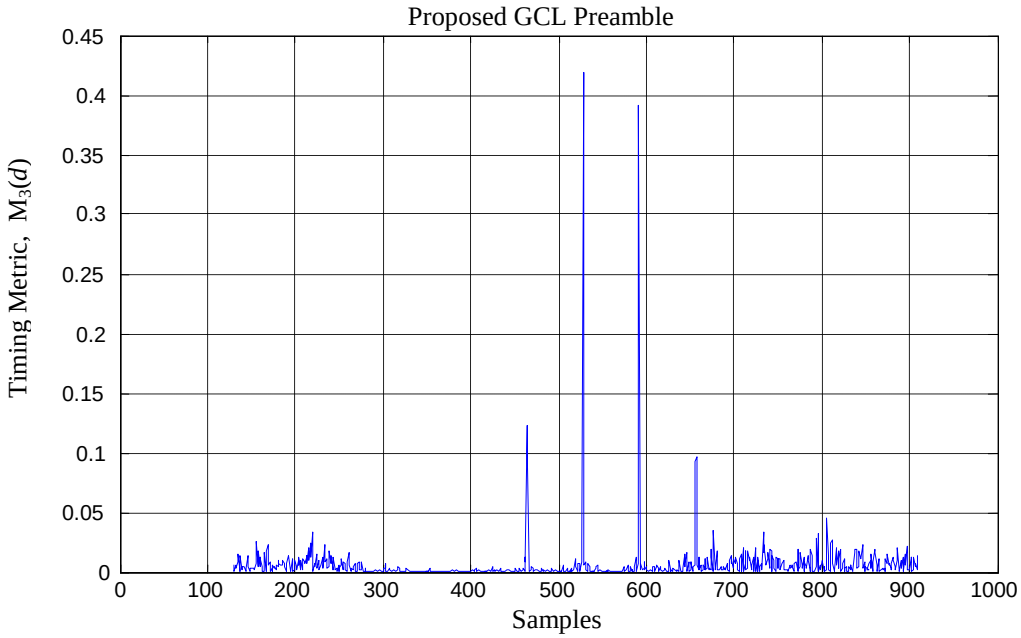

Fig. 4.12 Proposed GCL Preamble at SNR 10 dB with Frequency Offset 2.5

Fig. 4.11 shows the performance of the PN preamble in the presence of the frequency offset. It is seen from the figure that PN preamble produces so high unwanted sidelobes that the expected major peaks fail to appear. The presence of the frequency offset has destroyed the symmetric nature of correlation. It is shown that the standard PN preamble has less robustness to frequency offsets and fails to maintain the required characteristic.

On the other hand, Fig. 4.12 shows that the proposed GCL preamble still produces the major impulse peaks as though there is no frequency offset. GCL preamble again manages to maintain the required characteristic, symmetrical and conjugate part, just as when the signal has no frequency offset and produces the desired timing metric with sharp impulse like peaks. This means that GCL preamble still maintains the good correlation even in the presence of the frequency offset.

In order to compare the performance of PN preamble and GCL preamble in Park's method, Fig. 4.13 shows the probability of misdetection of the peaks while using the standard PN preamble and the proposed GCL preamble, with and without frequency offsets.

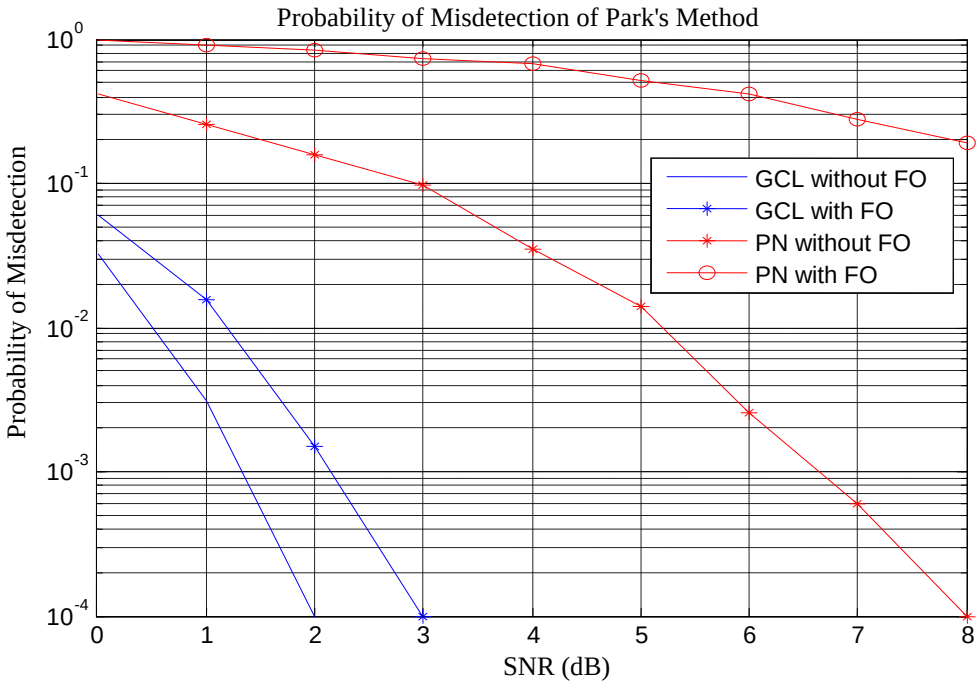

Fig. 4.13 Probability of Error Detection in Park's Timing Metric

From Fig. 4.13, we can see that, in the case of no frequency offset, the PN preamble has much higher probability of misdetection as compared to GCL preamble, in particular, the standard the standard PN preamble reaches SNR of 8 dB in order to get a probability of 10^{-4} while, for the same probability of misdetection GCL preamble only requires SNR of 2 dB. The proposed GCL preamble gives an advantage of 6 dB for the detection as compared to the standard PN preamble.

In the presence of frequency offset, the proposed GCL preamble has slightly higher probability of misdetection than in the absence of frequency offset. A seen from the figure, it requires 3 dB of SNR to achieve probability of 10^{-4} (+1 dB more than the case of no frequency offset). The performance of the standard PN preamble in this case is much worse as seen from Fig. 4.13. In the presence of frequency offset, the standard PN preamble has about 10^{-1} probability of misdetection at SNR of 8 dB.

The preambles were also tested in various multipath channels stipulated in SUI channels. Fig. 4.14 to 4.19 show the performance of preambles under SUI-channels.

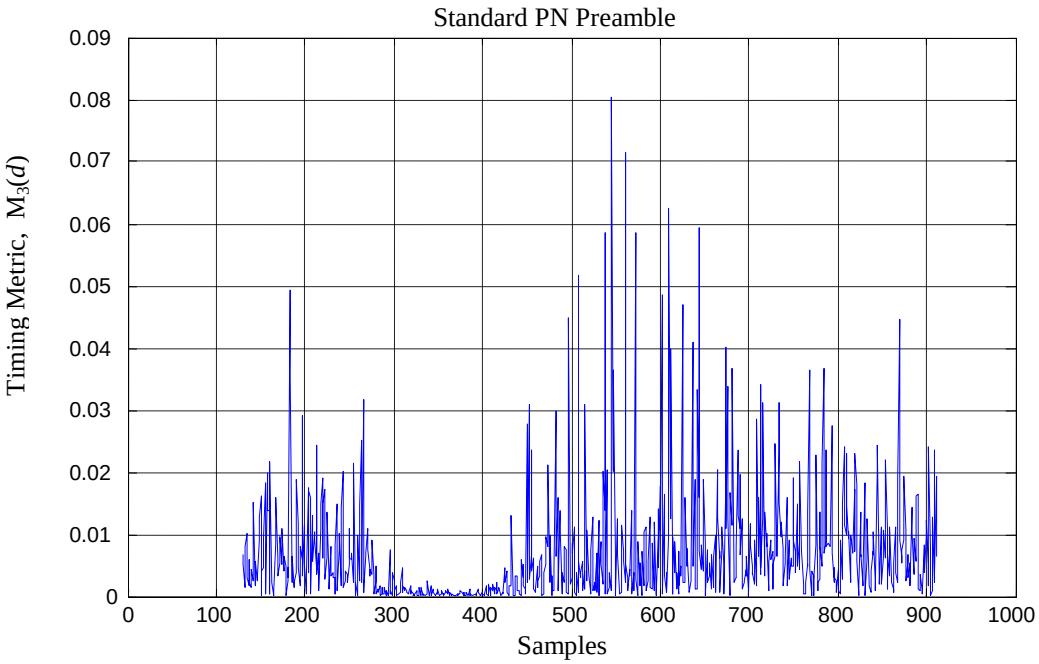

Fig. 4.14 Standard PN Preamble under SUI-2 with Frequency Offset 2.5

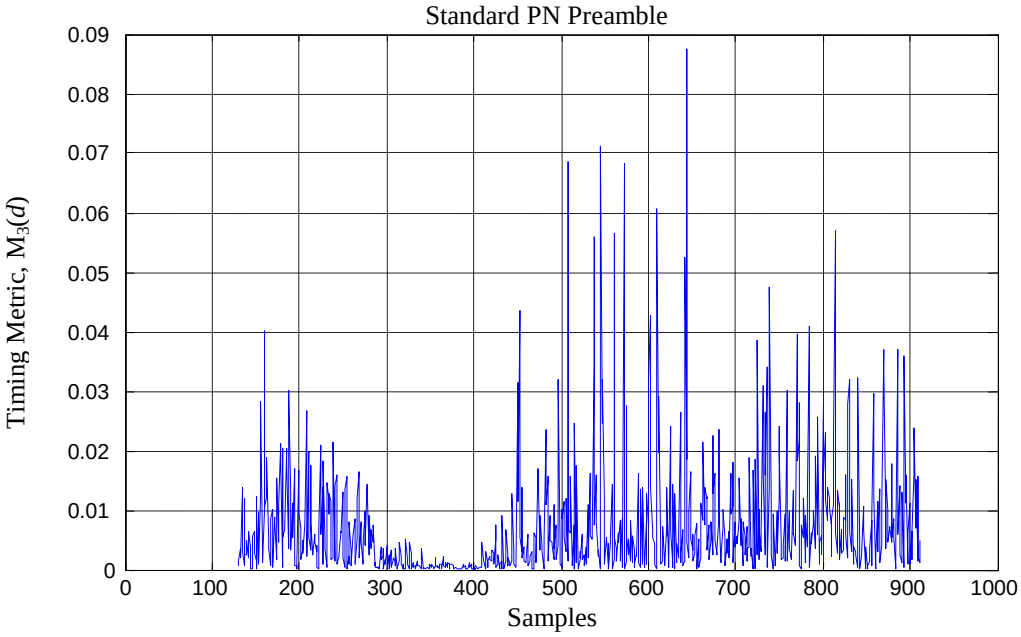

Fig. 4.15 Standard PN Preamble under SUI-3 with Frequency Offset 2.5

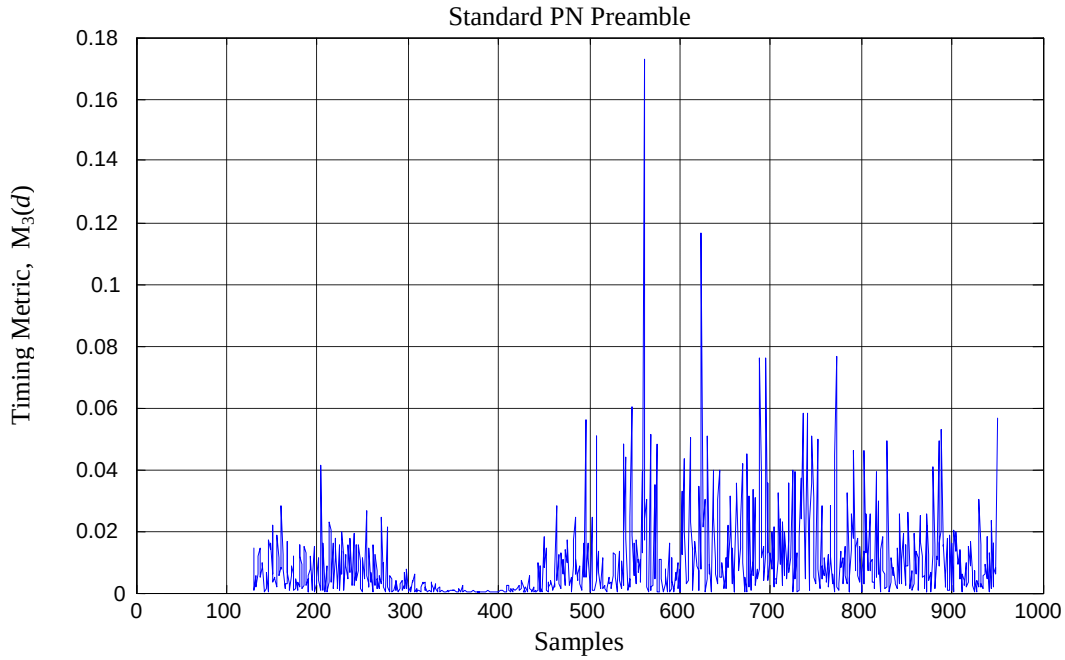

Fig. 4.16 Standard PN Preamble under SUI-6 with Frequency Offset 2.5

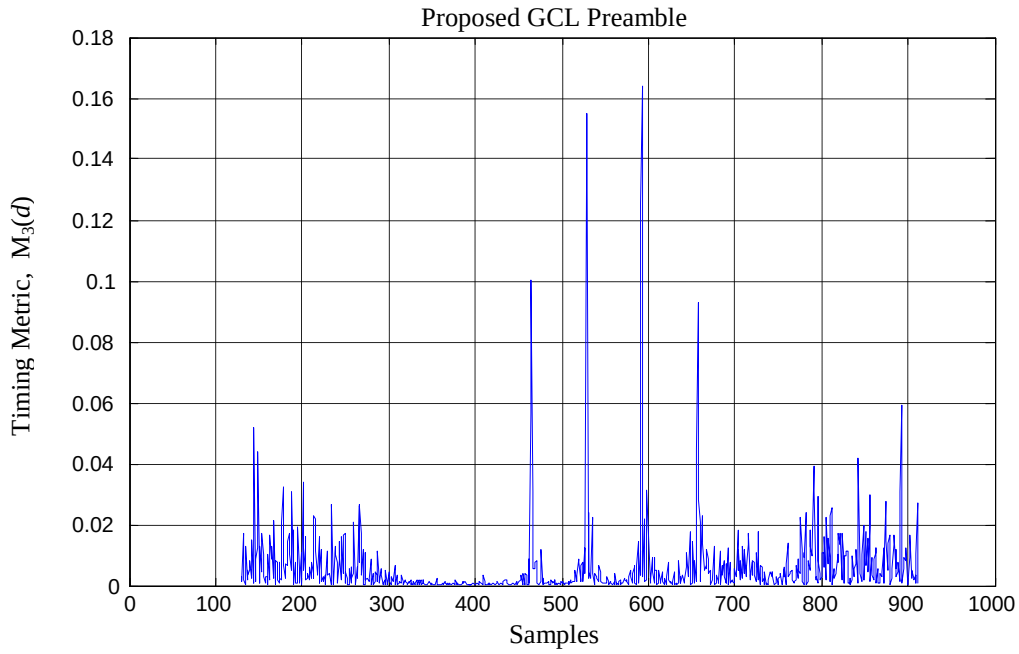

Fig. 4.17 Proposed GCL Preamble under SUI-2 with Frequency Offset 2.5

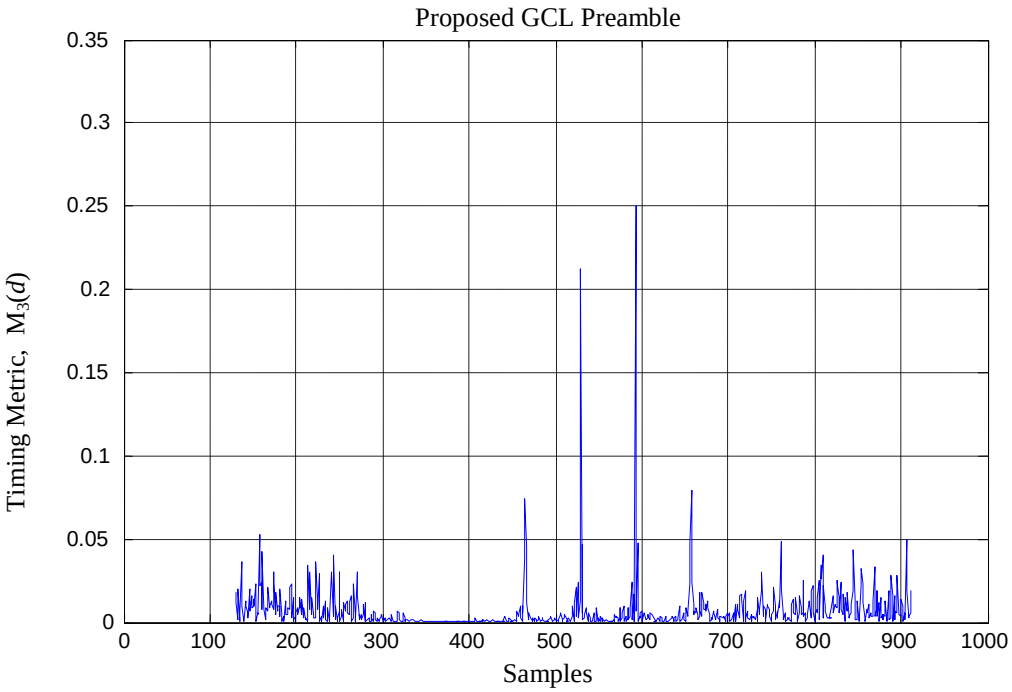

Fig. 4.18 Proposed GCL Preamble under SUI-3 with Frequency Offset 2.5

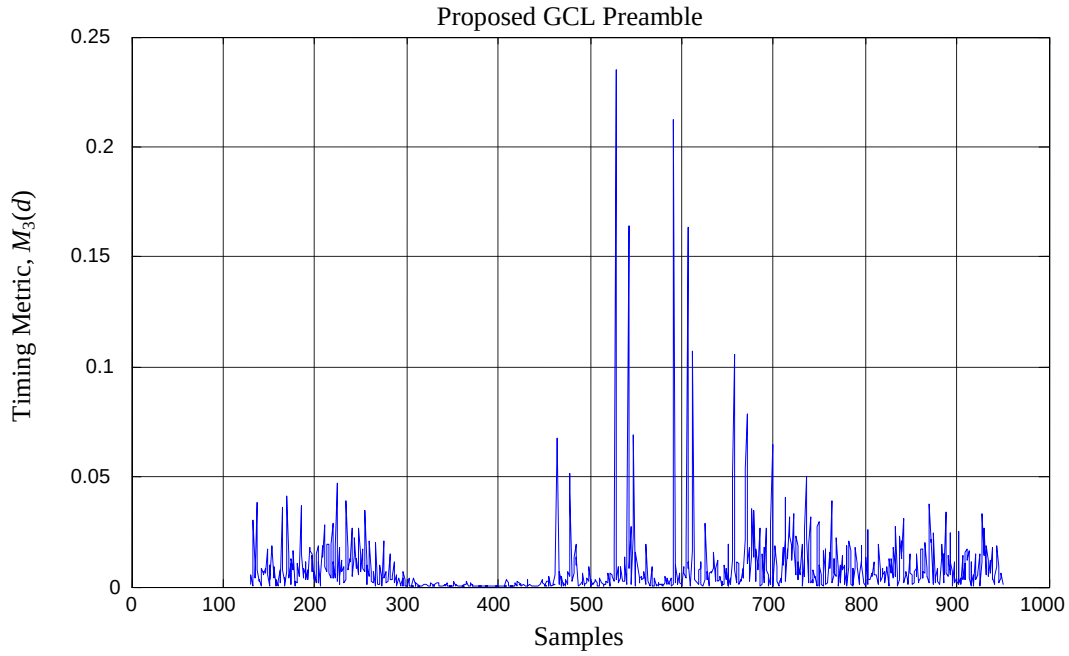

Fig. 4.19 Proposed GCL Preamble under SUI-6 with Frequency Offset 2.5

From Fig. 4.14 to 4.19, it can be seen that again the standard PN preamble suffers from the presence of the frequency offset in the multipath channels. The figures show

the unwanted high sidelobes appear in the correlation while the major impulse peak appears at the wrong location. Fig. 4.17 to 4.19 show that GCL preamble manages to produce the impulse like peak under the SUI-channels just like under the AWGN channel. The difference between the performance under the SUI-channel and the AWGN channel is that the sidelobes of the correlation under the former are higher compared to that of the AWGN channel. This is due to the signal received through multipath and noise. Again under the SUI-channel GCL preamble proves to preserve the required properties of Park's timing metric.

Although both preambles are designed in the same way yet GCL preamble proves a better characteristic compare to PN preamble. The results show that GCL sequence based preamble has better correlation property in the time domain especially in the presence of frequency offset as compared to the standard PN preamble.

4.2 Integer Frequency Synchronization Result and Analysis

In the frequency domain, integer offset shifts the subcarrier from its position to another position. The shift is detected by locating the main peak of cross-correlation. When there is no shift, the peak appears at zero lag location, while when there is a shift, the peak of the correlation is also shifted from zero lag location to a certain integer number equal to the shift

The simulation of integer offset estimation is run under the SUI-channel. The simulation is run for 1000 times and gives satisfied results. The performance of the integer offset frequency estimation is the probability of miss-detection of the integer offset. The range of SNR is from -8 dB to -2 dB. The reason of choosing this range of SNR is because the detection is made when the noise falsely detected as the signal. Fig. 4.20 to 4.25 present the performance of both preambles in each SUI-channel.

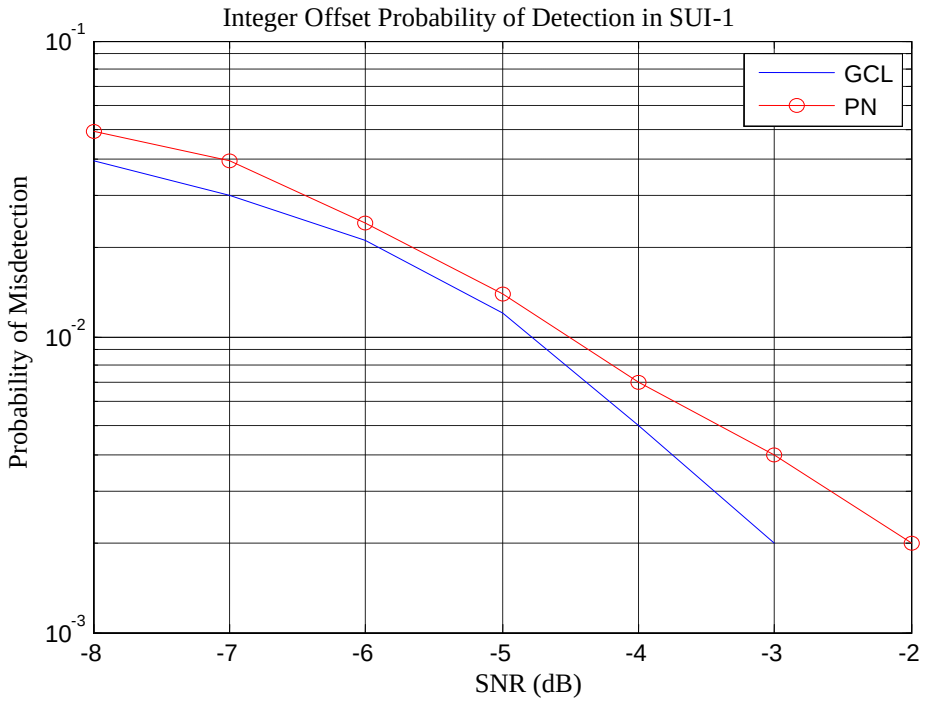

Fig. 4.20 Integer Offset Estimation in SUI-1

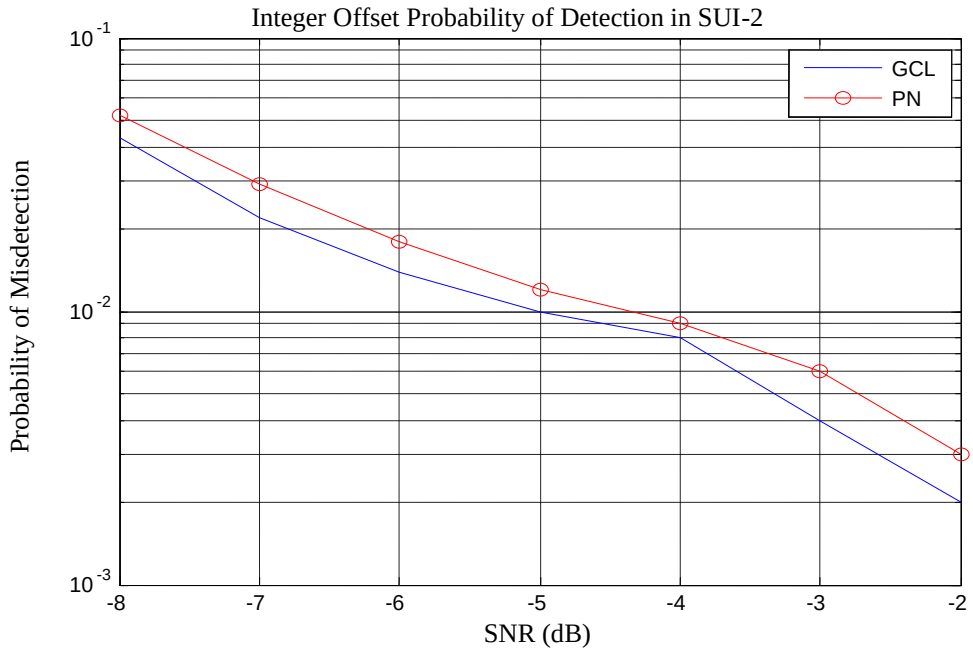

Fig. 4.21 Integer Offset Estimation in SUI-2

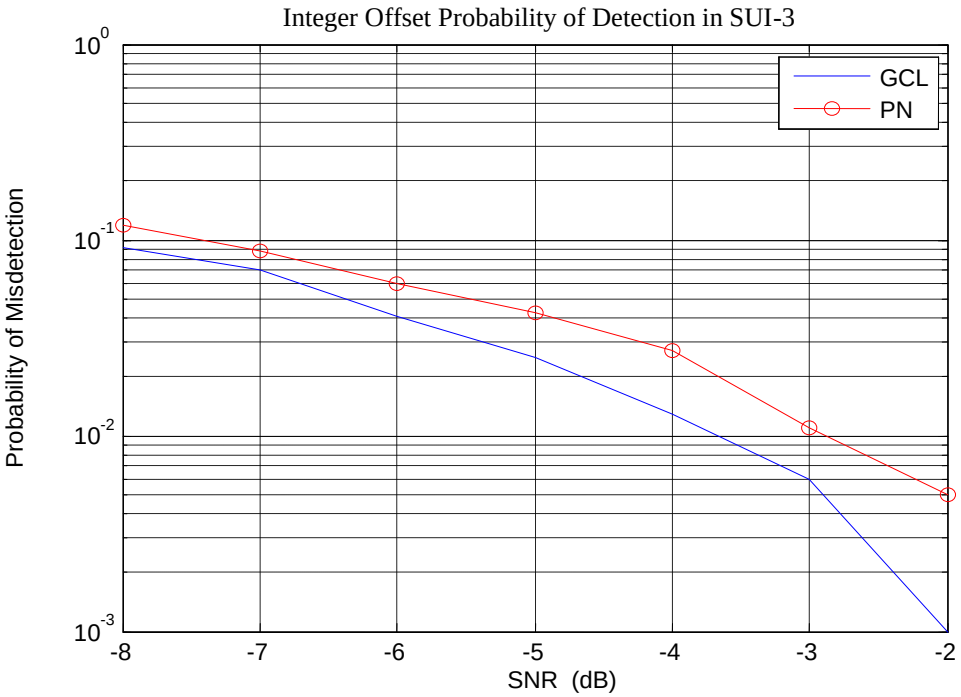

Fig. 4.22 Integer Offset Estimation in SUI-3

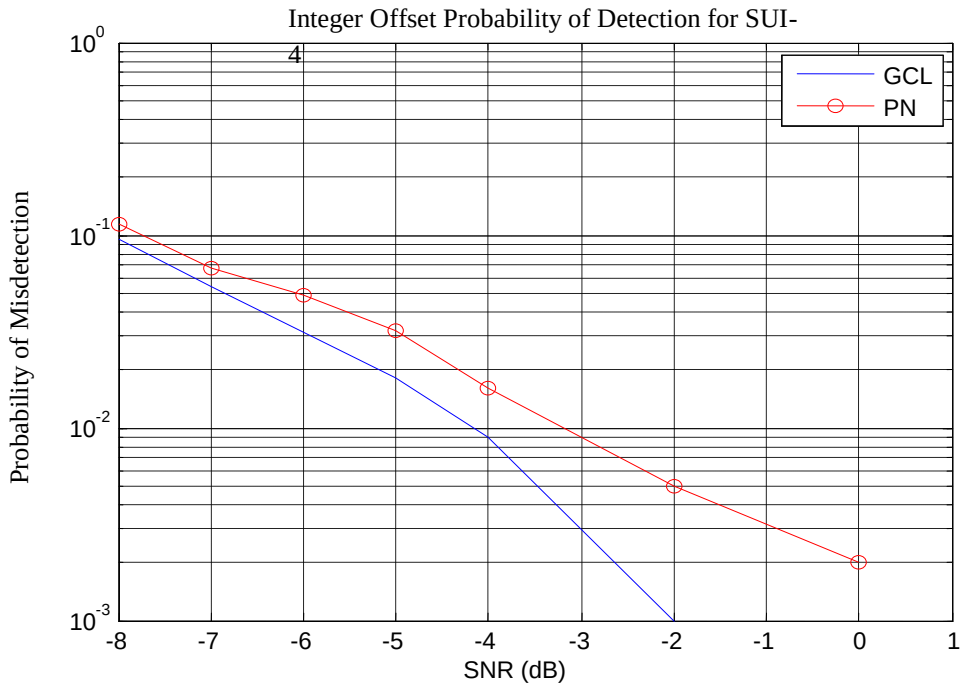

Fig. 4.23 Integer Offset Estimation in SUI-4

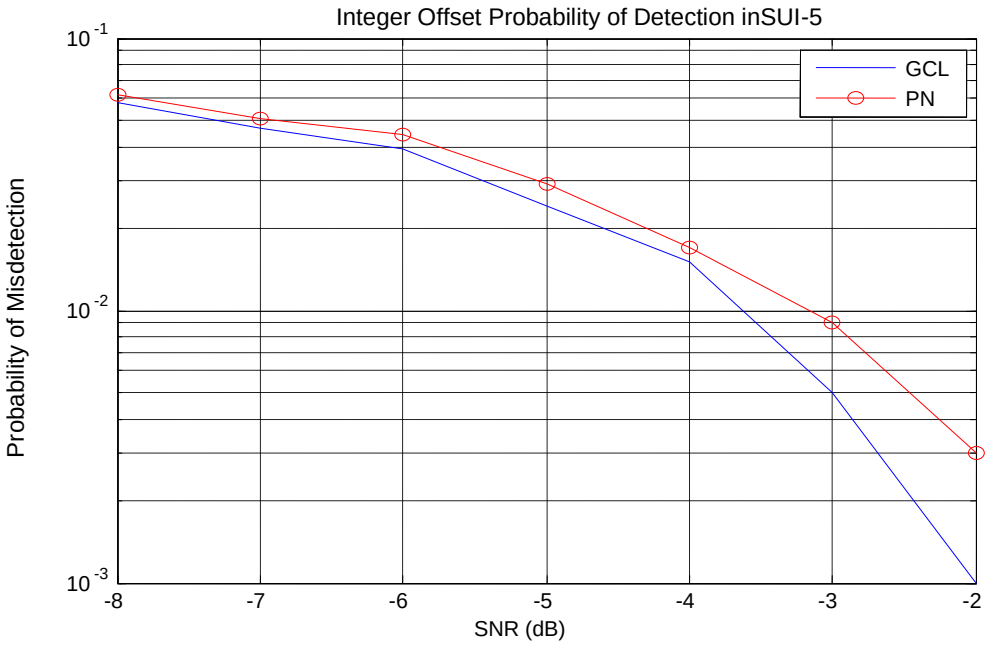

Fig. 4.24 Integer Offset Estimation in SUI-5

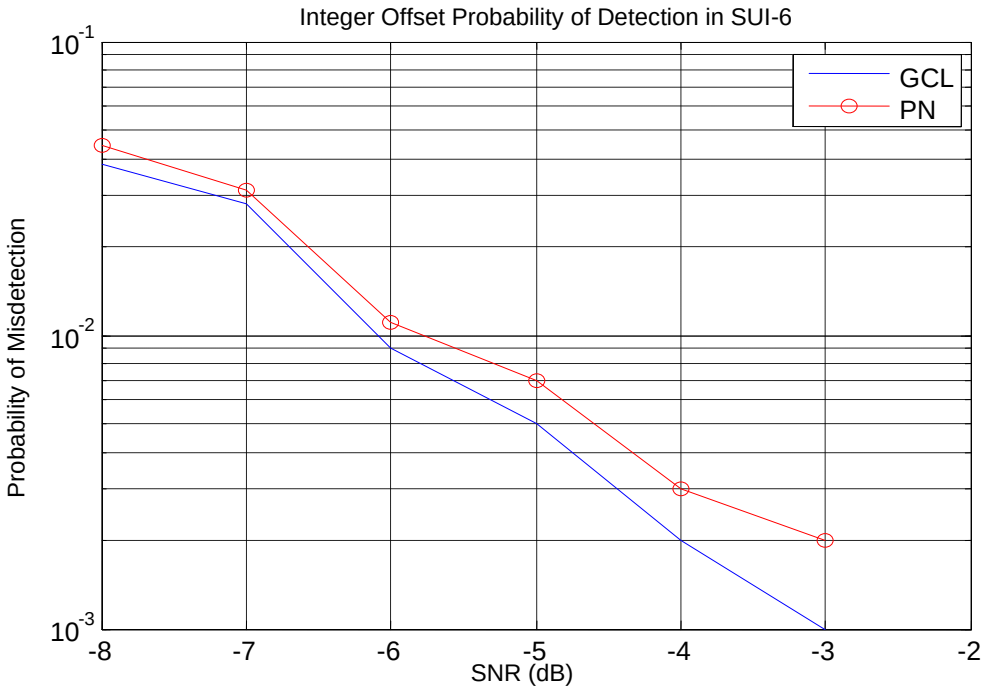

Fig. 4.25 Integer Offset Estimation in SUI-6

From Fig. 4.20 to 4.25 we can see that, the proposed GCL preamble performs better than the standard PN preamble where the probability of misdetection of the proposed GCL preamble is lower in each SNR than that of the standard PN preamble. For the

probability of 10^{-3}, the proposed GCL preamble gains 1 or 2 dB of SNR as compared to the standard PN preamble. This means that the proposed GCL preamble has an advantage of 1 or 2 dB of SNR to produce 1 error of detection over 1000 iteration.

In the integer frequency synchronization, again, proposed GCL preamble shows better performance than the standard PN preamble. This is due to its better cross-correlation property of in frequency domain as compared to the PN sequence. This was also argued in section 3.3.1.The results of the integer frequency synchronization proves that GCL based preamble has better correlation property not only in the time domain but also in the frequency domain than that of the standard PN preamble.

4.3 Time Domain Frequency Offset Correction Results and Analysis

The time domain frequency offset correction only use the proposed GCL preamble to obtain the probability of misdetection in the frequency offset correction since we only need to know the performance of time domain frequency offset correction scheme.

Fig. 4.26 shows the results of the time domain frequency offset estimation and correction with the integer frequency offset 2 and 3.

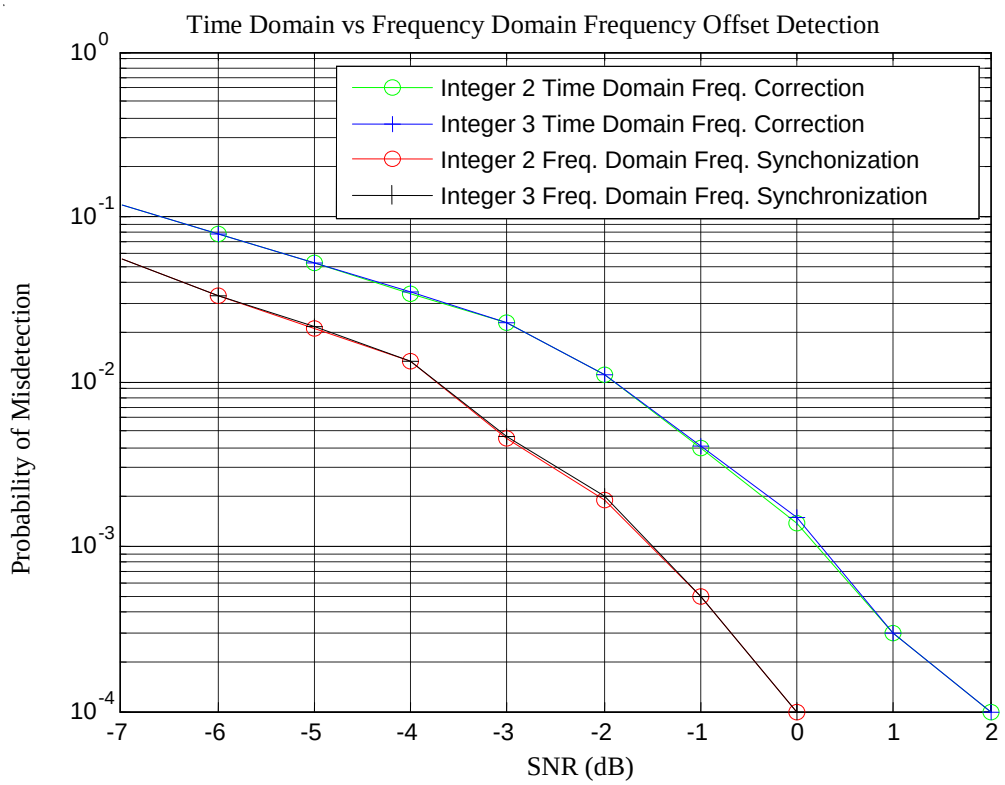

Fig. 4.26 Comparison of Frequency Correction and Estimation with Integer 2 and 3

It can be seen that the probability of misdetection for both of the integer frequency offset is similar to each other. Both figures show that the frequency offset correction achieves the same SNR for the same level of probability of misdetection. In conclusion, the figures show that the performance of the scheme is independent of the integer frequency offset.

Fig. 4.26 also shows the comparison of the performance of the time domain integer frequency correction using the proposed receiver scheme and the frequency domain integer frequency estimation of the typical receiver scheme. The purpose of this comparison is to obtain a comprehensive view of the time domain frequency correction and the frequency domain frequency estimation.

The result shows that the frequency offset estimation from the typical receiver has lower probability of miss-detection than the time domain frequency correction at each value of SNR. Although frequency correction and frequency estimation both rely on the correlation, but different domain characteristic affect the probability of misdetection differently.

From the explanation in Chapter section 3.3.1 and 3.3.2, it is known that the peak to sidelobe ratio of frequency domain correlation is 10 while that of time domain correlation is 4. If the ratio value is high, that means the magnitude of the sidelobe correlation is much smaller as compared to the magnitude of the main peak. Therefore, high ratio correlation is an advantage since lower sidelobe correlation has lower probability to disturb the detection of the main peak correlation. This effect showed in both of the figures , where the frequency domain estimation has lower probability of misdetection compared to that of the time domain. The advantage of the frequency domain correlation is 2 dB than the time domain correlation for the same level of probability of misdetection.

4.4 Time Domain Channel Estimation Results and Analysis

This subsection presents the simulation results of the time domain training based channel estimation of SUI channels. The SUI channels are the channel model meant for fixed wireless application. Since SUI-channel has three tap delays, the peaks expected to appear are also three peaks. Fig. 4.27 to 4.32 present the probability of the misdetection of the channel impulse response.

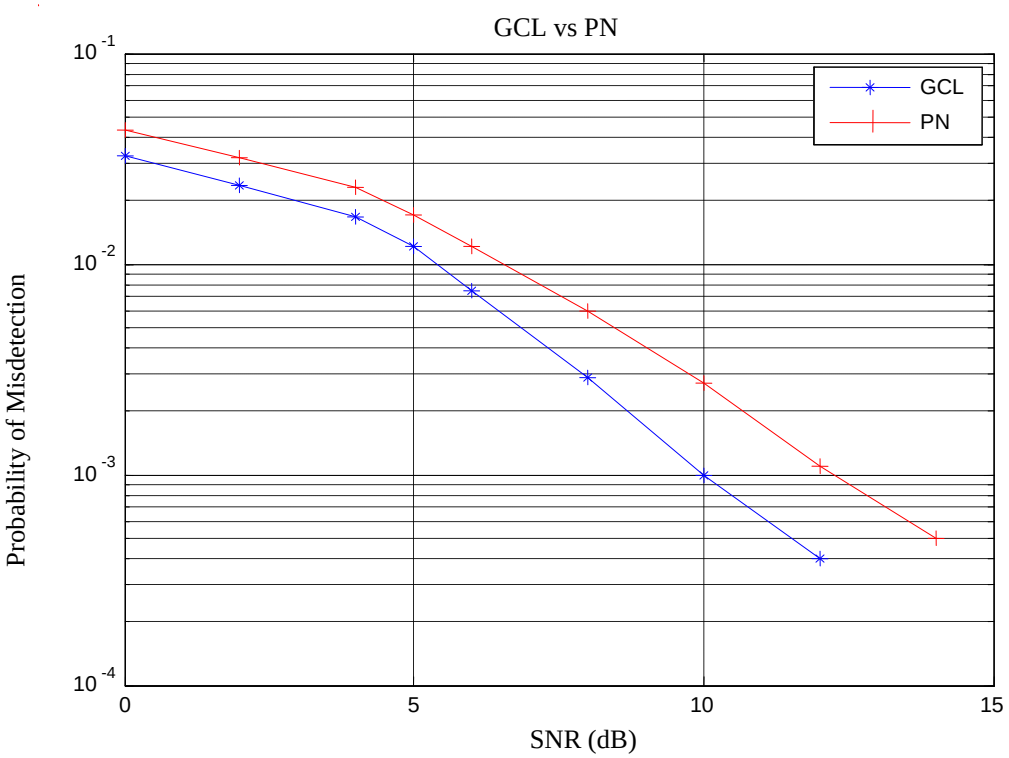

Fig. 4.27 Channel Estimation for SUI-1

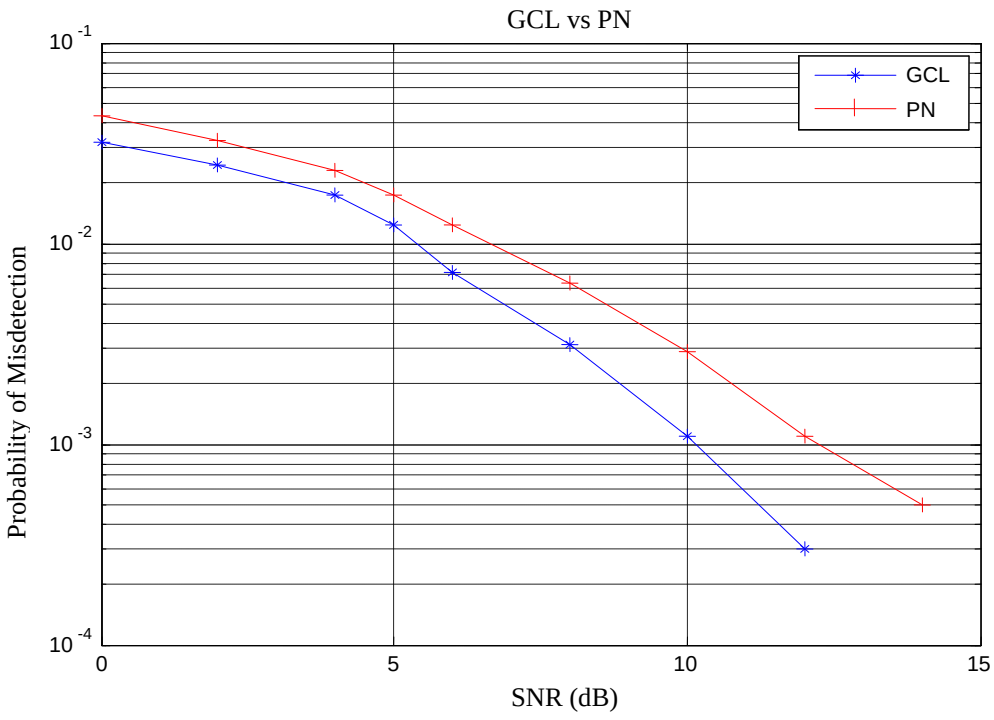

Fig. 4.28 Channel Estimation for SUI-2

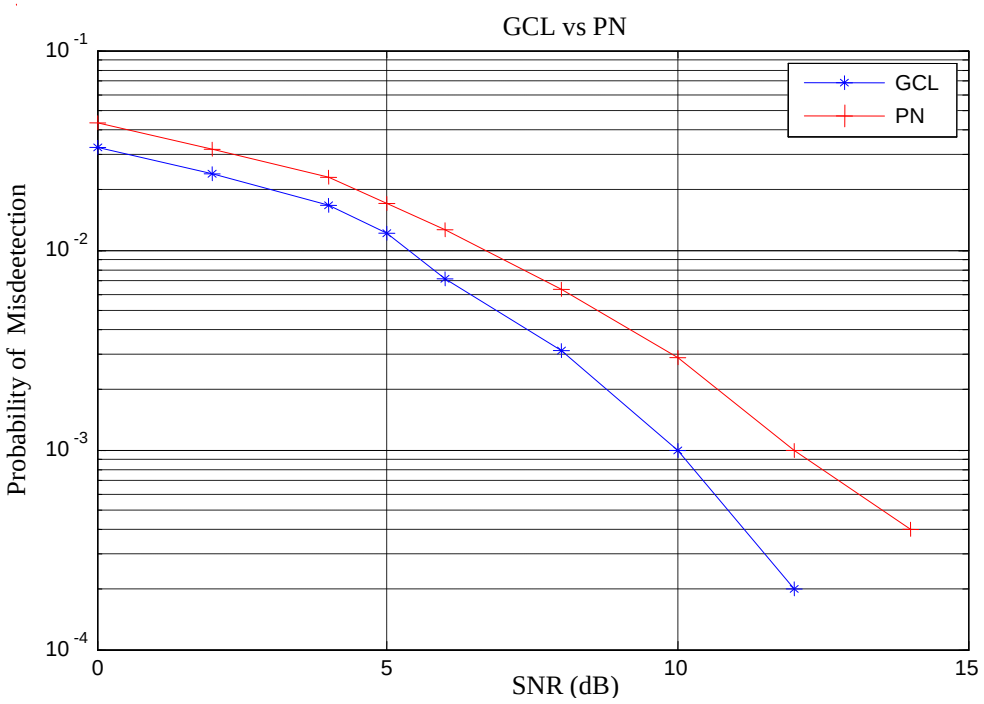

Fig. 4.29 Channel Estimation for SUI-3

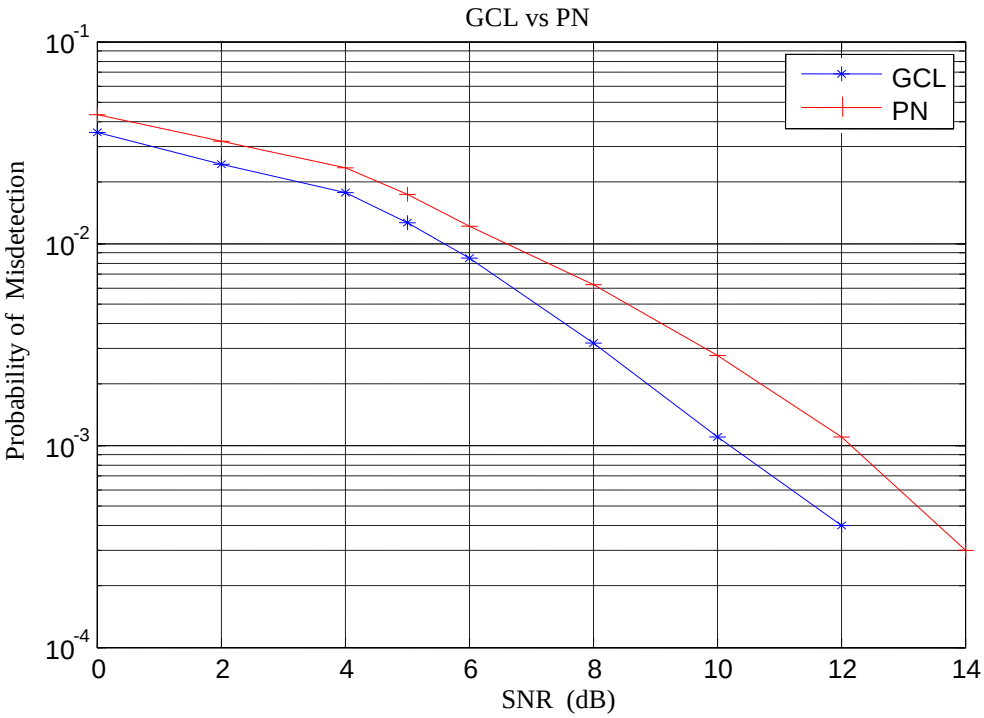

Fig.4.30 Channel Estimation in SUI-4

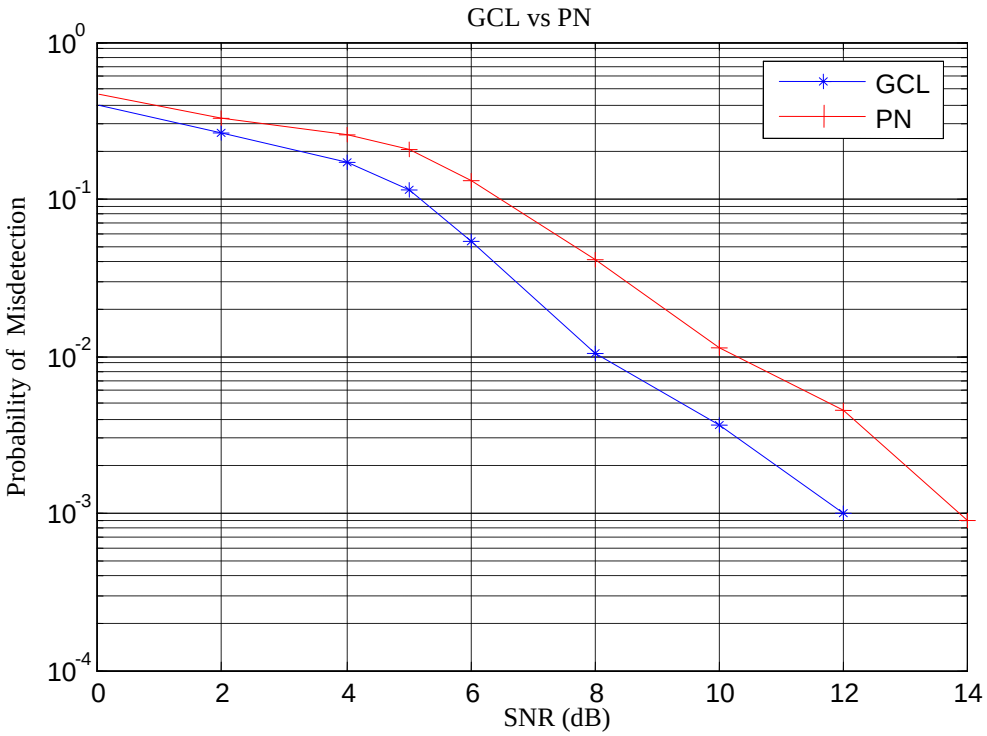

Fig. 4.31 Channel Estimation for SUI-5

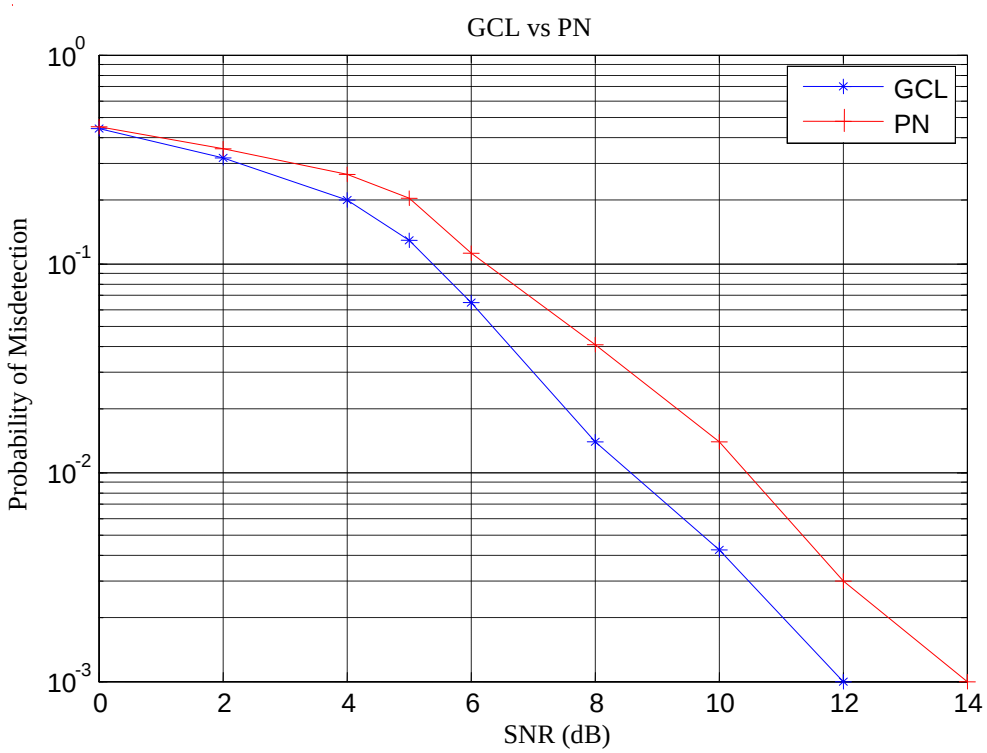

Fig. 4.32 Channel Estimation for SUI-6

The performance of the proposed GCL preamble for the first four SUI-channels is consistent where we can see that, for example, at SNR of 10 dB the probability reaches 10^{-3} or in other words that, one error occurs over 1000 times of detection. But, as we see in SUI-5 and SUI-6, the probability of misdetection is a bit higher than the rest of the SUI-channels for the same SNR. It can be seen that the probability of misdetection for SUI-5 and SUI-6 reach the same probability of misdetection such as 10^{-3} at SNR of 12 dB. The reason behind the difference is due to the distance length of the taps of SUI-5 and SUI-6. SUI-5 and SUI-6 has further distance and smaller power for the taps compared to other SUI-channels thus makes the probability of detection is lesser.

The same observation for the performance of the standard PN preamble gives information that the standard PN preamble reaches SNR of 12 dB to obtain the same level of probability, 10^{-3}, for the first four SUI-channels. In other words, the probability of one misdetection occurs over 1000 times detection happen at SNR of 12 dB. It is also shown from the results of SUI-5 and SUI-6 that the same probability reaches SNR of 14 dB for the same reason as mentioned in the above paragraph.

The results show that the time domain channel estimation performances are consistent, and this is due to the number of taps of the used channel in this work. As we have mentioned previously that SUI-channel has three taps, the probability of detecting three taps is good enough. But, this technique might not works well enough if the number of the channel taps are more than 3. The probability of detecting of more taps is lesser since the more taps is the more difficult to capture. In conclusion, this time domain channel estimation technique is suitable enough to apply in a WiMAX system that uses SUI-channels. Further observation is needed, to know whether a system like WLAN that has more than 3 taps can use the same technique. Therefore, it is a good suggestion for future work.

From Fig. 4.27 to 4.32, it is seen that the performance of the probability of misdetection of the proposed GCL preamble is better as compared to that of the standard PN preamble at each SNR. For example, with the probability of 10^{-3}, the proposed GCL preamble has better performance about 1 dB advantage as compared to that of the standard PN preamble.

Once again it is proved that the proposed GCL preamble showed superior performance in the time domain as compared to that of the standard PN preamble.

4.5 Hardware Complexity

The complexity of hardware implementation is measured by the number of the multiplication and addition of the applied scheme. In this scheme, for our new receiver scheme where we proposed the integer frequency offset is corrected in the time domain, we provide a bank of correlators in the time domain scheme. The number of multiplication in one correlator is $N(2N-1)$ or $2N^2-N$ multiplications and the number of addition is $N-1(2N-1)$ or $2N^2 - 3N + 1$ additions. And so for the whole correlators, we have 5 correlators, the total number of multiplications is $10N^2 - 5N$ and the total number of additions is $10N^2 - 15N + 5$. The proposed scheme also has a decision circuit which is used to decide the symmetrical correlation. The decision algorithm that included in our proposed scheme is a trivial scheme and therefore adds very little to the complexity.

For comparison with the frequency domain scheme, the frequency domain integer frequency offset estimation scheme has $2N^2-N$ multiplications and $2N^2 -3N + 1$ additions. It turns out that the proposed scheme has more complexity as compared to the frequency domain integer frequency offset estimation.

Although the proposed scheme is more complex than the frequency domain scheme, it is still desirable in order to estimate the channel in the time domain. The time domain channel estimation is known to be helpful in estimating the SNR that could be used in optimizing system performance by using it for adaptive power control, adaptive bit-loading or adaptive modulation. And, so, the proposed scheme is a desirable receiver scheme as no other receiver can perform the time domain channel estimation while also correcting the integer frequency offset.

4.6 Summary

This chapter presented the results of the works that are carried out in the Schmidl and Cox based typical OFDM receiver, time synchronization and integer synchronization and also the works that are carried out in the new proposed OFDM receiver, time domain frequency offset correction and time domain channel estimation.

The time synchronization results show that in the Schmidl and Cox's method, the proposed GCL preamble has better plateau shape than the standard PN preamble, more clearly obvious when the SNR goes below 5 dB. In Park et al.'s method, it shows that the proposed GCL preamble produces impulse like peaks that are much easier to detect than while using the standard PN preamble even in the presence of frequency offset. This is measured in terms of probability of misdetection of the said peaks.

Similarly, in the integer frequency synchronization, the proposed GCL preamble has lower probability of misdetection of the peaks as compared to the standard PN preamble.

In conclusion, the proposed GCL preamble shows superior performance over the standard PN preamble in the typical OFDM receiver system synchronization works, specifically it is shown that GCL based preamble in Park's method is a superior technique for time synchronization.

The performance evaluation of the time domain frequency offset correction is the probability of detection of the symmetrical correlation. It is shown that this scheme works well even when the SNR is low.

The proposed GCL preamble and the standard PN preamble from IEEE 802.16std are used in the time domain channel estimation. The performance of the estimation is measured in terms of misdetection probability that even one tap is not captured accurately. This performance is obtained for both the proposed GCL preamble and the standard IEEE 802.16 PN preamble and their respective performances are then compared.

The results show that the proposed GCL preamble has lower probability of misdetection of the channel impulse response compare to the standard PN preamble. It proves that the proposed GCL preamble has superior performance than the standard PN preamble.

As for the hardware complexity for our proposed receiver scheme, it is more complex than the standard receiver scheme. However, the proposed receiver scheme is still a desirable scheme as it perform the channel estimation as well the integer frequency offset correction in the time domain that has the advantages of adaptive power control, adaptive bit-loading and adaptive modulation.

CHAPTER 5

CONCLUSION

In Chapter III, we have presented the design of the proposed preamble based on GCL sequence and its application both in time as well as frequency synchronization. Similarly, in chapter IV, a new technique for integer frequency offset correction is presented together with its performance evaluation. This allows the channel estimation to be carried out in time domain. Accordingly, the chapter IV also carries out time domain channel estimation and presents its performance. In this chapter, we conclude the entire work and suggest future work to further this research work.

5.1 Conclusion

It is generally accepted that synchronization errors and large PAPR are among the main problems in the OFDM systems. Synchronization is the first task that any OFDM receiver carries out before any demodulation is done. In the burst transmission systems, like those of WiFi and WiMAX, to estimate the timing and frequency offsets and also the channel impulse response, correlation of a specially designed preamble is exploited. Accordingly, we set for ourselves the task of designing a new preamble that will help synchronize both in time and frequency domains better. Towards this end, we developed a GCL based preamble that has better correlation properties in time as well as frequency domain. This preamble has lower PAPR than the ones being used and also proves to be more robust against frequency offsets present in time domain.

In this thesis, we have shown, for the first time, the impairments caused by the residual frequency offset on both synchronization and time domain channel

estimation. Accordingly, we also set for ourselves the task of correcting both the fractional and integer frequency offsets in time domain. Doing so allows us to estimate the channel in time domain. Thus, we present a new receiver that carries out all synchronization tasks, as well as channel estimation, in time domain.

In order to estimate the performance of the proposed preamble, we make use of both Schmidl and Cox synchronization method and Park's method and compare it with that of PN sequence based preamble stipulated in IEEE 802.16 standard of WMAN.

Similarly, for frequency offset correction, we propose a bank-of-correlators based technique that looks for symmetrical correlation result. We evaluate its performance in terms of probability of wrong estimate as a function of SNR for some fixed value of integer offset.

Lastly, we carry out channel estimation in time domain and show that the scheme is feasible and also that the GCL based proposed preamble works better as compared to that based on PN sequence based preamble.

The contributions in the thesis are:

1. We have designed a new Generalized Chirp Like (GCL) sequence based preamble which has lower PAPR (1.82 dB) than the IEEE 802.16 standard preamble (3.0 dB) and better time domain and frequency domain correlation properties.

   The results show that in the time synchronization based on Schmidl-Cox' technique, the proposed GCL based preamble has better plateau-shape than the standard preamble even for SNR $\leq$ 5 dB. At the same time, when used in Park's technique, it gives more accurate and robust estimation of the time offset even in the presence of frequency offsets. This is measured in terms of probability of mis-detection of the peaks of the timing-metric as defined by Park's method. It has, thus, been shown that our proposed GCL based preamble outperforms the standard PN based preamble for time synchronization even in the presence of the frequency offset.

   When used for the integer frequency synchronization, following the Schmidl and Cox technique for integer-frequency-offset estimation, the results showed that

GCL based preamble has lower probability of misdetection at each SNR as compared to the standard PN preamble. It is because, as shown in the thesis, our proposed GCL preamble has better frequency domain correlation than the standard PN preamble.

In conclusion, the GCL based preamble has superior performance as compared to the standard PN preamble for both the time and frequency synchronization.

2. We have designed a new receiver scheme that corrects the integer frequency offset using a bank of correlators. Since the preambles usually have identical halves, the correlation is symmetrical if it has no residual frequency offset. Accordingly, the bank of correlators are so used that the one with symmetrical correlation is captured. The results show that the new receiver scheme is able to detect the symmetrical correlation quite accurately and the scheme has low probability of misdetection of the symmetrical correlation. In conclusion, for the frequency offset correction scheme, the receiver works well even in low SNR environment.

3. We have also performed the time domain channel estimation before pre-FFT which requires the above mentioned frequency offset correction to have been done before the channel estimation, without which, as shown in the thesis, the channel estimation is not feasible in time domain. We use the proposed GCL based preamble and also the standard PN based preamble to evaluate their relative performances in the time domain channel estimation. The results show that our proposed GCL based preamble has lower probability of misdetection at each SNR as compared to the standard PN preamble and thus is able to help detect better all the taps of the channel impulse response.

5.2 Future Works

There are many extensions possible to enhance this work.

1. A possible extension of this work is to first undertake the hardware implementation of the time and frequency synchronization works and analyze the actual complexity, both in terms of computational cost and also extra

processing delay, if any. This is essential to know how practical the proposals are.

2. Another interesting future work to be investigated is to compare the time domain channel estimation method with that applied in the frequency domain, particularly from hardware implementation point of view.
3. Similarly, the hardware implementation of the proposed receiver that estimates and corrects the frequency offset and carries out time domain channel estimation is also interesting and thus needs to be considered in the future work in order to evaluate the proposed receiver scheme for any OFDM system and compare it with other conventional systems.
4. It would also be an interesting work to extend time-domain channel estimation to SNR estimation and use it in diversity application or adaptive power control or adaptive modulation application.
5. The channel estimates are useful in many applications where feedback paths exist to the transmitter, so the transmitter can implement transmit-only diversity techniques, or even in space-time coding.

REFERENCES

[1] Park B., et. al.," A Novel Timing Estimation for OFDM Systems", Communication Letters, IEEE, Vol.7, No.5, pp.239-241, May, 2003.

[2] European Telecommunications Standards Institute (ETSI), Radio Broadcasting Systems; Digital Audio Broadcasting (DAB) to Mobile, Portable and Fixed Receivers, European Telecommunication Standard ETS 300 401, 1st edition, reference DE/JTC-DAB, Feb,1995.

[3] Asymmetric Digital Subscriber Line (ADSL) Transceivers. Telecommunication Standardization Sector of International Telecommunication Union, ITU-T G.992.1.

[4] Cooley, J. W. and J. W. Tukey, "An Algorithm for the Machine Computation of the Complex Fourier Series", Mathematics of Computation, Vol. 19, pp. 297-301, April 1965.

[5] Schmidl T.M., Cox D., "Robust Frequency and Timing Synchronization for OFDM", IEEE Transaction On Communication, Vol.45, No.12, pp.1613-1621, Dec, 1997.

[6] Minn H., Zeng M., Barghava V.K., "On timing Offset Estimation for OFDM Systems", Communication Letters, IEEE, Vol.4, No.7, pp.242-244, July, 2000.

[7] Van de Beek, et.al. ,"ML Estimation of Time and Frequency Offset in OFDM systems", IEEE Transaction On Signal Processing, Vol.47, No.7, pp.1800-1805, July, 1997.

[8] Prasad, R. & Van Nee, R.," OFDM for wireless for multimedia communication", London: Artec House, 2000.

[9] Li, C.P., Huang, W.C.,"Semi-Blind Channel Estimation Using Superimposed Training Sequences with Constant Magnitude in Dual Domain for OFDM Systems", Vehicular Technology Conference 2006, VTC2006-Spring, IEEE 3rd, Vol.4, pp.1575-1579, May, 2006.

[10] Drieberg,M.," MIMO Channel Estimation for Applications in Fixed Broadband Wiresless Access Systems", MSc Thesis, Electrical and Electronics Department, Universiti Teknologi Petronas, May, 2005.

[11] Magnus Sandell., Over Edfors, "A comparative study of pilot-based channel estimators for wireless OFDM", Research Report, Luleå University of Technology, Sweden,September,1996.

[12] Morelli, M., Mengali, U., "A Comparison of Pilot-Aided Channel Estimation Methods for OFDM Systems", IEEE Transactions On Signal Processing, Vol. 49, No.2, pp.3065-3073, Dec, 2001.

[13] Manzoor, S.,"A Novel SNR Estimation Technique for OFDM System", MSc Thesis, Electrical and Electronic Department, Universiti Teknologi Petronas, August, 2008.

[14] Witrisal, K., "OFDM Air-Interface for Multimedia Communications," Ph.D Thesis, Technische Universiteit Delft, Netherlands, April, 2002.

[15] Ersoy, O.Z., "A Comparison of Timing Methods in OFDM Systems", MSc Thesis, Naval Postgraduate School, Monterey, California, Sept, 2004.

[16] Mark Engels, "Wireless OFDM System How To Make Them Work?", Springer-Verlag, New York, LLC, July, 2002.

[17] Luc Deneire, Bert Gyselinckx, Marc Engels, "Training Sequence vs Cyclic Prefix. A new Look on Single Carrier Communication", Communication Letters, IEEE Vol.5, No.7, pp.292-294, July, 2001.

[18] IEEE 802.16a Standard for Local and Metropolitan Networks, Part 16: Air Interface for Fixed Broadband Wireless Access Systems, 2000.

[19] Paul H. Moose, "A Technique for Orthogonal Frequency Division Multiplexing Frequency Offset Correction", IEEE Transaction On Communication, Vol.42, No.10, pp.2908-2914, Oct,1994.

[20] Guoping, Xu, et al., " New OFDM Channel Estimation Algorithm with Low Complexity", Vehicular Technology Conference, 2007, VTC2007-Spring, IEEE 65th, pp.2257-2260, April, 2007.

[21] PingZhi Fan, Mike Darnell, F.Fan, “Sequence Design for Communication Application”, Research Studies Press Ltd, John Wiley & Sons Inc, New York, November, 1996.

[22] Frank, R.L, Zadoff, S.A, Heimiller, R., “Phase Shift Codes with Good Periodic Correlation Properties”, IEEE Transaction On IRE Information Theory, Vol.IT-8, pp.381-382, Oct, 1962.

[23] Chu, D.C.,” Polyphase Code with Good Correlation Properties”, IEEE Transactional On Information Theory, Vol.18, pp. 531-532, July, 1972.

[24] Suehiro, N., Hatori, M.,” Modulatable Orthogonal Sequences and their Application to SSMA Systems”, IEEE Transaction On Information Theory, Vol.34, No.1, pp. 93-100, Jan, 1988.

[25] Zhuang, J., et.al,” Ranging Improvement for 802.16e OFDMA PHY”, IEEE 802.16 Broadband Wireless Access Working Group, June, 2004.

[26] B. M. Popovic, “Generalized Chirp-Like Polyphase Sequences with Optimum Correlation Properties”, IEEE Transaction On Information Theory, Vol.38, No.4, pp.1406-1409, July, 1992.

[27] Zhuang, J., et.al, ”GCL-based preamble design for 1024,512 and 128 FFT sizes in the OFDMA PHY layer”, IEEE 802.16 Broadband Wireless Access Working Group, IEEE C80216e-04/241r1, Aug, 2004.

[28] Lotter, M.P., Linde. L.P, ” A Comparison of Three Families of Spreading Sequences for CDMA Applications”, COMSIG-94, Proceedings of 1994 IEEE South African Symposium On, pp.67-75, Oct, 1994.

[29] B.M., Popovic & Mauritz, O., ”Random Access Preambles for Evloved UTRA Cellular System”, Spread Spectrum Techniques and Applications, IEEE Ninth International Symposium On, pp.488-492, 28-31 Aug ,2006.

[30] Lee, D.H., ”OFDMA Uplink Ranging for IEEE 802.16e Using Modified Generalized Chirp-Like Polyphase Sequence”, The First IEEE and IFIP International Conference in Central Asia On, pp.5, Sept, 2005.

[31] Erceg, V., et.al, ”Channel Model for Fixed Broadband Wireless Applications”, IEEE 802.16 Broadband Wireless Access Working Group, July, 2001.

PUBLICATIONS

1. Yanti, D.K., Minn, Y.K., Jeoti, V.," A study of GCL sequence in frequency synchronization for IEEE 802.16-2004", Intelligent and Advance Systems, 2007, ICIAS 2007, International Conference On, IEEE, pp. 494-497, November, 2007.

2. Yanti, D.K., Jeoti, V., "On GCL Based Preamble for Time Synchronization in OFDM System", Signal and Image Processing Applications, 2009, ICSIPA 2009, International Conference On, IEEE, 18-19th November, 2009.

APPENDIX

Table1. Terrain A consisting of (a) SUI-1 channel and (b) SUI-2 channel [18]

SUI – 1 Channel				
	Tap 1	**Tap 2**	**Tap 3**	**Units**
Delay	0	0.4	0.9	µs
Power (omni ant.)	0	-15	-20	dB
90% K-fact. (omni)	4	0	0	
75% K-fact. (omni)	20	0	0	
Power (30° ant.)	0	-21	-32	dB
90% K-fact. (30°)	16	0	0	
75% K-fact. (30°)	72	0	0	
Doppler	0.4	0.3	0.5	Hz
Antenna Correlation: $\rho_{ENV} = 0.7$ **Gain Reduction Factor:** GRF = 0 dB **Normalization Factor:** $F_{omni} = -0.1771$ dB, $F_{30°} = -0.0371$ dB			**Terrain Type:** C **Omni antenna:** $\tau_{RMS} = 0.111$ µs, overall K: K = 3.3 (90%); K = 10.4 (75%) **30° antenna:** $\tau_{RMS} = 0.042$ µs, overall K: K = 14.0 (90%); K = 44.2 (75%)	

(a)

SUI – 2 Channel				
	Tap 1	**Tap 2**	**Tap 3**	**Units**
Delay	0	0.4	1.1	µs
Power (omni ant.)	0	-12	-15	dB
90% K-fact. (omni)	2	0	0	
75% K-fact. (omni)	11	0	0	
Power (30° ant.)	0	-18	-27	dB
90% K-fact. (30°)	8	0	0	
75% K-fact. (30°)	36	0	0	
Doppler	0.2	0.15	0.25	Hz
Antenna Correlation: $\rho_{ENV} = 0.5$ **Gain Reduction Factor:** GRF = 2 dB **Normalization Factor:** $F_{omni} = -0.3930$ dB, $F_{30°} = -0.0768$ dB			**Terrain Type:** C **Omni antenna:** $\tau_{RMS} = 0.202$ µs, overall K: K = 1.6 (90%); K = 5.1 (75%) **30° antenna:** $\tau_{RMS} = 0.069$ µs, overall K: K = 6.9 (90%); K = 21.8 (75%)	

(b)

Table2. Terrain B consisting of (a) SUI-3 channel and (b) SUI-4 channel [18]

SUI – 3 Channel				
	Tap 1	**Tap 2**	**Tap 3**	**Units**
Delay	0	0.4	0.9	µs
Power (omni ant.)	0	-5	-10	dB
90% K-fact. (omni)	1	0	0	
75% K-fact. (omni)	7	0	0	
Power (30° ant.)	0	-11	-22	dB
90% K-fact. (30°)	3	0	0	
75% K-fact. (30°)	19	0	0	
Doppler	0.4	0.3	0.5	Hz
Antenna Correlation: $\rho_{ENV} = 0.4$ **Gain Reduction Factor:** GRF = 3 dB **Normalization Factor:** $F_{omni} = -1.5113$ dB, $F_{30°} = -0.3573$ dB			**Terrain Type:** B **Omni antenna:** $\tau_{RMS} = 0.264$ µs, overall K: K = 0.5 (90%); K = 1.6 (75%) **30° antenna:** $\tau_{RMS} = 0.123$ µs, overall K: K = 2.2 (90%); K = 7.0 (75%)	

(a)

SUI – 4 Channel				
	Tap 1	**Tap 2**	**Tap 3**	**Units**
Delay	0	1.5	4	µs
Power (omni ant.)	0	-4	-8	dB
90% K-fact. (omni)	0	0	0	
75% K-fact. (omni)	1	0	0	
Power (30° ant.)	0	-10	-20	dB
90% K-fact. (30°)	1	0	0	
75% K-fact. (30°)	5	0	0	
Doppler	0.2	0.15	0.25	Hz
Antenna Correlation: $\rho_{ENV} = 0.3$ **Gain Reduction Factor:** GRF = 4 dB **Normalization Factor:** $F_{omni} = -1.9218$ dB, $F_{30°} = -0.4532$ dB			**Terrain Type:** B **Omni antenna:** $\tau_{RMS} = 1.257$ µs overall K: K = 0.2 (90%); K = 0.6 (75%) **30° antenna:** $\tau_{RMS} = 0.563$ µs overall K: K = 1.0 (90%); K = 3.2 (75%)	

(b)

Table3. Terrain C consisting of (a) SUI-5 channel and (b) SUI-6 channel [18]

SUI – 5 Channel				
	Tap 1	**Tap 2**	**Tap 3**	**Units**
Delay	0	4	10	µs
Power (omni ant.)	0	-5	-10	dB
90% K-fact. (omni)	0	0	0	
75% K-fact. (omni)	0	0	0	
50% K-fact (omni)	2	0	0	
Power (30° ant.)	0	-11	-22	dB
90% K-fact. (30°)	0	0	0	
75% K-fact. (30°)	2	0	0	
50% K-fact. (30°)	7	0	0	
Doppler	2	1.5	2.5	Hz
Antenna Correlation: $\rho_{ENV} = 0.3$ **Gain Reduction Factor:** GRF = 4 dB **Normalization Factor:** $F_{omni} = -1.5113$ dB, $F_{30°} = -0.3573$ dB			**Terrain Type:** A **Omni antenna:** $\tau_{RMS} = 2.842$ µs overall K: K = 0.1 (90%); K = 0.3 (75%); K = 1.0 (50%) **30° antenna:** $\tau_{RMS} = 1.276$ µs overall K: K = 0.4 (90%); K = 1.3 (75%); K = 4.2 (50%)	

(a)

SUI – 6 Channel				
	Tap 1	**Tap 2**	**Tap 3**	**Units**
Delay	0	14	20	µs
Power (omni ant.)	0	-10	-14	dB
90% K-fact. (omni)	0	0	0	
75% K-fact. (omni)	0	0	0	
50% K-fact. (omni)	1	0	0	
Power (30° ant.)	0	-16	-26	dB
90% K-fact. (30°)	0	0	0	
75% K-fact. (30°)	2	0	0	
50% K-fact. (30°)	5	0	0	
Doppler	0.4	0.3	0.5	Hz
Antenna Correlation: $\rho_{ENV} = 0.3$ **Gain Reduction Factor:** GRF = 4 dB **Normalization Factor:** $F_{omni} = -0.5683$ dB, $F_{30°} = -0.1184$ dB			**Terrain Type:** A **Omni antenna:** $\tau_{RMS} = 5.240$ µs overall K: K = 0.1 (90%); K = 0.3 (75%); K = 1.0 (50%) **30° antenna:** $\tau_{RMS} = 2.370$ µs overall K: K = 0.4 (90%); K = 1.3 (75%); K = 4.2 (50%)	

(b)